M. TECH (POWER SYSTEM) SHREYA GARG 2020

ANALYSIS AND CONTROL OF DC-DC CONVERTERS

A Dissertation
Submitted in partial fulfillment of
the requirements for the degree of

Master of Technology
In
Power System
By

SHREYA GARG

(2K19/PSY/18)

Under the supervision of

Prof. Dheeraj Joshi

DEPARTMENT OF ELECTRICAL ENGINEERING

Delhi Technological University

(Formerly Delhi College of Engineering)

Bawana Delhi-110042

August 2020

DEPARTMENT OF ELECTRICAL ENGINEERING

DELHI TECHNOLOGICAL UNIVERSITY

(Formerly Delhi College of Engineering)

Bawana Road, Delhi-110042

Candidate's Declaration

I, **Shreya Garg**, having roll no**. 2K19/PSY/18** of M.Tech (**Power System**), hereby declare that work presented in Major Project-II titled "**Analysis and Control of DC-DC converters**" in fulfillment of requirement for awarding the **Degree of Master of Technology in Power Systems** is submitted to the Department of Electrical Engineering, Delhi Technological University, Delhi, is legitimate and of my own, carried during January to July 2021, under the oversight of Prof. Dheeraj Joshi.

The composition presented in this dissertation has not been submitted by me for the award of any other degree of this or any other Institute/University.

Place: DELHI

Date: 8th sept 2021

Shreya Garg

DELHI TECHNOLOGICAL UNIVERSITY

(Formerly Delhi College of Engineering)

Bawana, Delhi-110042

Certificate

I hereby declare that the project Dissertation titled "**Analysis and Control of DC-DC Converters**" – which is submitted by **Shreya Garg**, having roll no. **2K19/PSY/18** of Electrical Engineering Department, Delhi Technological University, Delhi in partial fulfillment of the requirement for the award of the degree of Master of Technology, is a record of the project work carried out by the scholar under my supervision. To the best of my knowledge the work has not been submitted in part or full for any degree or diploma to this university or somewhere else.

Place: Delhi

Date:

Prof. Dheeraj Joshi

Project Supervisor

(Professor,EED)

ACKNOWLEDGEMENT

I want to convey my deepest appreciation to Prof. Dheeraj Joshi for his support in the dissertation. I owe him a debt of gratitude enabling me to work under his supervision, and for supplying me with all of the essential instructions and tools for my project. It would have not been possible to conclude my project in absence of his invaluable time and advice. I sincerely appreciate his readiness to address all my doubts and queries regarding the project work and his consistent encouragement to carry my work forward. Working under him has been a great experience and it aided me in gaining a lot of personal as well as professional insight.

I am thankful to Prof. Uma Nangia, Head of Department, Electrical Engineering, Delhi Technological University for their kind help, encouragement and extending support during course of study which helped me in completing my project work.

Shreya Garg

2k19/PSY/18

Delhi Technological University

ABSTRACT

The work presented in this dissertation is the study of non-isolated dc-dc converters and their control to provide a regulated output dc voltage with least ripples and fluctuations with the change in circuit parameters. Steady state modeling of dc-dc converters in continuous conduction mode using state space averaging is discussed. This provides with a clear insight into the behavior of dc-dc converters. The circuits that are considered in this dissertation are buck converter, elementary Luo converter, self-lift Luo converter, super-lift Luo converter and ultra-lift Luo converter.

Further, to control the outputs of these converters, PI control technique is implemented to improve the system performance and create fewer fluctuations during parameter changes to the circuit. A sliding mode controller is proposed and implemented on these converters that reduces the ripples in output voltage and can achieve better dynamic response than PI controllers.

MATLAB-Simulink models of these converters are designed and PI control and the proposed sliding mode control are implemented. Presented assay of proposed SMC can enact steady frequency of switching with reduced ripples in output . Error in steady state of the converters is reduced and the output tracks a desired reference voltage despite disturbances caused in the supple voltage and resistance at load. The devised sliding mode controller in this dissertation aims at achieving minimum steady state error & chattering in the converters. The results from an uncontrolled and PI controlled converter is compared with that of SMC and conclusions are drawn.

CONTENTS

LIST OF FIGURES

LIST OF TABLES

LIST OF SYMBOLS

A	State matrix of state space averaged model
A_s	State matrix of small signal state space averaged model
α	Coefficient for inductor current in sliding mode control
B	Input matrix for model
B_s	Input matrix for small signal model
β	Coefficient for output voltage in sliding mode control
D	Duty ratio (T_{on}/T)
γ	Coefficient for error between output and reference voltage in sliding mode control
I_{in} ,i_{in}	Input current to converter
I_{out} ,i_{out}	Output current from converter
i_x	Instantaneous current through any component labeled at X
I_x	Average current of component x
mH	Mili Henry
µH	Micro Henry
µF	Micro Farad
Ω	Ohm
R	Load resistance
s	Laplace operator
$s(x)$	Sliding surface function
T	Switching period
T_{on}	On time during one period of switch

T_{off}	Off time during one period of switch
u_{eq}	Equivalent control in SMC
V_{in} ,v_{in}	Input voltage to converter
V_{out} ,v_{out}	Output voltage from converter
V_{ref}	Reference Voltage

LIST OF ABBREVIATIONS

AC	Alternating Current
CCM	Continuous Conduction Mode
DC	Direct Current
CCM	Continuous Conduction Mode
MOSFET	Metal Oxide Silicon Field Effect Transistor
NOULLC	Negative Output Ultra-Lift Luo Converter
PI	Proportional Integral
PID	Proportional Integral Differential
POELC	Positive Output Elementary Luo Converter
POSLC	Positive Output Super-lift Luo Converter
POSLLC	Positive Output Self-Lift Luo Converter
PWM	Pulse Width Modulation
SMC	Sliding Mode Control
SSA	State Space Average
SSM	Small Signal model
VSS	Variable Structure System

CHAPTER 1

INTRODUCTION

Power electronic devices provide efficient way of energy conversion. This energy conversion is categorized into alteration of ac into dc, alteration of dc into dc, alteration of dc into ac and alteration of ac into ac. DC-DC converters find plethora of applications; huge power alteration systems like HVDC, electric vehicles, energy storage, renewable energy conversion to everyday appliances like cell phone chargers, computer peripherals and more [1-2], [5-6]. Some of the examples of such converters are buck converter, which gives a lesser voltage at output than input, boost, sepic converter which generates a higher output voltage. Buck-Boost converter both reduces and increases voltage at output but has opposite polarity in the output voltage. Cuk converter generates a higher output voltage but having opposite polarity.

Dc-dc power unit consists of a converter and a controller. Fig 1 represents the dc-dc power conversion unit. Some challenges to the present controllers for dc-dc converters are broadly divided into the following points.

1. The efficiency of the converter should not decrease when the controller is implemented.
2. The designed controller can work to lessen the presence of ripples in the output of the converter.
3. Stable outputs voltages should be generated which should not be affected by the changes brought in the parameters of the converters.
4. Controller can deal with nonlinearities of converter.
5. The controller must enable the converter output to track a reference signal despite the circuit disturbances.

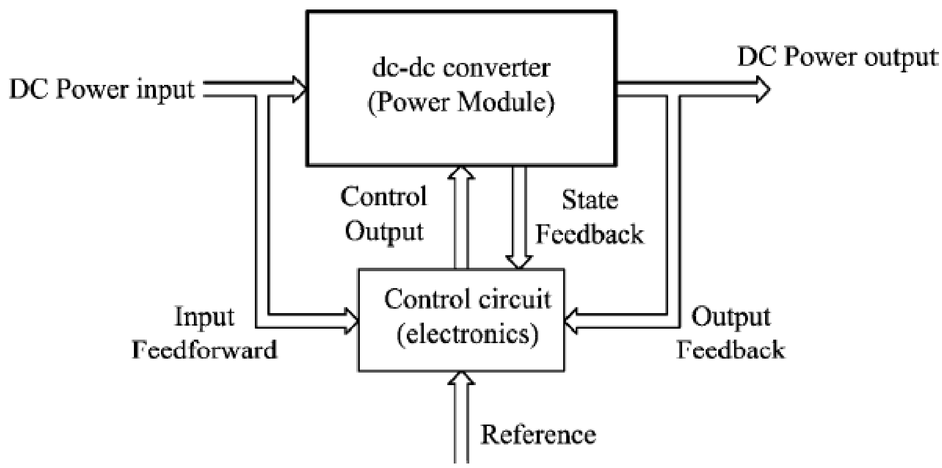

Fig 1.1 Representation of dc-dc power unit.

Nonlinearity and high switching frequency of these converters creates lots of difficulties while modeling the converters and controlling them. There is a range of methodologies of controlling designed due to requirement of regulated dc voltage at output regardless of fluctuations in load resistance and supply voltage

1.1 SCOPE OF THIS DISSERTATION

In this dissertation, a new class of DC-DC boost converters that is Luo converters has been studied and analyzed. The DC-DC luo converter was designed by F.L Luo [12], [13]. These converters have simple circuitry, high efficiency and almost zero ripples in output voltage and current. The voltage gain of these converters are higher than that of traditional step-up converters (boost, sepic, cuk converters). Voltage lift technique [14] implemented on luo converter and a family of luo converters is studied and analyzed.

State space modeling [21], [22] of these converters are performed in steady state and small signal modeling is done for each converter. Control of these converters is the main area of focus for these converters. Closed loop control guarantees satisfactory performance and high reliability for dc-dc converters. Control performance of these converters is analyzed under different conditions by implementing a proportional integral controller [28]-[31], which is a linear controller. More details about this controller are presented in chapter 5. Sliding mode controller [34]-[47] is also proposed for these converters which is discussed further in chapter 6. The goal of controllers is providing closed loop control to the converter and generate stable outputs for varying conditions. The goal of this dissertation is analyzing voltage at output w.r.t duty ratio of switch. Reference tracking of the output voltage under variations given to voltage given at supply and resistance at load and is noted. Performance parameters of the controlled converter which includes the rise time, system overshoot, ripple content, settling time are also noted and compared. Pros and cons of the methods of control are also considered.

This dissertation, presents the MATLAB- Simulink models of POELC, POSLLC, POSLC, NOULLC. PI control and the proposed SMC is designed and implemented on each of these converters. The output voltage waveform is observed for each converter under variations in load resistance and supply voltage. Reference voltage tracking of the output voltage is observed for these controllers and the results are tabulated and compared. A conclusion is drawn based on the data obtained.

1.2 STRUCTURE OF THIS DISSERTATION

The work presented in this dissertation can be divided into the following chapters.

Chapter 1 shows the scope of the work done and the structure of this dissertation.

In chapter 2, the literature survey is presented wherein the works done by other researchers related to the fields of mentioned in this dissertation are discussed.

Chapter 3 deals with the analysis of the dc-dc converters and its configurations. The performance and characteristics of different configurations of luo converters is derived and discussed.

In chapter 4, steady state model of the mentioned converters is performed. State space averaging method utilized to derive the models of the converters. A small perturbation is added to the state space variables, duty ratio, supply voltage to converters and the small signal models are obtained.

Theory of proportional integral controllers and their application to the Luo converters is presented in chapter 5. Values of proportional and integral controllers are derived using Zeigler-Nichols tuning method.

In chapter 6, SMC of dc converters is discussed and sliding surface is designed for the converters. The conditions for a system to be controlled using sliding mode control are also discussed.

Chapter 7 presents with the models for the converters and the controllers drawn using MATLAB-Simulink for all configurations of converters mentioned. System performance parameters and reference voltage tracking of the controlled converters are observed and tabulated.

Chapter 8 presents the conclusion of this dissertation where the performance of converters mentioned under both the controllers are compared and the pros and cons of controlling methodologies is also considered. Future applications of this work and further work which can be done is also discussed in this chapter.

Appendices present the tabulated data related to the work done. Appendix A contains the different converter parameters and their values which are designed in this work.

The work of researchers done in the fields of this dissertation which have acted as guiding references for this dissertation are presented in the last segment Bibliography and References.

CHAPTER 2

LITERATURE REVIEW

2.1 INTRODUCTION

This chapter expresses many papers & work done by other scholars related in controlling dc converters and SMC is reviewed. The review work is done for the areas mentioned below:

i. Topologies of dc converters
ii. Modeling and control of dc-dc converters
iii. Sliding Mode Controller

2.2 LITERATURE SURVEY

2.2.1 Topologies of dc converters

DC-DC converters are the most basic power electrical circuits that convert one dc voltage level to another. They are smaller, more efficient, have a higher power density, and are easier to manage. Dc converters perform wide range of applications from electric vehicles aircrafts, telecommunication, computer peripherals, power system, electric drives and many more [1]-[6]. Due to several advantages and utilization of such converters, several dc-dc converter topologies have been developed in recent years. Buck, boost & buck-boost converters are the first generation topologies having simple structures [7],[8],[9]. Buck converter's operation is to provide lower voltage at output as compared to supply. Boost converters gives higher value of output than the input. Buck-boost converters are able to execute both buck and boost converter functions but with a negative output voltage. Almost all the next stage converters are developed using these converters. These developments may include addition of more inductors and capacitors, or adding more switches, isolation using a transformer or some other methodology. Cuk [10], sepic, zeta converter, flyback, interleaved dc-dc converters are some topologies , performing high level voltage transfer with high efficiency[11] ,[12].

DC-DC luo topology is a new topology of dc converters with design objective to providing even higher gain of voltage, & reducing ripples present at output voltage and inductor current. They have high efficiency [12]-[19]. Voltage lift technique can be easily applied to the luo converters which can increase the voltage by ten or hundred times than the supply voltage [12], [20]. Self-lift [12], re-lift [18], super-lift [16], [17] and ultra-lift [19] are some of the configurations of voltage lifted luo converters derived from the elementary luo converter topology. These configurations are discussed in detail in this dissertation.

2.2.2 Control and modeling of dc-dc converters

DC-DC converters have non-linear and vary with time systems. Certain modeling methods to deal with the nonlinearity of these converters has been studied. Modeling of dc converters requires some methods like averaging method [21], [22] sampled data modeling [23], phase plane trajectory analysis [24] are some of the examples. In [25], the author has performed state space modeling including parasitic components. Almost all these modeling methods will generate multi variable systems with state space equations. Since these have non-linear dynamic behavior, to perform model analysis or provide linear control, linear models are developed around a given operating point. Small signal analysis can be used to generate these linear models for the converters. This is done by introducing a small perturbation in the system. More details on this can be found in chapter 4.

Controlling converters is an essential step. Dc regulated voltage at output is needed, with least ripples and less fluctuations to parameters changes for applications into renewable energy, power system, electric vehicles [26]. The controllers can be categorized as classical controllers and modern controllers [27]. Classical controllers are easy to implement and find application in a variety of home and industrial settings. Some examples of these are PI, PID controllers, sliding mode controller [28], [30].The controllers can also be divided into two categories linear and non-linear. Controllers termed linear are those which implement linearized models of the converters like PI /PID controllers. Some papers mentioned in references [33],[34] show the implementation of linearization technique on nonlinear dc-dc converters. Nonlinear controllers do not require any linearized model like sliding mode control, fuzzy control or robust control techniques. Linear controller like PI is easy to implement and for a long time, they've been used in a variety of industrial settings.. Well-tuned PI controller provides good performance to the converters. Authors of papers [29],[30] give insight into the PI control and various tuning techniques. In this dissertation, Ziegler- Nichols tuning method is used to find the values for a PI controller [31]. The performance is sensitive to load and line variations.

2.2.3 Control of dc-dc converter using sliding mode.

Nonlinear control theory is an approach to overcome the problem of linear controllers. Implementation of nonlinear controllers is a bit sophisticated in dc-dc converters. SMC is a non-linear mode of control for variable structure systems. References [34]-[37] presented some earlier works done in sliding mode control.[38]-[39] presented some earliest works in implementing SMC to converters. The conventional PWM Controllers implemented on dc-dc converters were small signal based, so a new approach of implementing PWM controllers with sliding mode controllers for better regulation were implemented in [38], [39]. The works were mainly focused on buck, boost & buck-boost converters.

In later years, authors of papers [40] ,[41] extended the works as order increases of dc converters such as cuk and sepic converters. Sira-Ramirez in [42] presented sliding mode controller using a PI controller to boost the system's efficiency for a buck converter. In [43], a PWM based SMC was designed to have constant switching frequency. Reference [44] analyzes some previous works done in the field of SMC. In [45], SMC is implemented on converters operating in DCM.

Some of the works presenting SMC of luo converters are mentioned here. In [46], the proposed SMC is designed using input voltage feed forward and information feedback for buck and positive elementary luo converter. This adaptive sliding mode control gave finer performance under parameter variations and operating point changes. Sliding mode control for an elementary luo converter is designed to obtain constant switching frequency in [47].

2.3 CONCLUSION

Literature review is carried out for presented work “Analysis and Control of DC-DC Luo Converters’. Literature review is carried out to realize the scope of dc-dc luo converters and its modeling. It also helped in understanding the implementation of PI controllers and SMC in dc-dc converters. An understanding of the problems encountered by the proposed method of control like high switching frequency, circuit complexity, designing of sliding surface and ways to overcome these problems can be developed from the past works presented in the literature review.

CHAPTER 3

ANALYSIS OF DC-DC CONVERTERS

3.1 INTRODUCTION

DC-DC converters as the name implies, are power electronics circuits taking dc voltage as input and converting it into dc voltage at another level. These are electronic voltage regulators which consist of inductors, capacitors, diodes and transistors. Diodes and transistors act as switches and inductors and capacitors are the energy storage devices. DC-DC converters can either generate load voltage lower than supply or can increase the level of output dc voltage by providing accurate duty ratio to the switches. Due to wide range of applications of these converters, there have been developed a number of topologies of dc-dc converters [7]-[10]. Detailed examination and characteristics of some topologies of converters are discussed in the upcoming sections.

3.2 BUCK CONVERTER

Buck Converter generates voltage at load lesser or equal to supply. It is also known as step-down converter. Diagram shown in fig. 3.1 is the circuitry of a buck converter. LC components are energy storage elements and provide filtering for low frequency for the circuit. Diode connected gets forward biased When S has been opened. This provides path for inductor current When S has been opened.

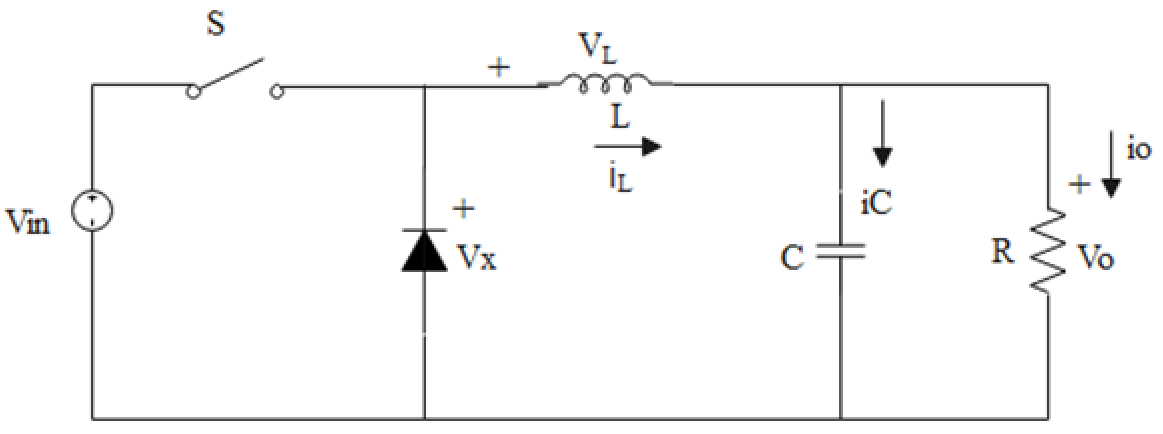

Fig 3.1: Circuitry of buck converter

V_s is voltage of input battery, V_0 is output voltage, v_L,i_L are Voltage across inductor and current respectively, i_c is current through capacitor, v_X is diode voltage and i_O is current in load. Figure 3.2 and 3.3 present the circuits for buck converter When S has been closed /opened respectively.

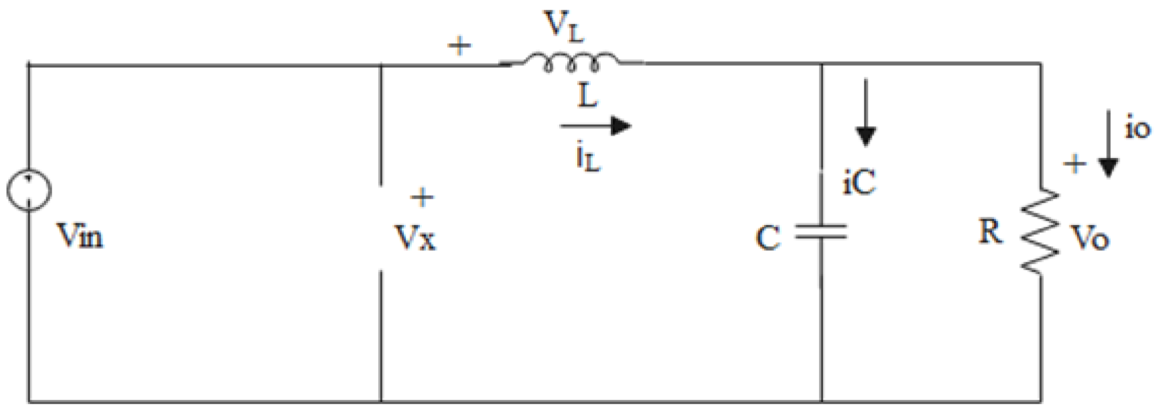

Fig 3.2: Circuitry of buck When S has been closed

In figure 3.2, as S gets closed, diode opens and supply current runs through the inductor, capacitor and resistance.

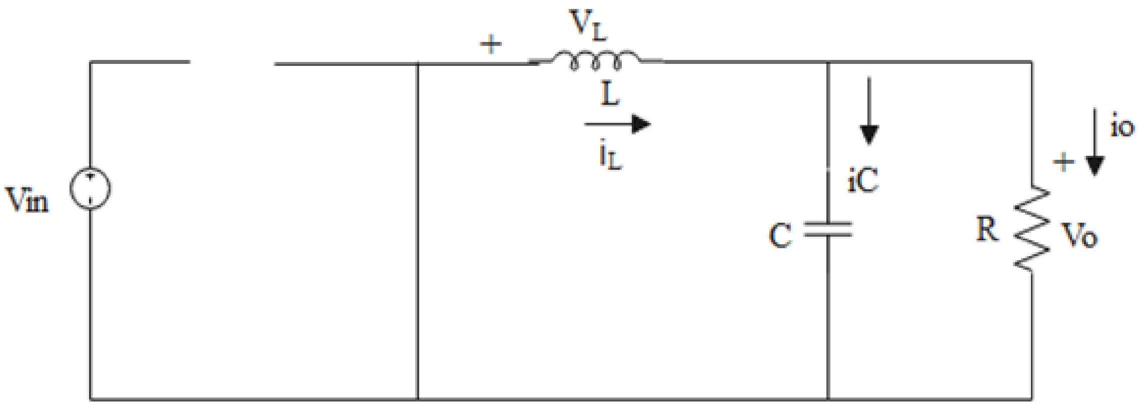

Fig 3.3: Circuitry of buck when S is open

In figure 3.3, as S gets opened, diode gets forward biased. Supply gets disconnected from circuit and inductor acts as current source.

3.2.1 Analysis of buck converter circuit in CCM

CCM means that current in inductor is positive throughout the operation.

Analyzing circuit from fig 3.2 When S has been closed ,

$$v_L = V_S - V_0 \tag{3.1}$$

Since, $v_L = L\frac{di_L}{dt}$ (3.2)

$$=> \frac{di_L}{dt} = \frac{v_L}{L} = \frac{V_s - V_0}{L} \tag{3.3}$$

Since ON time of S is DT (t_{on} time). D being duty ratio of the converter

$$\frac{di_L}{dt} = \frac{\Delta i}{DT} = \frac{V_s - V_0}{L} \tag{3.4}$$

$$=> \Delta il_{open} = \frac{(V_s - V_0)DT}{L} \tag{3.5}$$

Δi_L is peak to peak variation of inductor current for converter.

Analyzing circuit from fig 3.3 When S has been opened,

$$v_L = -V_o \tag{3.6}$$

Similarly, $\Delta il_{closed} = \frac{(-V_0)(1-D)T}{L}$ (3.7)

During steady state, inductor current in one switching cycle is zero.

$$\Delta il_{open} + \Delta il_{closed} = 0 \tag{3.8}$$

$$\frac{(V_S-V_0)DT}{L} + \frac{(-V_0)(1-D)T}{L} = 0 \tag{3.9}$$

The gain of voltage transferfor buck converter in CCM can be given as:

$$=> \frac{V_o}{V_{in}} = D \tag{3.10}$$

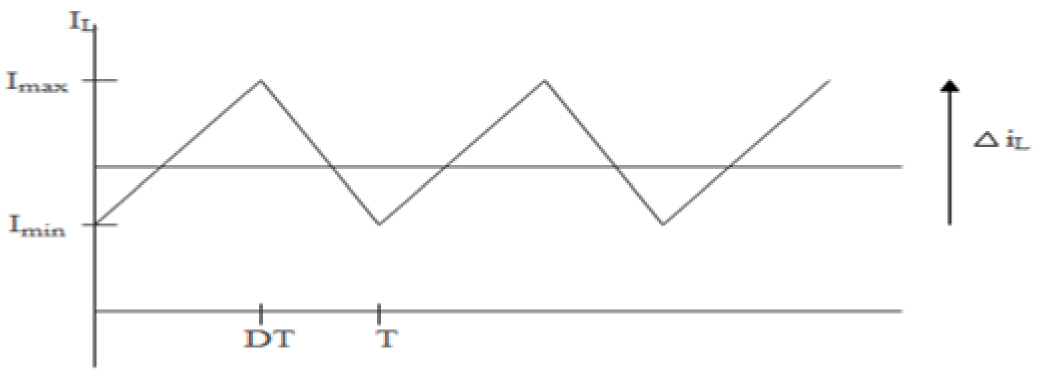

Fig 3.4: Current through inductor in CCM

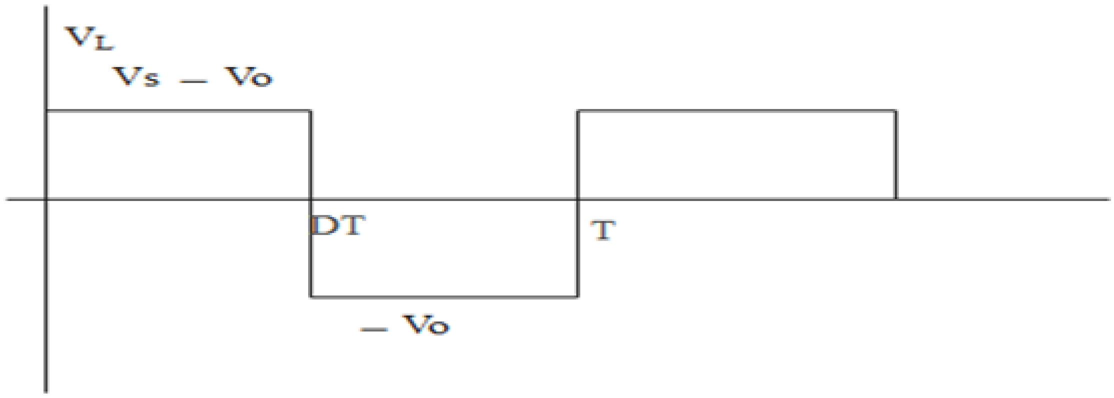

Fig 3.5: Voltage across inductor in CCM.

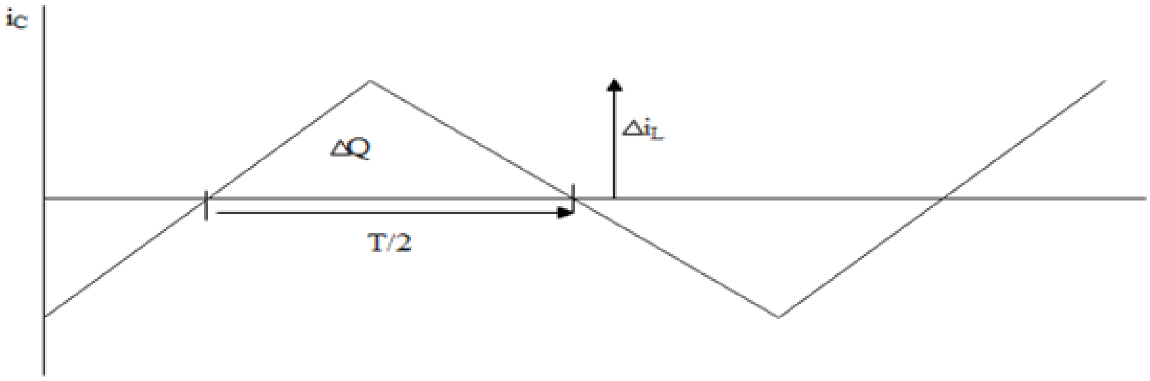

Fig 3.6: Capacitor current in CCM.

From eq. (3.5) and (3.7), values of minimum and maximum inductor current are derived.

$$I_{L\,max} = I_L + \frac{\Delta i_L}{2} \tag{3.11}$$

$$I_{L\,min} = I_L - \frac{\Delta i_L}{2} \tag{3.12}$$

Equating $I_{L\,min} = 0$, we get the critical value of inductor which is the minimum value needed for CCM.

$$=> L_{min} = \frac{(1-D)R}{f} \tag{3.13}$$

Where R is resistance at load. f is frequency of switching.

In figure 3.6, ripple in Vc is given by

$$\Delta V_0 = \frac{\Delta Q}{C} \tag{3.14}$$

The change in charge ΔQ of the capacitor is given by

$$\Delta Q = \frac{T \Delta i_L}{8} \tag{3.15}$$

Ripple in output voltage as fraction of output voltage is given by

$$\frac{\Delta V_0}{V_0} = \frac{(1-D)}{8LCf^2} \tag{3.16}$$

3.2.2 Analysis of buck converter circuit in DCM

DCM means current through inductor is not always positive during operation.

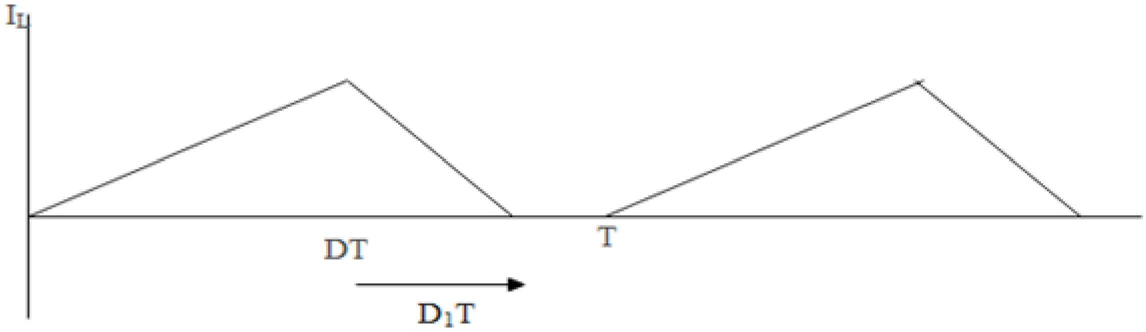

Fig 3.7: Current through inductor in DCM

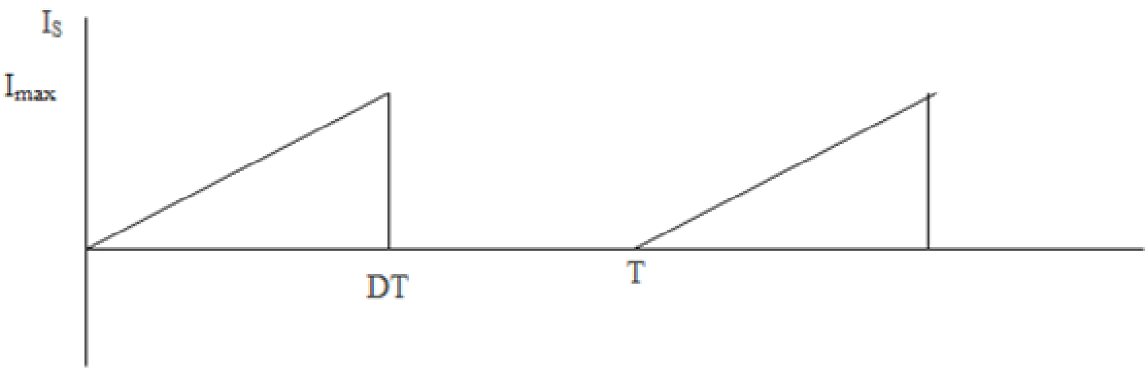

Fig 3.8: Current from supply in DCM

From figure 3.7, D_1T is the time when current through inductor is decreasing and hits zero . This gives average Voltage across inductor as:

$$(V_S - V_0)D - V_0D_1 = 0 \qquad (3.17)$$

The boundary for CCM and DCM happens when $D=D_1$.

The average value of Current through inductor in DCM is given as

$$I_{L\,max} = I_L + \frac{\Delta i_L}{2} \qquad (3.18)$$

$$I_{L\,max} = \frac{V_0 D_1 T}{L} \qquad (3.19)$$

Solving equations (3.17) and (3.18), gives the value of D_1. Voltage gain for buck converter in DCM is given as:

$$=> \frac{V_o}{V_{in}} = \frac{2D}{D + \sqrt{D^2 + 8\frac{L}{RT}}} \qquad (3.20)$$

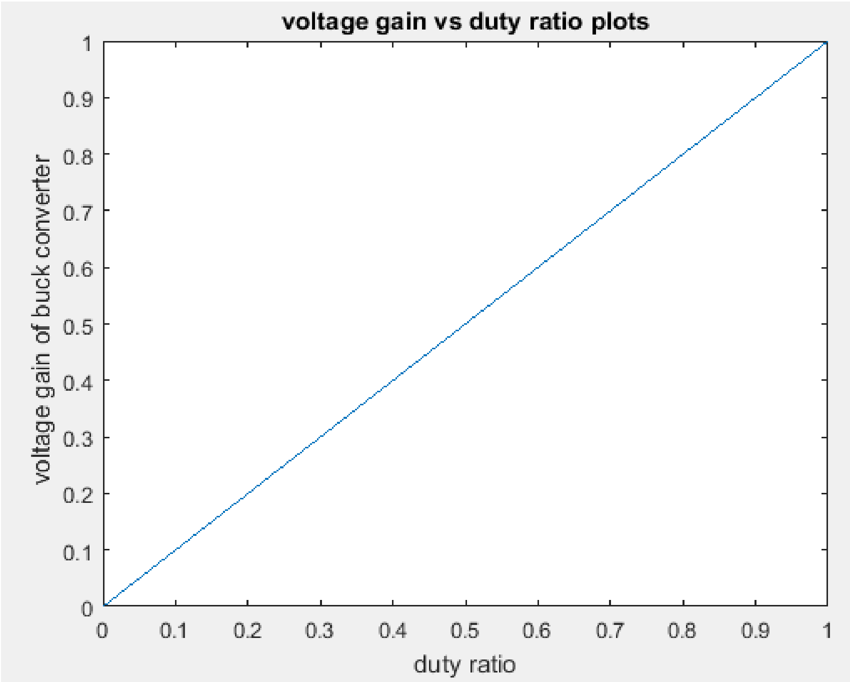

Fig 3.9: Gain of voltage transferversus duty ratio of switch for buck .

Fig. 3.9 shows gain of voltage transferversus duty ratio of switch for buck. Gain of voltage transferand duty ratio have a linear connection.

3.3 POSITIVE OUTPUT ELEMENTARY LUO CONVERTER

Elementary Luo converters recently developed topology of dc converter which is derived from fundamental converters [12], [13]. Figure 3.10 shows circuitry of POELC. Capacitor C_a is the primary energy storage and transferring element via pump inductor L_a. Fig 3.11, fig 3.12 give circuitry when S is ON and OFF respectively.

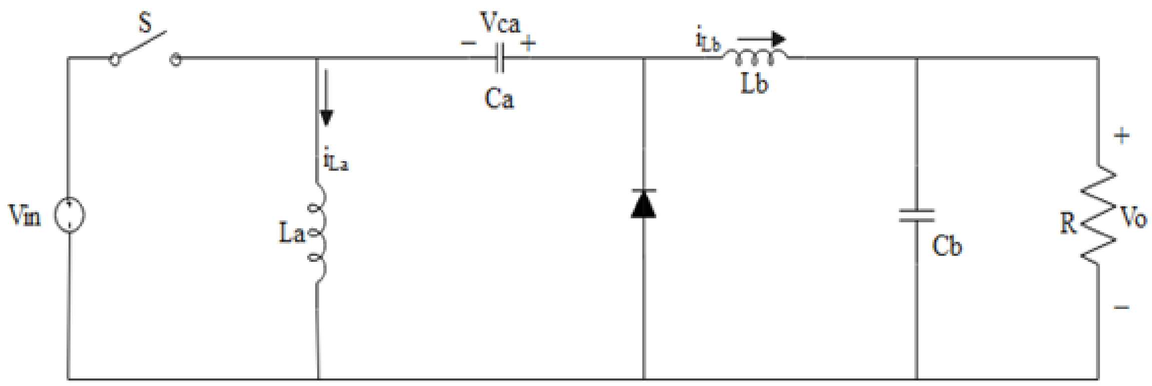

Fig 3.10: Circuit representation of POELC

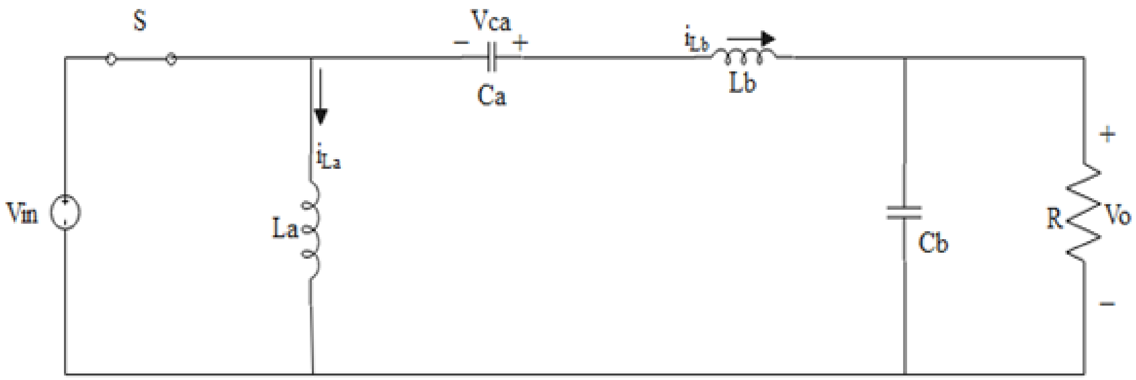

Fig 3.11: Circuit representation of POELC When S has been closed

Fig 3.11, When S has been closed , diode is off and current from supply is given as:

$$i_s = i_{L\,a} + i_{L\,b} \tag{3.21}$$

Inductor L_a and L_b absorbs energy from source and their currents increases.

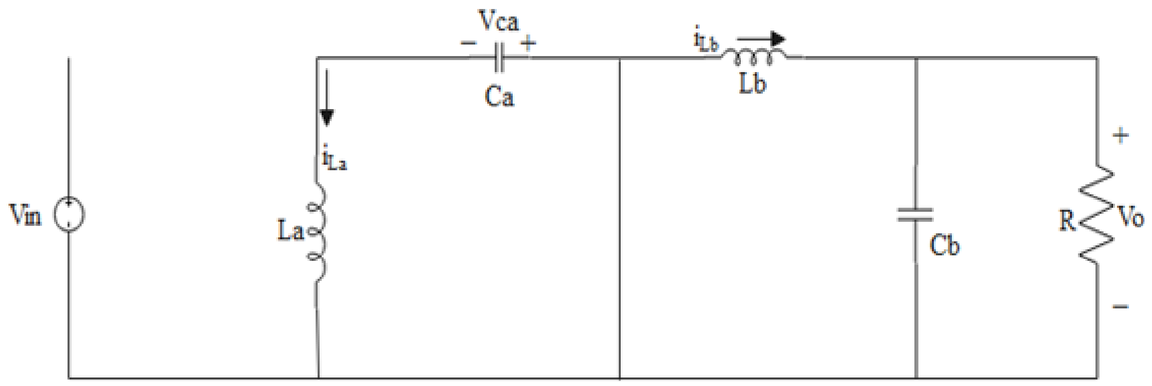

Fig 3.12: Circuit representation of POELC when switch is opened

In figure 3.11, S is opened, diode gets connected and supply current is disconnected. $i_{L\,a}$ runs through it and charges C_a . $i_{L\,b}$ flows through C_b and R. Inductor L_a and L_b release energy from source and their currents decreases. The variations present in currents I_{La} and I_{Lb} are negligible, ie $i_{L\,a} \approx I_{La}$ and $i_{L\,b} \approx I_{Lb}$

3.3.1 Analysis of POELC circuit in CCM

Analyzing circuit from fig 3.11, S is closed,

The charge on capacitor C_a is given by

$$Q_{Ca\ close} = dI_{Lb}T \tag{3.22}$$

Analyzing circuit from fig 3.12, S is opened,

The charge on capacitor C_a is given by

$$Q_{Ca\ open} = (1-d)I_{La}T \tag{3.23}$$

Since, $$Q_{Ca\ close} + Q_{Ca\ open} = 0 \tag{3.24}$$

Therefore, $$Q_{Ca\ close} + Q_{Ca\ open} = 0 \tag{3.25}$$

$$=> I_{Lb} = \frac{1-d}{d} I_{La} \tag{3.26}$$

The source current when S closes is given as

$$i_s = i_{La} + i_{Lb}$$

$$=> I_s = d\left(I_{La} + \frac{1-d}{d} I_{La}\right) \tag{3.27}$$

Therefore, average source current is

$$I_s = I_{La} \tag{3.28}$$

and output current is

$$I_o = \frac{1-d}{d} I_{La} \tag{3.29}$$

Voltage at output of POELC is

$$V_o = \frac{d}{1-d} V_{in} \tag{3.30}$$

The gain of voltage transferof elementary Luo converter is given as:

$$M_E = \frac{V_o}{V_{in}} = \frac{d}{1-d} \tag{3.31}$$

Figure 3.13 shows the plot between gain of voltage transferand duty ratio of an elementary Luo converter.

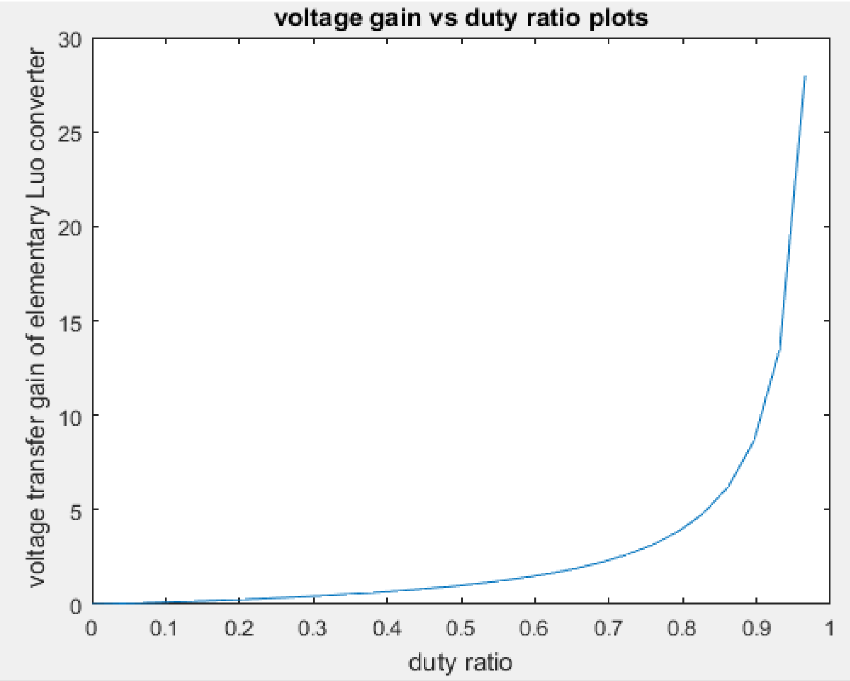

Fig 3.13: Gain of voltage transfervs duty ratio for POELC

From figure 3.11, the VL_a when S closes is given as $V_{La} = V_{in}$

The variation of peak to peak inductor current i_{La} is given as:

$$\Delta i_{La} = \frac{dV_{in}T}{L_a} \qquad (3.32)$$

Ratios for the current variations in inductor are shown below:

$$\eta = \frac{\Delta i_{La}/2}{I_{La}} = \frac{dTV_{in}}{2L_a I_s} = \frac{1-d}{2M_E}\frac{R}{fL_a} \qquad (3.33)$$

$$\varsigma = \frac{\Delta i_{Lb}/2}{I_{Lb}} = \frac{dTV_{in}}{2L_b I_O} = \frac{d}{2M_E}\frac{R}{fL_b} \qquad (3.34)$$

The variation of peak to peak capacitor voltage v_{Ca} is:

$$\Delta v_{Ca} = \frac{Q_{Ca\ open}}{C_a} = \frac{dI_{Lb}T}{C_a} \qquad (3.35)$$

Ratio for the variation in v_{Ca} is:

$$\rho = \frac{\Delta v_{ca}/2}{V_{Ca}} = \frac{(1-d)TI_s}{2C_a V_O} = \frac{d}{2}\frac{1}{fC_a R} \qquad (3.36)$$

Ratio for the variation in output voltage is:

$$\epsilon = \frac{\Delta v_o/2}{V_o} = \frac{dT^2 V_{in}}{16C_b L_b V_O} = \frac{dT^2}{16M_E C_b L_b} \qquad (3.37)$$

The inductor currents during CCM operation for POELC is similar to buck.

3.3.2 Analysis of POELC circuit in DCM

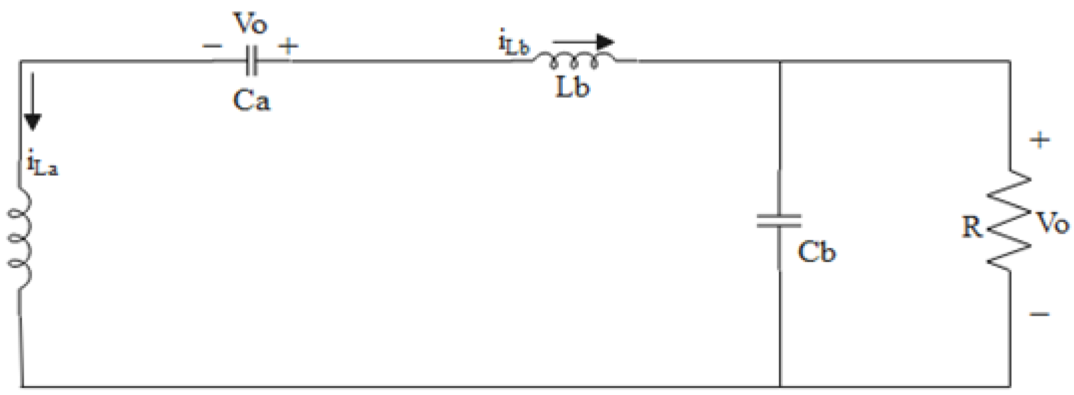

Fig 3.14: Circuit representation of POELC under DCM operation

Fig 3.14 shows the DCM operation of elementary Luo converter. The diode current becomes zero When S has been opened before it is closed again. The condition for DCM is that the ratio of variation of diode current must be greater than 1. This is given by equation (3.38).

$$\epsilon = \frac{\Delta i_D/2}{I_D} = \frac{d^2 R}{{M_E}^2 2fL} \geq 1 \tag{3.38}$$

$$=> \; M_E \leq d\sqrt{\frac{R}{2fL}} \tag{3.39}$$

Where, $L=L_a \parallel L_b$

The current i_D that used to exists in the interval between dT as well as $[d+(1-d)m_E]T$, such that m_E is considered to be the filling efficiency and can be defined as:

$$m_E = \frac{d^2 R}{{M_E}^2 2fL} \tag{3.40}$$

Voltage across load in DCM is:

$$V_O = \left[\frac{d}{(1-d)m_E}\right] V_{in} = \frac{d(1-d)RV_{in}}{2fL} \tag{3.41}$$

From equation (3.41) , the output voltage is directly proportional to R.

3.4 POSITIVE OUTPUT SELF-LIFT LUO CONVERTER

Voltage lifting method is applied to converters to get higher gain of voltage transfer. In the basic voltage lifting technique, a passive switch is realized along with diode as well as a charged capacitor is included. This charged capacitor voltage is arranged with the circuit of elementary Luo converter. Therefore, the output voltage gets lifted even higher. For instance, if diode and capacitor included to the POELC (Figure 3.15-3.17), we can get a positive output self-lift Luo converter [12]-[14].

Though, while analyzing these circuits, we assume that capacitance is as large as required and we can ignore the variation of voltage in the voltage lifting capacitor. If we consider the capacitance in the analysis, there are several influences of voltage lifting on performance of the converter. It helps in making gain of voltage transfera function of the R and f. CCM and DCM have a boundary between them which is influenced because of the parameters of voltage lifting. POSLLC increase the gain of voltage transfer of POELC in arithmetic progression.

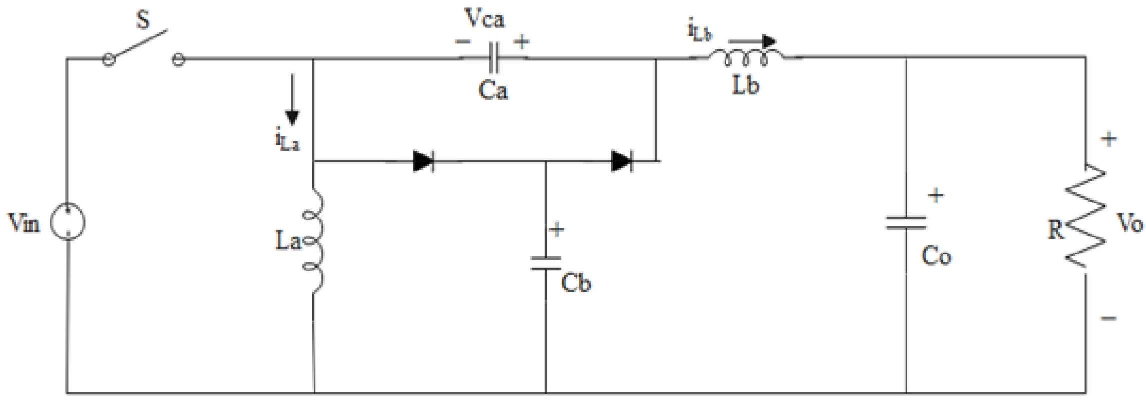

Fig 3.15: Circuit representation of POSLLC

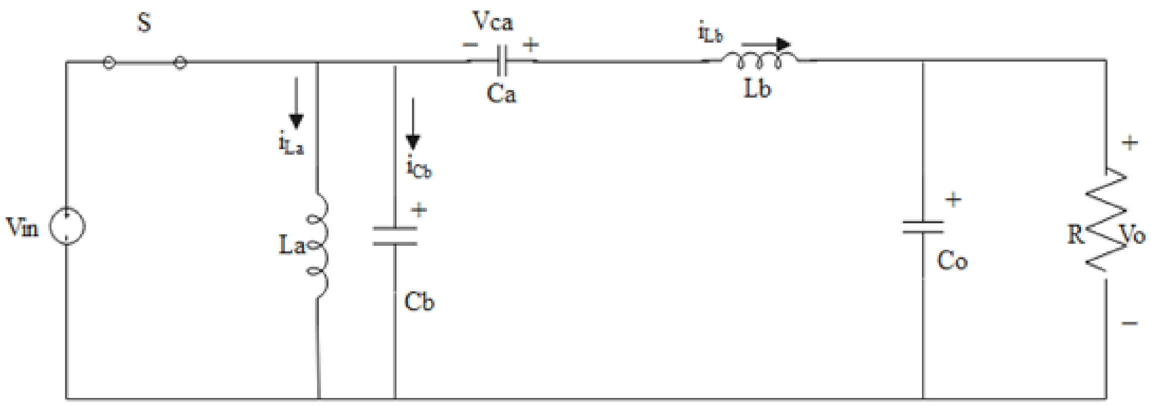

Fig 3.16: Circuit representation of POSLLC when switch is closed

If S is closed, diode D_a goes into conduction. D_b gets disconnected. Capacitor C_b is the voltage lifting capacitor. It lifts the capacitor voltage V_{ca} by supply voltage Vin

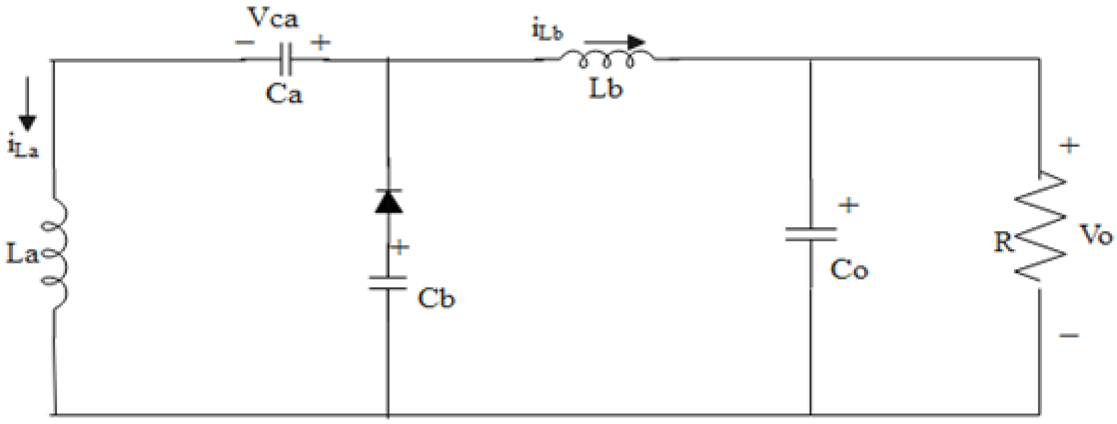

Fig 3.17: Circuit representation of POSLLC when S is open

When S opens, diode D_a gets disconnected. D_b goes into conduction.

3.4.1 Analysis of POSLLC circuit in CCM

Analysis of POSLLC is performed similar to positive output elementary Luo converter. Analyzing circuitry from fig 3.16 and figure 3.17,

Voltage across inductor L_a When S has been closed is V_{in} .When S opens the voltage is equal to $-(v_{ca} - v_{cb})$. Vavg across L_a is zero; this gives relationship between output voltage and supply for POSLLC given by equation (3.42)

$$V_o = \frac{1}{1-d} V_{in} \tag{3.42}$$

The gain of voltage transfer of POSLLC is given in equation (3.43)

$$M_E = \frac{V_o}{V_{in}} = \frac{1}{1-d} \tag{3.43}$$

For an ideal converter, the supply current and output current can be given below

$$I_{in} = \frac{1}{1-d} I_o \tag{3.44}$$

The charge on capacitor C_a when S closes is

$$Q_{Ca\,close} = dI_0T \tag{3.45}$$

The charge on capacitor C_a is given by

$$Q_{Ca\,open} = (1-d)I_{La}T \tag{3.46}$$

Average charge stored by capacitor in one cycle equals zero. Using eq (3.45) and (3.46), below mentioned equation can be derived.

$$I_{La} = \frac{d}{1-d} I_o \tag{3.47}$$

Current i_{La} increases when S closes and charged by supply voltage. Therefore, the current variation of i_{La} can be given by

$$\Delta i_{La} = \frac{dV_{in}T}{L_a} \tag{3.48}$$

Ratio for the current variation in inductor L_a is shown below:

$$\eta = \frac{\Delta i_{La}/2}{I_{La}} = \frac{TV_{in}}{2L_a I_s} = \frac{1}{2{M_E}^2}\frac{R}{fL_a} \tag{3.49}$$

Current i_{Lb} also increases When S has been closed and is charged by supply voltage. Therefore, the current variation of i_{Lb} can be given by

$$\Delta i_{Lb} = \frac{dV_{in}T}{L_b} \tag{3.50}$$

Ratio for the current variation in inductor L_b is shown below:

$$\varsigma = \frac{\Delta i_{Lb}/2}{I_{Lb}} = \frac{dTV_{in}}{2(1-d)L_b I_s} = \frac{d}{2M_E}\frac{R}{fL_b} \tag{3.51}$$

The variation in peak to peak v_{Ca} is given as:

$$\Delta v_{Ca} = \frac{Q_{Ca\,open}}{C_a} = \frac{(1-d)T}{C_a} \tag{3.52}$$

Ratio for the variation in capacitor voltage C_a is:

$$\rho = \frac{\Delta v_{ca}/2}{V_{Ca}} = \frac{d}{2}\frac{1}{fC_a R} \tag{3.53}$$

The variation in peak to peak v_{Cb} is given as:

$$\Delta v_{Cb} = \frac{Q_{Cb\,open}}{C_b} = \frac{dTI_{in}}{C_b} \tag{3.54}$$

Ratio for the variation in capacitor voltage C_b is:

$$\rho = \frac{\Delta v_{cb}/2}{V_{Cb}} = \frac{d}{2}\frac{I_{in}}{f C_a R} = \frac{M_E}{2 f C_b R} \tag{3.55}$$

Ratio for the variation in output voltage is:

$$\epsilon = \frac{\Delta v_o/2}{V_o} = \frac{d(1-d)T^2 V_{in}}{8 C_b L_b V_O} = \frac{dT^2}{8 M_E C_b L_b} \tag{3.56}$$

Fig 3.18 gives plot between gain of voltage transferand duty ratio for self-lift Luo converter.

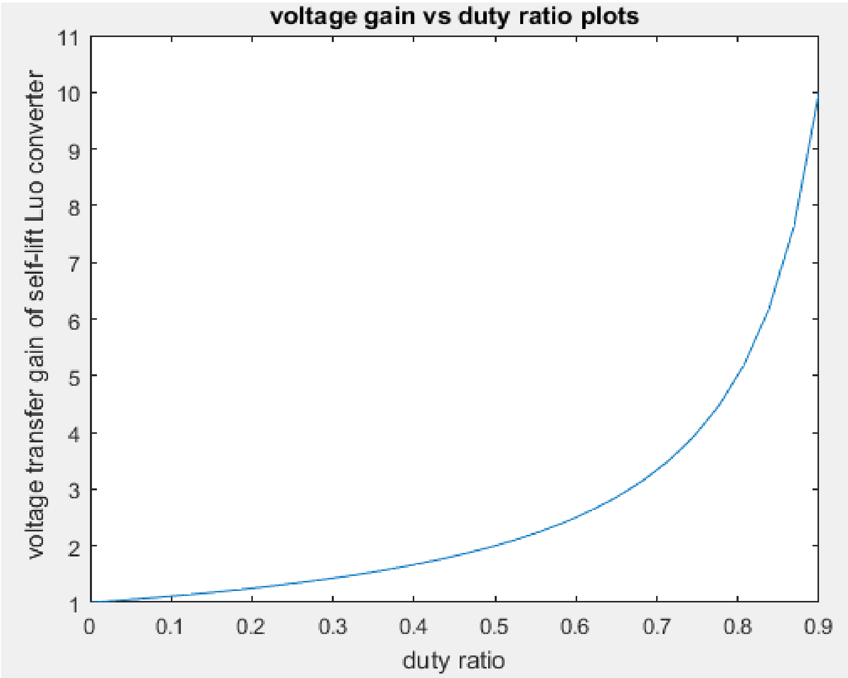

Fig 3.18: Gain of voltage transfervs duty for POSLLC

3.4.2 Analysis of POSLLC circuit in DCM

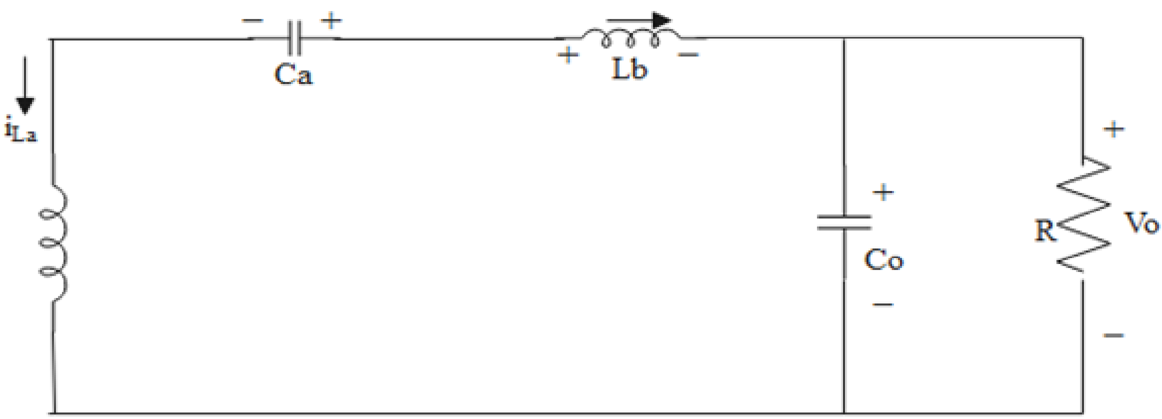

Fig 3.19: Circuit representation of POSLLC in DCM

Figure 3.19 shows the DCM operation of self-lift Luo converter. The diode current becomes zero when S has been opened before it has been closed again. Condition for DCM is that the ratio of variation of diode current must be greater than 1. This is given by equation (3.57).

$$\epsilon = \frac{\Delta i_D/2}{I_D} = \frac{dR}{{M_E}^2 2fL} = 1 \tag{3.57}$$

$$M_E = \sqrt{\frac{Rd}{2fL}} \tag{3.58}$$

Where, $L=L_a \parallel L_b$

3.5 POSITIVE OUTPUT SUPER-LIFT LUO CONVERTER

The super-lift technique of increasing the gain of voltage transferis more effective than voltage lift. Super-lift technique provides increment of voltage in stages in geometric progression; therefore the voltage gain can attain high values. Super-lift Luo converter is designed by implementing the super-lift technique on elementary Luo converter [12], [16]. The circuit representation of super-lift Luo converter is in fig 3.20.

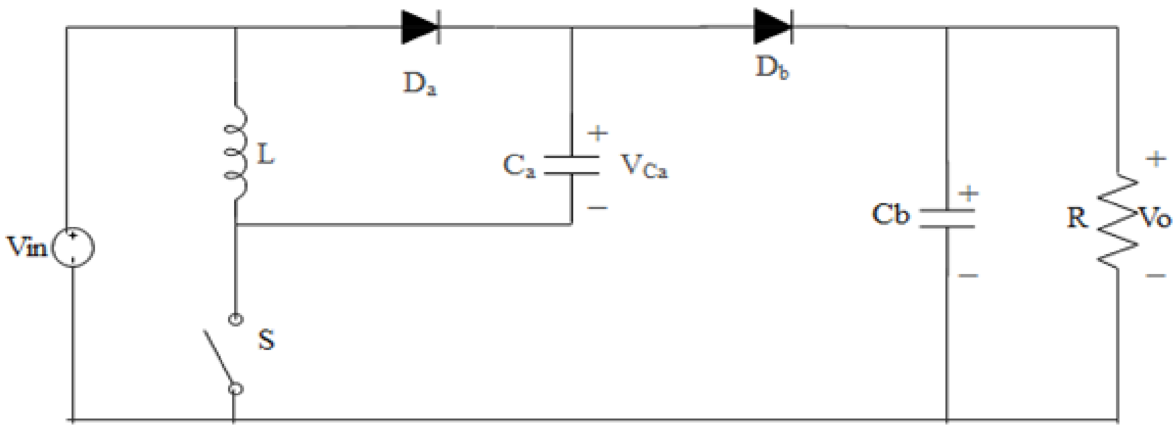

Fig 3.20: Circuitry of POSLC

Figure 3.21 and 3.22 shows the circuit representation for POSLC when S has been closed and has been opened respectively.

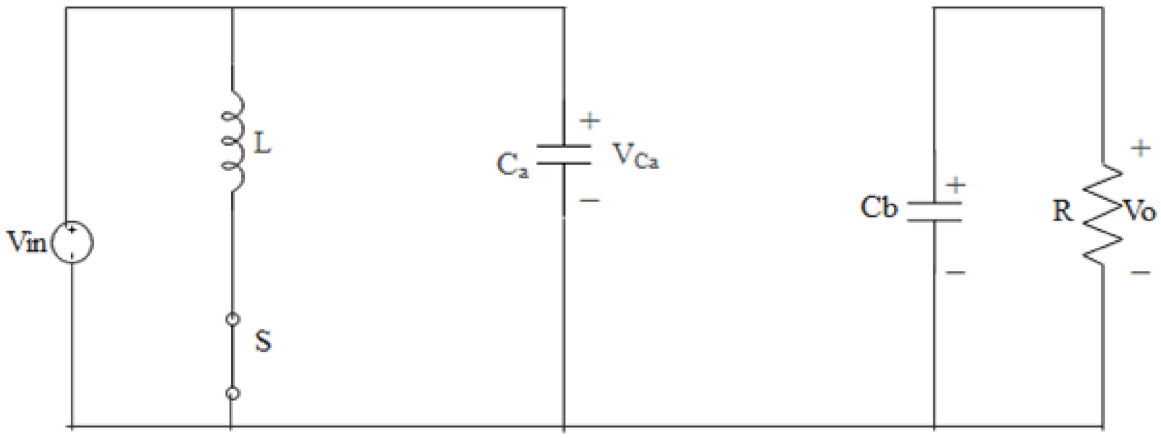

Fig 3.21: Circuitry of POSLC when switch is closed

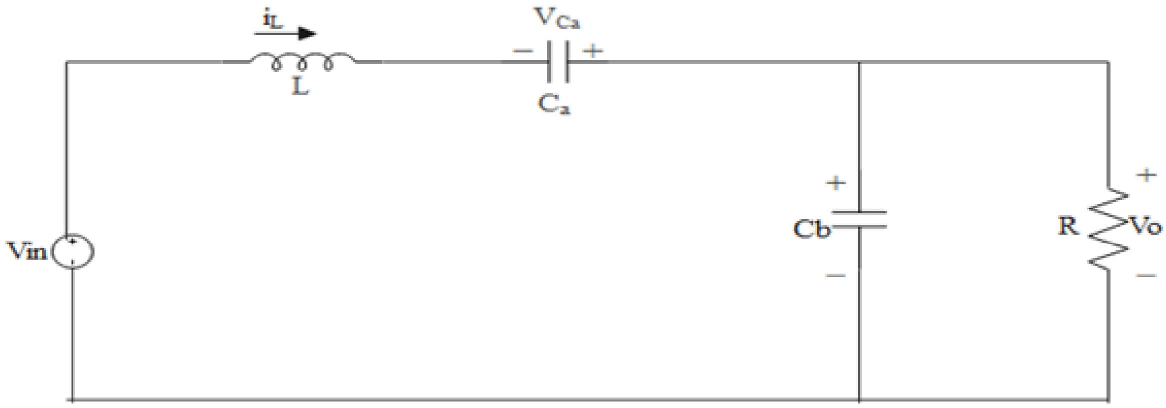

Fig 3.22: Circuitry of POSLC when switch is opened

When S has been closed (fig 3.21), D_a gets into conduction and V_{ca} across C_a rises to V_{in} in less time period. Therefore, the diode D_b gets blocked. Current from supply runs through L and $C_{a.}$

When S has been opened (fig 3.22), D_a gets blocked and D_b goes into conduction. L supplies current to C_a and $C_{b.}$

3.5.1 Analysis of POSLC circuit in CCM

Current in inductor L when S has been closed rises along V_{in}. When S has been opened, current falls along – (V_o-2V_{in}). Average voltage across L should be nill, therefore we get relationship between supply and output in a super-lift Luo converter.

$$V_o = \frac{2-d}{1-d} V_{in} \tag{3.59}$$

The gain of voltage transfer for POSLC is

$$M_E = \frac{V_o}{V_{in}} = \frac{2-d}{1-d} V_{in} \tag{3.60}$$

The inductance L is considered large enough to say that i_L is equal to average current I_L

From the circuit analysis of figure 3.21 and 3.22, the supply current is given as (I_L +$i_{c\text{-}on}$) when S has been closed and I_L when S has been opened. Average supply current given as

$$I_s = (2-d)I_L \tag{3.61}$$

The current variation of i_L can be given by

$$\Delta i_L = \frac{dV_{in}T}{L} \tag{3.62}$$

Ratio for the current variation in inductor L is shown below:

$$\varsigma = \frac{\Delta i_L/2}{I_L} = \frac{dTV_{in}}{LI_L} = \frac{d(1-d)^2}{2(2-d)} \frac{R}{fL} \tag{3.63}$$

Since,

$$\frac{V_{in}}{I_s} = \left(\frac{(1-d)}{(2-d)}\right)^2 R \tag{3.64}$$

The voltage variation of v_{cb} can be given by

$$\Delta v_o = \frac{\Delta v_o}{C_b} = \frac{dV_oT}{C_bR} \tag{3.65}$$

Ratio for the current variation in inductor L is shown below:

$$\epsilon = \frac{\Delta v_o/2}{V_o} = \frac{d}{2RC_bf} \tag{3.66}$$

Figure 3.23 shows the plot between gain of voltage transfer and duty ratio of super-lift Luo converter.

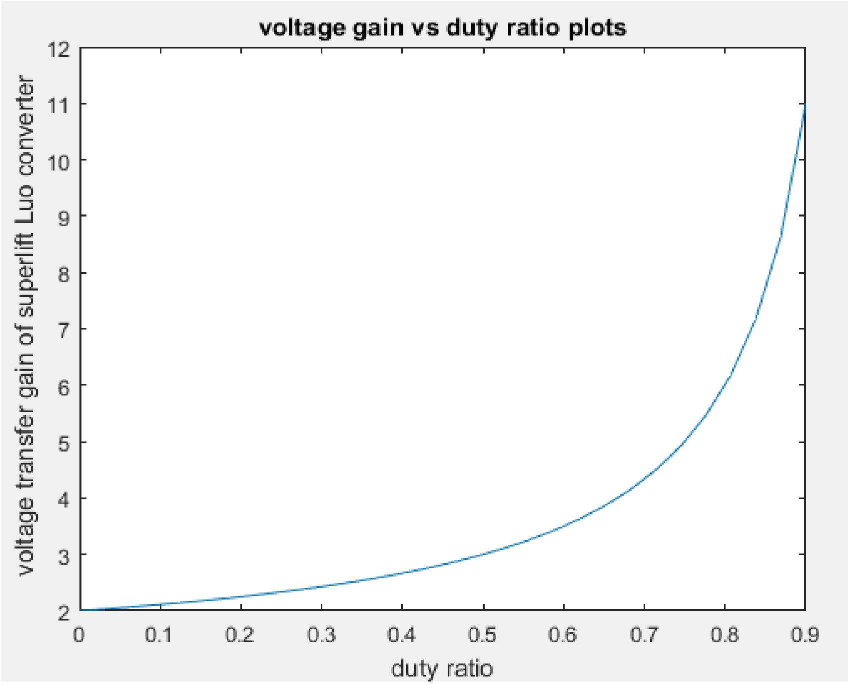

Fig 3.23: Gain of voltage transfervs duty ratio for POSLC

3.5.2 Analysis of POSLC circuit in DCM

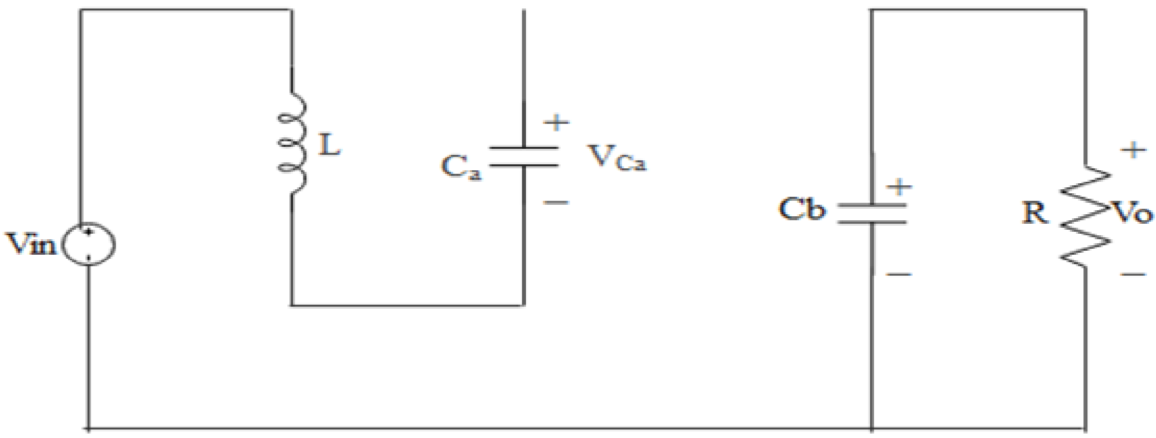

Fig 3.24: Circuitry of POSLC operating in DCM

The gain of voltage transfer in DCM of POSLC is given by equation (3.67)

$$M_E = \frac{V_O}{V_{in}} = \frac{R\xi d(1-d)}{2fL_1} \tag{3.67}$$

Where, ξ is the filling efficiency

Filling efficiency is defined as:

$$\xi = \frac{t_1 - dT}{(1-d)T} \tag{3.68}$$

This means after a time lapse of $\xi(1-d)T$ from the instance when S has been opened, diode current will become zero.

3.6 NEGATIVE OUTPUT ULTRA-LIFT LUO CONVERTER

Ultra-lift tactic provides even higher gain of voltage transfer than voltage lift and super-lift techniques [12],[19]. Increment of voltage is in stages in geometric progression. NOULLC is presented in fig 3.25.

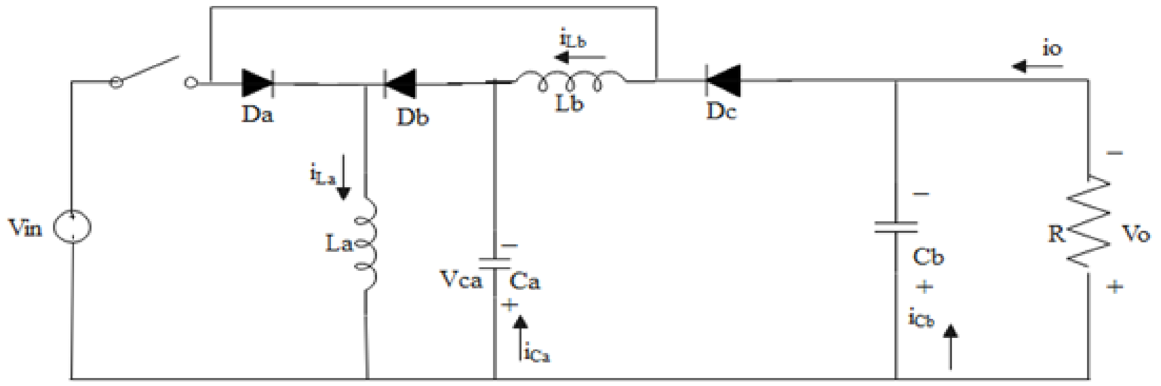

Fig 3.25: Circuitry of NOULLC

Figure 3.26 and 3.27 show the circuit representation of NOULLC when S has been closed and opened respectively.

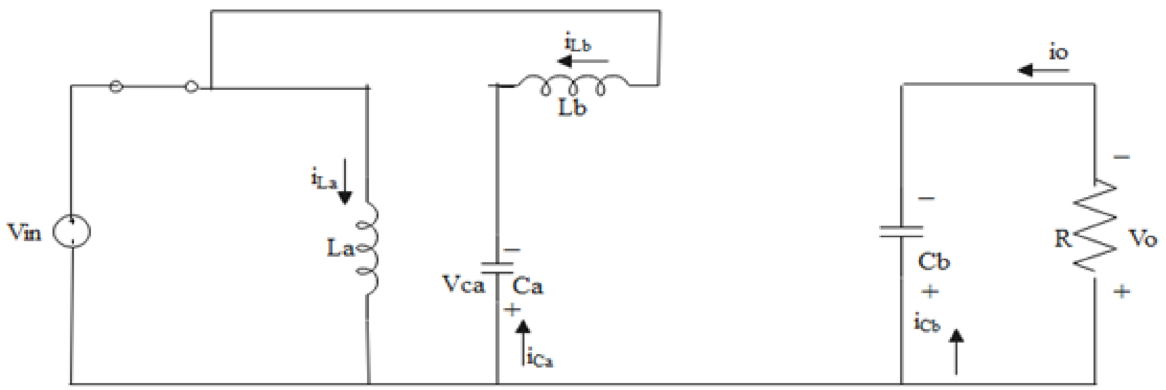

Fig 3.26: Circuitry of NOULLC when switch is closed

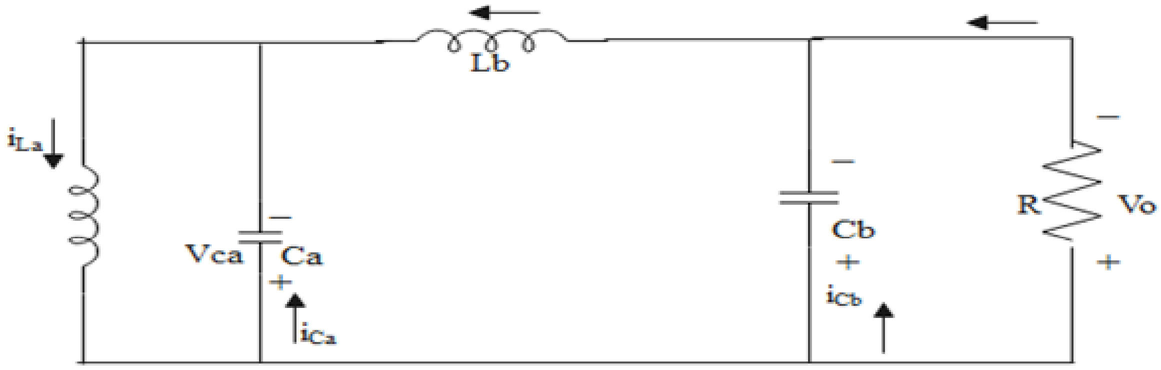

Fig 3.27: Circuitry of NOULLC when switch is opened

3.6.1 Analysis of NOULLC circuit in CCM

On referring the figures 3.26 and 3.27, the current i_{La} increases with slope $+\frac{V_{in}}{L_a}$ when S has been closed and falls with slope $-\frac{V_{in}}{L_a}$ when S has been opened. Increment and decrement in i_l equals for time T given as:

$$dT\frac{V_{in}}{L_a} = (1-d)T\frac{V_{in}}{L_a} \tag{3.69}$$

Thus,

$$V_{ca} = \frac{d}{1-d}V_{in} \tag{3.70}$$

The current i_{Lb} increases with slope $\frac{V_{in}-V_{ca}}{L_b}$ when S has been closed and decreases with slope $\frac{V_{ca}-V_o}{L_b}$ When S has been opened. The increment and decrement in inductor current is equal for time T. This can be showed as:

$$dT\frac{V_{in}+V_{ca}}{L_b} = (1-d)T\frac{V_o-V_{ca}}{L_b} \tag{3.71}$$

Thus,

$$V_o = \frac{d(2-d)}{(1-d)^2}V_{in} \tag{3.72}$$

From equation (3.72), it can be concluded that ultra-lift Luo converter are very sensitive to duty ratio. A slight change in duty can cause large changes in voltage at output.

The gain of voltage transfer of NOULLC is given as:

$$M_E = \frac{V_O}{V_{in}} = \frac{d(2-d)}{(1-d)^2} \tag{3.73}$$

The plot between gains of voltage transfer and duty ratio for ultra-lift Luo converter is given in figure 3.30. It shows small gains when duty is small, but as duty rises, the gain of voltage transfer increases drastically.

The plot between gain of voltage transfer and duty ratio for NOULLC is given in fig 3.28. Small gains when duty is less is shown. With rise in duty, gain of voltage transfer increases drastically.

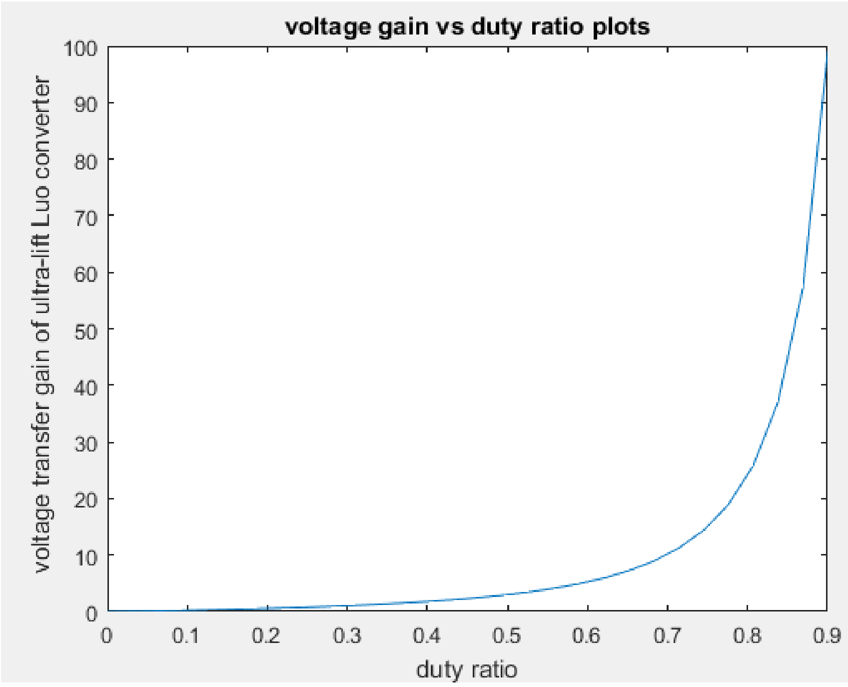

Fig 3.28 Gain of voltage transfer vs duty ratio of NOULLC

Relationship of supply and output average current of NOULLC is in equation (3.74)

$$I_o = \frac{(1-d)^2}{d(2-d)} I_{in} \tag{3.74}$$

The relation of I_{La} & I_{Lb} is given in equation (3.75)

$$I_{Lb} = (1-d) I_{La} \tag{3.75}$$

The inductor current variation in L_a is:

$$\Delta i_{La} = dT \frac{V_{in}}{L_a} \tag{3.76}$$

The ratio of variation of I_{La} is given as:

$$\xi_{La} = \frac{(1-d)^4 TR}{2(2-d) f L_a} \tag{3.77}$$

The inductor current variation is

$$\Delta i_{Lb} = dT\frac{V_{in}}{(1-d)L_a} \tag{3.78}$$

The ratio of variation of I_{La} is given as:

$$\xi_{Lb} = \frac{(1-d)^2 TR}{2(2-d)fL_b} \tag{3.79}$$

The capacitor voltage v_{ca} variation is

$$\Delta v_{ca} = dT\frac{I_o}{(1-d)C_a} \tag{3.80}$$

The ratio of variation of v_{ca} is given as:

$$\sigma_1 = \frac{\Delta V_{Ca}/2}{V_{Ca}} = \frac{d(2-d)T}{2f(1-d)^2 C_a R} \tag{3.81}$$

The capacitor voltage v_{cb} variation is

$$\Delta v_{cb} = dT\frac{I_o}{C_b} \tag{3.82}$$

The ratio of variation of v_{ca} is given as:

$$\sigma_2 = \frac{\Delta V_{Cb}/2}{V_{Cb}} = \frac{d}{2fC_b R} \tag{3.83}$$

3.6.2 Analysis of NOULLC circuit in DCM

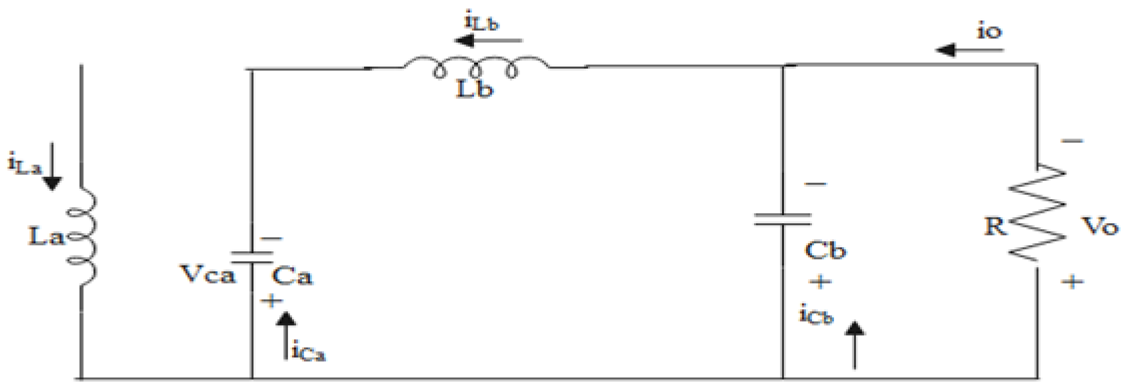

Fig 3.29 Circuitry of NOULLC in DCM

The condition for CCM is given as

$$\xi_1 \leq 1 \tag{3.84}$$

The condition for DCM is given as

$$\xi_1 \geq 1 \tag{3.85}$$

Boundary of CCM and DCM is in equation (3.86)

$$G = \frac{d(1-d)^2}{2}\frac{R}{fL_a} \tag{3.86}$$

Current i_{La} increases having slope $+\frac{V_{in}}{L_a}$ When S has been closed and decreases with slope $-\frac{V_{ca}}{L_a}$ when S opened. i_{L1} reduces to zero earlier than time T in DCM. Increment in inductor current equals decrement in steady state for the whole period of time T. The relation obtained is:

$$dT\frac{V_{in}}{L_a} = (1-d)\,\xi\,T\frac{V_{ca}}{L_a} \tag{3.87}$$

Thus,

$$V_{ca} = \frac{d}{(1-d)\xi}V_{in} \tag{3.88}$$

Current i_{Lb} increases having slope $\frac{V_{in}-V_{ca}}{L_b}$ When S has been closed and decreases with slope $\frac{V_{ca}-V_o}{L_b}$ when S opened. The increment in inductor current equals decrement in steady state for whole period of time T. The relation obtained is:

$$V_o = \frac{d(2-d)}{\xi(1-d)^2}V_{in} \tag{3.89}$$

The gain of voltage transfer in DCM operation is:

$$M_E = \frac{V_O}{V_{in}} = \frac{d(2-d)}{\xi(1-d)^2} \tag{3.90}$$

3.7 CONCLUSION

The analysis of a few topologies of dc converters was done in previous sections. The gain of voltage transfer of these converters is increased using voltage lift, super-lift and ultra-lift technique. Table 3.1 provides a glance over the gain of voltage transfer and is analyzed and a conclusion can be reached.

Table 3.1 Gain of voltage transfer for DC-DC converter topologies

	Gain of voltage transfer in CCM. (vo/vin)

Duty ratio	**Buck converter**	**POELC**	**POSLLC**	**POSLC**	**NOULLC**
0.1	0.1	0.11	1.11	2.11	0.23
0.3	0.3	0.42	1.42	2.42	1.04
0.5	0.5	1	2	3	3
0.7	0.7	2.33	3.33	4.33	10.11
0.9	0.9	9	10	11	99

From Table 3.1, we can observe that for buck converter the gain of voltage transfer is equal to duty ratio. It follows a linear curve as was evident from figure 3.9. Elementary Luo converters step down the output voltage for lower values of duty ratio but provide boost to output voltage for higher duty values. Self-lift Luo converters provider higher gain to the t voltage at output. As duty increases, higher gain of voltage transfer is achieved. It increases voltage in stages in arithmetic progression. POSLC have provided even higher gain than POSLLC. It increases voltage at output from one stage to other in geometric progression. Ultra-lift Luo converters perform step down operation at lower values of duty cycle. However, as duty increase, the gain of voltage transfer rises drastically. Higher values of duty ratio, the voltage gain is almost hundred times, which is higher than any converter topology. But this also makes the ultra-lift Luo converters highly sensitive to duty ratio. Small deviation in duty cycle brings huge changes in voltage. This makes controlling of NOULLC complicated. Luo converters are applied in industrial applications when high voltages are required. Control of dc converters, has been considered in following section.

CHAPTER 4

STATE SPACE MODELING OF DC-DC CONVERTERS

4.1 INTRODUCTION

Modeling of dc converters is mechanism of representing converter in a mathematical framework based on observation and analyzing its significant characteristics for a particular application. Modeling of converters is an essential step required to design controllers for the converter. A relation between converter's inputs and outputs with elements of the circuits can be derived from the modeling.

In [21], [22] two modeling methods are discussed. State space model provides a description of all power levels for any converter. State space equations of the converters are utilized for deriving this model under different switching conditions. State space averaging implemented in obtaining overall model of converter. Second method of averaging technique built upon overall behavior of circuit. It provides a single model for converter. In the dissertation, state space modeling of dc converters operating in CCM is performed. A flowchart representing the steps to realize state space model in fig 4.1.

Dc converters being non-linear circuits. Applying linear controllers on these, linearized model has to be developed. Small signal model gives linearized equivalence to converter. It is obtained by adding small perturbation to state space variables, inputs and outputs to converters. A generalized method showing modeling of converter using state space is described in the next section.

4.2 STATE SPACE MODEL OF DC-DC CONVERTERS

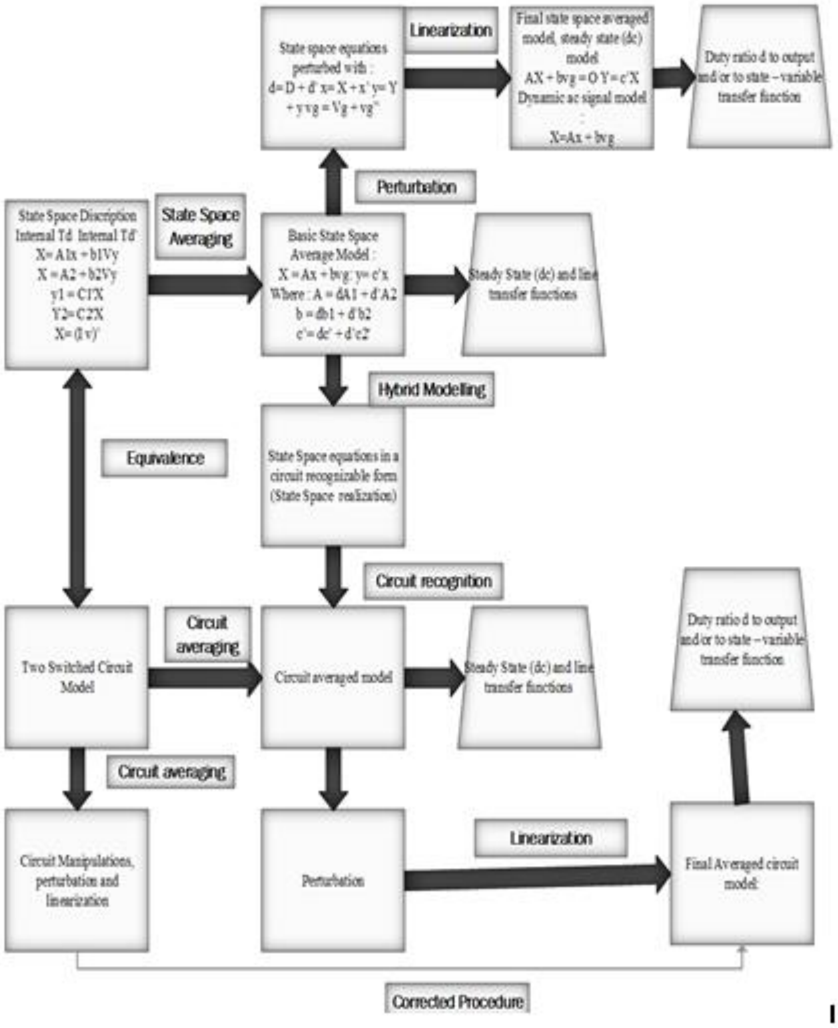

Figure 4.1 Block diagram for state space modeling of power converters

From figure 4.1, a state space description of the converters is formed both when S has been closed and when S has been opened. State space variables give a set of linear independent models. In converters, i_L and v_C are considered as state space variables (x). These are energy storing elements and determine the order of the converter. The state space is as it is depicted by

When switch has been closed — When switch has been opened

$$\dot{x} = A_a x + B_a v_{in} \qquad \dot{x} = A_b x + B_b v_{in}$$

$$y_a = C_a x \qquad y_b = C_b x$$

A_a and A_b give state matrix, B_a and B_b give input matrix, C_a and C_b are output matrix.

The individual state space models for the converter are merged to form a single state space model for switching time T. State space averaging method is used to do so. It can be shown as:

$$\dot{x} = d(A_a x + B_a v_{in}) + (1 - d)(A_b x + B_b v_{in})$$

$$y = d(y_a) + (1 - d)(y_b) => d(C_a x) + (1 - d)(C_b x) \quad (4.1)$$

Equation (4.1) is expressed as

$$\dot{x} = Ax + Bvin$$

$$y = Cx \quad (4.2)$$

Where, $A = A_a d + A_b(1 - d)$

$$B = B_a d + B_b(1 - d)$$

$$C = C_a d + C_b(1 - d)$$

The above mentioned modeling is steady state modeling. Linearized modeling is obtained by adding a small perturbation to the state space variables, supply, load voltage, duty of converter. Controlling of output is provided with respect to duty in this dissertation.

$$(\dot{x} + \dot{\hat{x}}) = A(x + \hat{x}) + B(vin + \widehat{v_{in}})$$

$$(y + \hat{y}) = C(x + \hat{x}) \quad (4.3)$$

Steady state modeling gives dc model of plant defined in equation (4.2). Separation of dc model from equation (4.3) gives the dynamic or ac model of the plant.

$$\dot{\hat{x}} = A\hat{x} + B\widehat{v_{in}}$$

$$\hat{y} = C\hat{x} \quad (4.4)$$

4.3 SMALL SIGNAL MODEL OF DC-DC CONVERTERS

Approximations in linearized model are deviations from the steady state approach. It's very small as compared to steady state values.. Second order nonlinear terms are not considered while modeling and steady state (dc) & dynamic terms (ac) were separated.

This can be shown in equation (4.5).

$$\dot{\hat{x}} = A\hat{x} + B_a\widehat{v_{in}} + B_b\hat{d}$$

$$\hat{y} = C\hat{x} + (C_a^T - C_b^T)X \quad (4.5)$$

$$B_2 = (A_a - A_b)X + (B_a - B_b)vin \quad (4.6)$$

$$X = A^{-1}B_b\, vin \quad (4.7)$$

4.4 STATE SPACE ANALYSIS OF BUCK CONVERTER

For a buck converter, i_l and v_c are state variables. v_o is voltage at output. Circuitry analysis given in fig (3.1),(3.2) and (3.3), helps in deriving state space equations by applying KVL and KCL. The converter working is in CCM.

When S has been closed,

$$v_L = V_{in} - V_0 \quad (4.8)$$

$$L\frac{di_L}{dt} = V_{in} - v_c \quad (4.9)$$

$$=> \frac{di_L}{dt} = \frac{V_{in}}{L} - \frac{V_c}{L} \quad (4.10)$$

$$i_c = i_l - i_0 \quad (4.11)$$

$$C\frac{dv_c}{dt} = i_L - \frac{v_c}{R} \quad (4.12)$$

$$=> \frac{dv_c}{dt} = \frac{i_L}{C} - \frac{v_c}{RC} \quad (4.13)$$

This is rewritten as

$$\begin{matrix} \dot{\iota_L}(t) \\ \dot{v_c}(t) \end{matrix} = \begin{pmatrix} 0 & -\frac{1}{L} \\ \frac{1}{C} & -\frac{1}{RC} \end{pmatrix}\begin{pmatrix} i_l(t) \\ v_c(t) \end{pmatrix} + \begin{pmatrix} \frac{1}{L} \\ 0 \end{pmatrix} v_{in} \quad (4.14)$$

When S has been opened,

$$v_l = -V_0 \quad (4.15)$$

$$L\frac{di_L}{dt} = -V_c \quad (4.16)$$

$$=> \quad \frac{di_L}{dt} = \quad -\frac{V_c}{L} \quad (4.17)$$

$$i_c = i_l - i_0 \quad (4.18)$$

$$C\frac{dv_c}{dt} = i_L - \frac{v_c}{R} \quad (4.19)$$

$$=> \frac{dv_c}{dt} = \frac{i_L}{C} - \frac{v_c}{RC} \quad (4.20)$$

This is rewritten as

$$\begin{matrix}\dot{\iota_L}(t) \\ \dot{v_c}(t)\end{matrix} = \begin{pmatrix} 0 & -\frac{1}{L} \\ \frac{1}{C} & -\frac{1}{RC} \end{pmatrix}\begin{pmatrix} i_l(t) \\ v_c(t) \end{pmatrix} + \begin{pmatrix} \frac{1}{L} \\ 0 \end{pmatrix} v_{in} \quad (4.21)$$

The state space average equations for a Buck converter are:

$$=> \frac{di_L}{dt} = \quad \frac{dV_{in}}{L} - \frac{V_c}{L} \quad (4.22)$$

$$=> \frac{dv_c}{dt} = \frac{i_L}{C} - \frac{v_c}{RC} \quad (4.23)$$

The average state space matrix of buck is given as

$$\begin{matrix}\dot{\iota l}(t) \\ \dot{v}c(t)\end{matrix} = \begin{pmatrix} 0 & -\frac{1}{L} \\ \frac{1}{C} & -\frac{1}{RC} \end{pmatrix}\begin{pmatrix} i_l(t) \\ v_c(t) \end{pmatrix} + \begin{pmatrix} \frac{V_{in}d}{L} & 0 \end{pmatrix} \quad (4.24)$$

$$=> \begin{matrix}\dot{x}1(t) \\ \dot{x}2(t)\end{matrix} = \begin{pmatrix} 0 & -\frac{1}{L} \\ \frac{1}{C} & -\frac{1}{RC} \end{pmatrix}\begin{pmatrix} i_l(t) \\ v_c(t) \end{pmatrix} + \begin{pmatrix} \frac{V_{in}d}{L} & 0 \end{pmatrix} \quad (4.25)$$

4.4.1 Small signal model of buck converter

Linearized model of buck is acquired by adding perturbations to state space vectors, V_{in}, d. This is done by substituting the following variables into the state space model.

$$i_l = I_L + \hat{\imath_l}$$

$$v_c = V_c + \hat{v_c}$$

$$v_{in} = V_{in} + \widehat{v_{in}}$$

$$d = D + \hat{d}$$

Thus the linearized model of buck from large signal model is:

When S has been closed ,

$$\frac{d(I_L + \hat{\imath_l})}{dt} = \frac{V_{in} + \widehat{v_{in}}}{L} - \frac{V_c + \hat{v_c}}{L} \tag{4.26}$$

$$\frac{d(V_c + \hat{v_c})}{dt} = \frac{I_L + \hat{\imath_l}}{C} - \frac{V_c + \hat{v_c}}{RC} \tag{4.27}$$

When S has been opened,

$$\frac{d(I_L + \hat{\imath_l})}{dt} = -\frac{V_c + \hat{v_c}}{L} \tag{4.28}$$

$$\frac{d(V_c + \hat{v_c})}{dt} = \frac{I_L + \hat{\imath_l}}{C} - \frac{V_c + \hat{v_c}}{RC} \tag{4.29}$$

The small signal state space average equations of buck are”

$$\frac{d(I_L + \hat{\imath_l})}{dt} = \frac{(D + \hat{d})(V_{in} + \widehat{v_{in}})}{L} - \frac{V_c + \hat{v_c}}{L} \tag{4.30}$$

$$\frac{d(V_c + \hat{v_c})}{dt} = \frac{I_L + \hat{\imath_l}}{C} - \frac{V_c + \hat{v_c}}{RC} \tag{4.31}$$

Eliminating all the nonlinear terms like second order terms and not considering the steady state (dc) terms, we get the dynamic (ac) equation of converter.

$$\frac{d(\hat{\imath_l})}{dt} = \frac{D}{L}\widehat{v_{in}} + \frac{V_{in}}{L}\hat{d} - \frac{1}{L}\hat{v_c} \tag{4.32}$$

$$\frac{d(\widehat{v_c})}{dt} = \frac{1}{C}\widehat{\iota_l} - \frac{1}{RC}\ \widehat{v_c} \tag{4.33}$$

State Space Matrix of the small signal model for buck becomes,

$$\begin{pmatrix} \widehat{\dot{x_1}} \\ \widehat{\dot{x_2}} \end{pmatrix} = \begin{pmatrix} 0 & -\frac{1}{L} \\ \frac{1}{C} & -\frac{1}{RC} \end{pmatrix} \begin{pmatrix} \widehat{\iota_l} \\ \widehat{v_c} \end{pmatrix} + \begin{pmatrix} \frac{D}{L} & \frac{V_{in}}{L} \\ 0 & 0 \end{pmatrix} (\widehat{v_{\iota n}} \quad \hat{d}) \tag{4.34}$$

4.5 STATE SPACE ANALYSIS OF ELEMENTARY LUO CONVERTER

For elementary Luo converter, inductor current i_{la} , i_{lb} and capacitor voltage v_{ca} , v_{cb} are the state variables. v_o is voltage at load. Circuitry analysis of POELC given in fig (3.10), (3.11) , (3.12), succeeding state space equations may be calculated by combing KVL and KCL. Working of converter is in CCM.

State space variables for this converter can be defined as:

$x_1 = i_{la}$

$x_2 = i_{lb}$

$x_3 = v_{ca}$

$x_4 = v_{Cb}$

When S has been closed :

State space equations is:

$$\dot{x}_1 = \frac{v_{in}}{L_a} \tag{4.35}$$

$$\dot{x}_2 = \frac{v_{in}}{L_b} + \frac{x_3}{L_b} - \frac{x_4}{L_b} \tag{4.36}$$

$$\dot{x}_3 = -\frac{x_2}{C_a} \tag{4.37}$$

$$\dot{x}_4 = \frac{x_2}{C_b} - \frac{x_4}{RC_b} \tag{4.38}$$

This is rewritten as

$$\begin{pmatrix} \dot{x}_1 \\ \dot{x}_2 \\ \dot{x}_3 \\ \dot{x}_4 \end{pmatrix} = \begin{pmatrix} 0 & 0 & 0 & 0 \\ 0 & 0 & \frac{1}{L_b} & -\frac{1}{L_b} \\ 0 & \frac{-1}{C_a} & 0 & 0 \\ 0 & \frac{1}{C_b} & 0 & -\frac{1}{RC_b} \end{pmatrix} \begin{pmatrix} x_1 \\ x_2 \\ x_3 \\ x_4 \end{pmatrix} + \begin{pmatrix} \frac{1}{L_a} \\ \frac{1}{L_b} \\ 0 \\ 0 \end{pmatrix} v_{in} \tag{4.39}$$

When S has been opened:

State space equation is:

$$\dot{x}_1 = -\frac{x_3}{L_a} \tag{4.40}$$

$$\dot{x}_2 = -\frac{x_4}{L_b} \tag{4.41}$$

$$\dot{x}_3 = \frac{x_1}{C_a} \tag{4.42}$$

$$\dot{x}_4 = \frac{x_2}{C_b} - \frac{x_4}{RC_b} \tag{4.43}$$

This is rewritten as

$$\begin{pmatrix} \dot{x}_1 \\ \dot{x}_2 \\ \dot{x}_3 \\ \dot{x}_4 \end{pmatrix} = \begin{pmatrix} 0 & 0 & -\frac{1}{L_a} & 0 \\ 0 & 0 & 0 & -\frac{1}{L_b} \\ 0 & \frac{-1}{C_a} & 0 & 0 \\ 0 & \frac{1}{C_b} & 0 & -\frac{1}{RC_b} \end{pmatrix} \begin{pmatrix} x_1 \\ x_2 \\ x_3 \\ x_4 \end{pmatrix} + \begin{pmatrix} \frac{1}{L_a} \\ \frac{1}{L_b} \\ 0 \\ 0 \end{pmatrix} v_{in} \tag{4.44}$$

The state space average equations for elementary luo converter are:

$$\dot{x}_1 = \frac{v_{in}d}{L_a} - \frac{(1-d)}{L_a} x_3 \tag{4.45}$$

$$\dot{x}_2 = \frac{v_{in}d}{L_b} + \frac{d}{L_b} x_3 - \frac{x_4}{L_b} \tag{4.46}$$

$$\dot{x}_3 = \frac{(1-d)}{C_a} x_1 + \frac{d}{C_a} x_2 \tag{4.47}$$

$$\dot{x}_4 = \frac{x_2}{C_b} - \frac{x_4}{RC_b} \tag{4.48}$$

This is rewritten as

$$\begin{pmatrix} \dot{x}_1 \\ \dot{x}_2 \\ \dot{x}_3 \\ \dot{x}_4 \end{pmatrix} = \begin{pmatrix} 0 & 0 & -\frac{(1-d)}{L_a} & 0 \\ 0 & 0 & \frac{d}{L_b} & -\frac{1}{L_b} \\ \frac{(1-d)}{C_a} & \frac{d}{C_a} & 0 & 0 \\ 0 & \frac{1}{C_b} & 0 & -\frac{1}{RC_b} \end{pmatrix} \begin{pmatrix} x_1 \\ x_2 \\ x_3 \\ x_4 \end{pmatrix} + \begin{pmatrix} \frac{1}{L_a} \\ \frac{1}{L_b} \\ 0 \\ 0 \end{pmatrix} v_{in} \tag{4.49}$$

4.5.1 Small signal model of elementary Luo converter

Small signal model of POELC is caluclated by adding perturbations to state space vectors, V_{in}, d. This is done by substituting the following variables into the state space model.

$$i_{la} = I_{La} + \widehat{\imath_{la}}$$

$$i_{lb} = I_{Lb} + \widehat{\imath_{lb}}$$

$$v_{ca} = V_{ca} + \widehat{v_{ca}}$$

$$v_{cb} = V_{cb} + \widehat{v_{cb}}$$

$$v_{in} = V_{in} + \widehat{v_{in}}$$

$$d = D + \hat{d}$$

When switch is closed

State space equation is:

$$\frac{d(x_1 + \widehat{x_1})}{dt} = \frac{V_{in} + \widehat{v_{in}}}{L_a} \tag{4.50}$$

$$\frac{d(x_2+\widehat{x_2})}{dt}=\frac{V_{in}+\widehat{v_{in}}}{L_b}+\frac{x_3+\widehat{x_3}}{L_b}-\frac{x_4+\widehat{x_4}}{L_b} \tag{4.51}$$

$$\frac{d(x_3+\widehat{x_3})}{dt}=-\frac{x_2+\widehat{x_2}}{C_a} \tag{4.52}$$

$$\frac{d(x_4+\widehat{x_4})}{dt}=\frac{x_2+\widehat{x_2}}{C_b}-\frac{x_4+\widehat{x_4}}{RC_b} \tag{4.53}$$

When S has been opened:

State space equation is:

$$\frac{d(x_1+\widehat{x_1})}{dt}=\frac{x_3+\widehat{x_3}}{L_a} \tag{4.54}$$

$$\frac{d(x_2+\widehat{x_2})}{dt}=-\frac{x_4+\widehat{x_4}}{L_b} \tag{4.55}$$

$$\frac{d(x_3+\widehat{x_3})}{dt}=\frac{x_1+\widehat{x_1}}{C_a} \tag{4.56}$$

$$\frac{d(x_4+\widehat{x_4})}{dt}=\frac{x_2+\widehat{x_2}}{C_b}-\frac{x_4+\widehat{x_4}}{RC_b} \tag{4.57}$$

The state space average equations for elementary luo converter are:

$$\frac{d(x_1+\widehat{x_1})}{dt}=\frac{V_{in}+\widehat{v_{in}}}{L_a}\left(D+\hat{d}\right)+\frac{\left(1-D-\hat{d}\right)}{L_a}(x_3+\widehat{x_3}) \tag{4.58}$$

$$\frac{d(x_2+\widehat{x_2})}{dt}=\frac{V_{in}+\widehat{v_{in}}}{L_b}(D+\hat{d})+\frac{(x_3+\widehat{x_3})}{L_b}(D+\hat{d})-\frac{x_4+\widehat{x_4}}{L_b} \tag{4.59}$$

$$\frac{d(x_3+\widehat{x_3})}{dt}=\frac{\left(1-D-\hat{d}\right)}{C_a}(x_1+\widehat{x_1})+\frac{d(D+\hat{d})}{C_a}(x_2+\widehat{x_2}) \tag{4.60}$$

$$\frac{d(x_4+\widehat{x_4})}{dt}=\frac{(x_2+\widehat{x_2})}{C_b}-\frac{x_4+\widehat{x_4}}{RC_b} \tag{4.61}$$

Eliminating all the nonlinear terms like 2nd order & not considering steady state terms, we get the dynamic (ac) of converter.

State Space Matrix of small signal model of POELC becomes,

This is rewritten as

$$\begin{pmatrix} \dot{\hat{x}}_1 \\ \dot{\hat{x}}_2 \\ \dot{\hat{x}}_3 \\ \dot{\hat{x}}_4 \end{pmatrix} = \begin{pmatrix} 0 & 0 & \frac{(1-D)}{L_a} & 0 \\ 0 & 0 & \frac{D}{L_b} & -\frac{1}{L_b} \\ \frac{(1-D)}{C_a} & \frac{D}{C_a} & 0 & 0 \\ 0 & \frac{1}{C_b} & 0 & -\frac{1}{RC_b} \end{pmatrix} \begin{pmatrix} \hat{x}_1 \\ \hat{x}_2 \\ \hat{x}_3 \\ \hat{x}_4 \end{pmatrix} + \begin{pmatrix} \frac{D}{L_a} & \frac{V_{in}+x_3}{L_a} \\ \frac{D}{L_b} & \frac{V_{in}+x_4}{L_b} \\ 0 & \frac{-(x_1+x_2)}{C_a} \\ 0 & 0 \end{pmatrix} (\widehat{V}_{in} \quad \hat{d}) \tag{4.62}$$

4.6 STATE SPACE ANALYSIS OF SELF-LIFT LUO CONVERTER

For POSLLC, inductor current i_{la} , i_{lb} and capacitor voltage v_{ca} , v_{cb} are the state variables. v_o is voltage at output. Circuital analysis of POSLLC given in fig (3.15),(3.16) and (3.17), the following state space may be calculated by combining KVL and KCL. Converter is considered working in CCM.

State space variables for this converter can be defined as:

$x_1 = i_{la}$

$x_2 = i_{lb}$

$x_3 = v_{ca}$

$x_4 = v_{Cb}$

When S has been closed :

State space equation is:

$$\dot{x}_1 = \frac{v_{in}}{L_a} \tag{4.63}$$

$$\dot{x}_2 = \frac{v_{in}}{L_b} + \frac{x_3}{L_b} - \frac{x_4}{L_b} \tag{4.64}$$

$$\dot{x}_3 = -\frac{x_2}{C_a} \tag{4.65}$$

$$\dot{x}_4 = \frac{x_2}{C_b} - \frac{x_4}{RC_b} \tag{4.66}$$

This is rewritten as

$$\begin{pmatrix} \dot{x}_1 \\ \dot{x}_2 \\ \dot{x}_3 \\ \dot{x}_4 \end{pmatrix} = \begin{pmatrix} 0 & 0 & 0 & 0 \\ 0 & 0 & \frac{1}{L_b} & -\frac{1}{L_b} \\ 0 & \frac{-1}{C_a} & 0 & 0 \\ 0 & \frac{1}{C_b} & 0 & -\frac{1}{RC_b} \end{pmatrix} \begin{pmatrix} x_1 \\ x_2 \\ x_3 \\ x_4 \end{pmatrix} + \begin{pmatrix} \frac{1}{L_a} \\ \frac{1}{L_b} \\ 0 \\ 0 \end{pmatrix} v_{in} \tag{4.67}$$

When S has been opened:

State space equation is:

$$\dot{x}_1 = \frac{v_{in}}{L_a} - \frac{x_3}{L_a} \tag{4.68}$$

$$\dot{x}_2 = \frac{v_{in}}{L_b} - \frac{x_4}{L_b} \tag{4.69}$$

$$\dot{x}_3 = \frac{x_1}{C_a} \tag{4.70}$$

$$\dot{x}_4 = \frac{x_2}{C_b} - \frac{x_4}{RC_b} \tag{4.71}$$

This is rewritten as

$$\begin{pmatrix} \dot{x}_1 \\ \dot{x}_2 \\ \dot{x}_3 \\ \dot{x}_4 \end{pmatrix} = \begin{pmatrix} 0 & 0 & -\frac{1}{L_a} & 0 \\ 0 & 0 & 0 & -\frac{1}{L_b} \\ 0 & \frac{1}{C_a} & 0 & 0 \\ 0 & \frac{1}{C_b} & 0 & -\frac{1}{RC_b} \end{pmatrix} \begin{pmatrix} x_1 \\ x_2 \\ x_3 \\ x_4 \end{pmatrix} + \begin{pmatrix} \frac{1}{L_a} \\ \frac{1}{L_b} \\ 0 \\ 0 \end{pmatrix} v_{in} \tag{4.72}$$

The state space average equations for self-lift Luo converter are:

$$\dot{x}_1 = \frac{v_{in}}{L_a} - \frac{(1-d)}{L_a} x_3 \tag{4.73}$$

$$\dot{x}_2 = \frac{v_{in}}{L_b} + \frac{d}{L_b} x_3 - \frac{x_4}{L_b} \tag{4.74}$$

$$\dot{x}_3 = \frac{(1-d)}{C_a} x_1 - \frac{d}{C_a} x_2 \tag{4.75}$$

$$\dot{x}_4 = \frac{x_2}{C_b} - \frac{x_4}{RC_b} \tag{4.76}$$

This is rewritten as

$$\begin{pmatrix} \dot{x}_1 \\ \dot{x}_2 \\ \dot{x}_3 \\ \dot{x}_4 \end{pmatrix} = \begin{pmatrix} 0 & 0 & -\frac{(1-d)}{L_a} & 0 \\ 0 & 0 & \frac{d}{L_b} & -\frac{1}{L_b} \\ \frac{(1-d)}{C_a} & \frac{-d}{C_a} & 0 & 0 \\ 0 & \frac{1}{C_b} & 0 & -\frac{1}{RC_b} \end{pmatrix} \begin{pmatrix} x_1 \\ x_2 \\ x_3 \\ x_4 \end{pmatrix} + \begin{pmatrix} \frac{1}{L_a} \\ \frac{1}{L_b} \\ 0 \\ 0 \end{pmatrix} v_{in} \tag{4.77}$$

4.6.1 Small signal model of self-lift Luo converter

Small signal model of POSLLC is computed by adding perturbations to state space vectors, V_{in}, d. This is done by substituting the following variables into the state space model.

$$i_{la} = I_{La} + \widehat{i_{la}}$$

$$i_{lb} = I_{Lb} + \widehat{i_{lb}}$$

$$v_{ca} = V_{ca} + \widehat{v_{ca}}$$

$$v_{cb} = V_{cb} + \widehat{v_{cb}}$$

$$v_{in} = V_{in} + \widehat{v_{in}}$$

$$d = D + \hat{d}$$

When S has been closed

State space equation is:

$$\frac{d(x_1 + \widehat{x_1})}{dt} = \frac{V_{in} + \widehat{v_{in}}}{L_a} \tag{4.78}$$

$$\frac{d(x_2 + \widehat{x_2})}{dt} = \frac{V_{in} + \widehat{v_{in}}}{L_b} + \frac{x_3 + \widehat{x_3}}{L_b} - \frac{x_4 + \widehat{x_4}}{L_b} \tag{4.79}$$

$$\frac{d(x_3 + \widehat{x_3})}{dt} = -\frac{x_2 + \widehat{x_2}}{C_a} \tag{4.80}$$

$$\frac{d(x_4 + \widehat{x_4})}{dt} = \frac{x_2 + \widehat{x_2}}{C_b} - \frac{x_4 + \widehat{x_4}}{RC_b} \tag{4.81}$$

When S has been opened:

State space equation is:

$$\frac{d(x_1 + \widehat{x_1})}{dt} = \frac{V_{in} + \widehat{v_{in}}}{L_a} - \frac{x_3 + \widehat{x_3}}{L_a} \tag{4.82}$$

$$\frac{d(x_2 + \widehat{x_2})}{dt} = \frac{V_{in} + \widehat{v_{in}}}{L_b} - \frac{x_4 + \widehat{x_4}}{L_b} \tag{4.83}$$

$$\frac{d(x_3 + \widehat{x_3})}{dt} = \frac{x_1 + \widehat{x_1}}{C_a} \tag{4.84}$$

$$\frac{d(x_4 + \widehat{x_4})}{dt} = \frac{x_2 + \widehat{x_2}}{C_b} - \frac{x_4 + \widehat{x_4}}{RC_b} \tag{4.85}$$

The state space average equations for self-lift luo converter are:

$$\frac{d(x_1+\widehat{x_1})}{dt}=\frac{V_{in}+\widehat{v_{in}}}{L_a}\left(D+\hat{d}\right)+\frac{\left(1-D-\hat{d}\right)}{L_a}(x_3+\widehat{x_3}\ ) \tag{4.86}$$

$$\frac{d(x_2+\widehat{x_2})}{dt}=\frac{V_{in}+\widehat{v_{in}}}{L_b}(D+\hat{d})+\frac{(x_3+\widehat{x_3}\ )}{L_b}(D+\hat{d})-\frac{x_4+\widehat{x_4}}{L_b} \tag{4.87}$$

$$\frac{d(x_3+\widehat{x_3})}{dt}=\frac{\left(1-D-\hat{d}\right)}{C_a}(x_1+\widehat{x_1})+\ \frac{d(D+\hat{d})}{C_a}(x_2+\widehat{x_2}) \tag{4.88}$$

$$\frac{d(x_4+\widehat{x_4})}{dt}=\frac{(x_2+\widehat{x_2})}{C_b}-\frac{x_4+\widehat{x_4}}{RC_b} \tag{4.89}$$

Eliminating all the nonlinear terms like 2nd order and not considering steady state terms, we get the dynamic or linear state space equation.

State Space Matrix of the small signal model of self-lift Luo converter becomes,

This is rewritten as

$$\begin{pmatrix}\dot{\hat{x}}_1\\ \dot{\hat{x}}_2\\ \dot{\hat{x}}_3\\ \dot{\hat{x}}_4\end{pmatrix}=\begin{pmatrix}0 & 0 & -\frac{(1-D)}{L_a} & 0\\ 0 & 0 & \frac{D}{L_b} & -\frac{1}{L_b}\\ \frac{(1-D)}{C_a} & -\frac{D}{C_a} & 0 & 0\\ 0 & \frac{1}{C_b} & 0 & -\frac{1}{RC_b}\end{pmatrix}\begin{pmatrix}\hat{x}_1\\ \hat{x}_2\\ \hat{x}_3\\ \hat{x}_4\end{pmatrix}+\begin{pmatrix}\frac{D}{L_a} & \frac{x_3}{L_a}\\ \frac{D}{L_b} & \frac{x_3}{L_b}\\ 0 & \frac{-(x_1+x_2)}{C_a}\\ 0 & 0\end{pmatrix}\left(\hat{V}_{in}\quad \hat{d}\ \right) \tag{4.90}$$

4.7 STATE SPACE ANALYSIS OF SUPER-LIFT LUO CONVERTER

For POSLC, i_l , v_{ca} , v_{cb} are considered as state variables. v_o is voltage from output. Circuitry analysis of POSLC given in fig (3.20),(3.21) and (3.22), the following state space equations may be computed using KVL and KCL. Converter works in CCM.

State space variables for this converter can be defined as:

$x_1 = i_l$

$x_2 = v_{ca}$

$x_3 = v_{cb}$

When S has been closed :

State space equation is:

$$\dot{x}_1 = \frac{v_{in}}{L} \tag{4.91}$$

$$\dot{x}_2 = \frac{(1-d)x_1}{dC_a} \tag{4.92}$$

$$\dot{x}_3 = -\frac{x_3}{RC_b} \tag{4.93}$$

This is rewritten as

$$\begin{pmatrix} \dot{x}_1 \\ \dot{x}_2 \\ \dot{x}_3 \end{pmatrix} = \begin{pmatrix} 0 & 0 & 0 \\ \frac{(1-d)}{dC_a} & 0 & 0 \\ 0 & 0 & -\frac{1}{RC_b} \end{pmatrix} \begin{pmatrix} x_1 \\ x_2 \\ x_3 \end{pmatrix} + \begin{pmatrix} \frac{1}{L} \\ 0 \\ 0 \end{pmatrix} v_{in} \tag{4.94}$$

When S has been opened:

State space equation is:

$$\dot{x}_1 = \frac{v_{in}}{L} - \frac{x_2}{L} - \frac{x_3}{L} \tag{4.95}$$

$$\dot{x}_2 = \frac{x_1}{C_a} \tag{4.96}$$

$$\dot{x}_3 = \frac{x_1}{C_b} - \frac{x_3}{RC_b} \tag{4.97}$$

This is rewritten as

$$\begin{pmatrix} \dot{\hat{x}}_1 \\ \dot{\hat{x}}_2 \\ \dot{x}_3 \end{pmatrix} = \begin{pmatrix} 0 & -\frac{1}{L} & -\frac{1}{L} \\ \frac{1}{C_a} & 0 & 0 \\ \frac{1}{C_b} & 0 & -\frac{1}{RC_b} \end{pmatrix} \begin{pmatrix} x_1 \\ x_2 \\ x_3 \end{pmatrix} + \begin{pmatrix} \frac{1}{L} \\ 0 \\ 0 \end{pmatrix} v_{in} \tag{4.98}$$

The state space average equations for super-lift luo converter are:

$$\dot{x}_1 = \frac{V_{in}}{L_1} - (1-d)\frac{x_2}{L_1} - (1-d)\frac{x_3}{L_1} \tag{4.99}$$

$$\dot{x}_2 = \frac{2(1-d)x_1}{C_a} \tag{4.100}$$

$$\dot{x}_3 = \frac{x_1}{C_b}(1-d) - \frac{x_3}{RC_b} \tag{4.101}$$

This is rewritten as

$$\begin{pmatrix} \dot{x}_1 \\ \dot{x}_2 \\ \dot{x}_3 \end{pmatrix} = \begin{pmatrix} 0 & -\frac{(1-d)}{L_1} & -\frac{(1-d)}{L_1} \\ \frac{2(1-d)}{C_a} & 0 & 0 \\ \frac{(1-d)}{C_b} & 0 & -\frac{x_3}{RC_b} \end{pmatrix} \begin{pmatrix} x_1 \\ x_2 \\ x_3 \end{pmatrix} + \begin{pmatrix} \frac{1}{L} \\ 0 \\ 0 \end{pmatrix} v_{in} \tag{4.102}$$

4.7.1 Small signal model of super-lift Luo converter

Linearized model of POSLC may be calculated by adding perturbations to state space vectors, V_{in}, d. This is done by substituting the following variables into the state space model.

$$i_{la} = I_{La} + \widehat{i_{la}}$$

$$v_{ca} = V_{ca} + \widehat{v_{ca}}$$

$$v_{cb} = V_{cb} + \widehat{v_{cb}}$$

$$v_{in} = V_{in} + \widehat{v_{in}}$$

$$d = D + \hat{d}$$

When S has been closed

State space equation is:

$$\frac{d(x_1 + \widehat{x_1})}{dt} = \frac{V_{in} + \widehat{v_{in}}}{L} \tag{4.103}$$

$$\frac{d(x_2 + \widehat{x_2})}{dt} = \frac{\left(1 - D - \hat{d}\right)}{(D + \hat{d})C_a}(x_1 + \widehat{x_1}) \tag{4.104}$$

$$\frac{d(x_3 + \widehat{x_3})}{dt} = -\frac{x_3 + \widehat{x_3}}{C_b} \tag{4.105}$$

When S has been opened:

State space equation is:

$$\frac{d(x_1 + \widehat{x_1})}{dt} = \frac{V_{in} + \widehat{v_{in}}}{L} - \frac{x_2 + \widehat{x_2}}{L} - \frac{x_3 + \widehat{x_3}}{L} \tag{4.106}$$

$$\frac{d(x_2 + \widehat{x_2})}{dt} = \frac{x_1 + \widehat{x_1}}{C_a} \tag{4.107}$$

$$\frac{d(x_3 + \widehat{x_3})}{dt} = \frac{x_1 + \widehat{x_1}}{C_b} - \frac{x_3 + \widehat{x_3}}{RC_b} \tag{4.108}$$

The state space average equations for super-lift Luo converter are:

$$\frac{d(x_1+\widehat{x_1})}{dt}=\frac{V_{in}+\widehat{v_{in}}}{L}-\frac{\left(1-D-\hat{d}\right)}{L}(x_2+\widehat{x_2})-\frac{\left(1-D-\hat{d}\right)}{L}(x_3+\widehat{x_3}) \quad (4.109)$$

$$\frac{d(x_2+\widehat{x_2})}{dt}=2\left(1-D-\hat{d}\right)\frac{x_1+\widehat{x_1}}{C_a} \quad (4.110)$$

$$\frac{d(x_3+\widehat{x_3})}{dt}=\frac{\left(1-D-\hat{d}\right)}{C_a}(x_1+\widehat{x_1})+\frac{(D+\hat{d})}{C_a}(x_2+\widehat{x_2}) \quad (4.111)$$

Eliminating all the nonlinear terms like second order terms and not considering the steady state (dc) terms, we get the dynamic (ac) or linearized state space equation of converter.

State Space Matrix of the linearized model of POSLC becomes,

This is rewritten as

$$\begin{pmatrix}\dot{\hat{x}}_1\\ \dot{\hat{x}}_2\\ \dot{\hat{x}}_3\end{pmatrix}=\begin{pmatrix}0 & -\frac{(1-D)}{L_1} & -\frac{(1-D)}{L_1}\\ \frac{2(1-D)}{C_a} & 0 & 0\\ \frac{(1-D)}{C_b} & 0 & -\frac{x_3}{RC_b}\end{pmatrix}\begin{pmatrix}\widehat{x_1}\\ \widehat{x_2}\\ \widehat{x_3}\end{pmatrix}+\begin{pmatrix}\frac{1}{L} & \frac{\widehat{x_2}+\widehat{x_3}}{L}\\ 0 & -\frac{2\widehat{x_1}}{C_a}\\ 0 & -\frac{(\widehat{x_1}-\widehat{x_2})}{L}\end{pmatrix}\begin{pmatrix}\widehat{v_{in}} & \hat{d}\end{pmatrix} \quad (4.112)$$

4.8 STATE SPACE ANALYSIS OF ULTRA-LIFT LUO CONVERTER

For NOULLC, inductor current i_{la} , i_{lb} and capacitor voltage v_{ca} , v_{cb} are the state variables. v_o is voltage at output. Circuitry analysis of NOULLC given in fig (3.25),(3.26) and (3.27), the following state space equations may be computed using KVL and KCL. Converter works in CCM.

State space variables of NOULLC can be defined as:

$x_1 = i_{la}$

$x_2 = i_{lb}$

$x_3 = v_{ca}$

$x_4 = v_{Cb}$

When S has been closed :

State space equation is:

$$\dot{x}_1 = \frac{v_{in}}{L_a} \tag{4.113}$$

$$\dot{x}_2 = \frac{v_{in}}{L_b} - \frac{x_3}{L_b} \tag{4.114}$$

$$\dot{x}_3 = -\frac{x_2}{C_a} \tag{4.115}$$

$$\dot{x}_4 = \frac{x_2}{C_b} - \frac{x_4}{RC_b} \tag{4.116}$$

This is rewritten as

$$\begin{pmatrix} \dot{x}_1 \\ \dot{x}_2 \\ \dot{x}_3 \\ \dot{x}_4 \end{pmatrix} = \begin{pmatrix} 0 & 0 & 0 & 0 \\ 0 & 0 & -\frac{1}{L_b} & 0 \\ 0 & \frac{-1}{C_a} & 0 & 0 \\ 0 & \frac{1}{C_b} & 0 & -\frac{1}{RC_b} \end{pmatrix} \begin{pmatrix} x_1 \\ x_2 \\ x_3 \\ x_4 \end{pmatrix} + \begin{pmatrix} \frac{1}{L_a} \\ \frac{1}{L_b} \\ 0 \\ 0 \end{pmatrix} v_{in} \tag{4.117}$$

When S has been opened:

State space equation is:

$$\dot{x}_1 = -\frac{x_3}{L_a} \tag{4.118}$$

$$\dot{x}_2 = -\frac{x_3}{L_b} + \frac{x_4}{L_b} \tag{4.119}$$

$$\dot{x}_3 = \frac{x_1}{C_a} - \frac{x_2}{C_a} \tag{4.120}$$

$$\dot{x}_4 = -\frac{x_4}{RC_b} \tag{4.121}$$

This is rewritten as

$$\begin{pmatrix} \dot{x}_1 \\ \dot{x}_2 \\ \dot{x}_3 \\ \dot{x}_4 \end{pmatrix} = \begin{pmatrix} 0 & 0 & -\frac{1}{L_a} & 0 \\ 0 & 0 & -\frac{1}{L_b} & \frac{1}{L_b} \\ \frac{1}{C_a} & -\frac{1}{C_a} & 0 & 0 \\ 0 & 0 & 0 & -\frac{1}{RC_b} \end{pmatrix} \begin{pmatrix} x_1 \\ x_2 \\ x_3 \\ x_4 \end{pmatrix} + \begin{pmatrix} 0 \\ 0 \\ 0 \\ 0 \end{pmatrix} v_{in} \tag{4.122}$$

The state space average equations for ultra-lift Luo converter are:

$$\dot{x}_1 = \frac{v_{in}}{L_a} d - \frac{(1-d)}{L_a} x_3 \tag{4.123}$$

$$\dot{x}_2 = \frac{v_{in}}{L_b} d - \frac{1}{L_b} x_3 + \frac{(1-d) x_4}{L_b} \tag{4.124}$$

$$\dot{x}_3 = \frac{(1-d)}{C_a} x_1 - \frac{1}{C_a} x_2 \tag{4.125}$$

$$\dot{x}_4 = \frac{x_2 d}{C_b} - \frac{x_4}{RC_b} \tag{4.126}$$

This is rewritten as

$$\begin{pmatrix} \dot{\hat{x}}_1 \\ \dot{\hat{x}}_2 \\ \dot{\hat{x}}_3 \\ \dot{\hat{x}}_4 \end{pmatrix} = \begin{pmatrix} 0 & 0 & -\frac{(1-d)}{L_a} & 0 \\ 0 & 0 & -\frac{1}{L_b} & \frac{(1-d)}{L_b} \\ \frac{(1-d)}{C_a} & \frac{-1}{C_a} & 0 & 0 \\ 0 & \frac{d}{C_b} & 0 & -\frac{1}{RC_b} \end{pmatrix} \begin{pmatrix} \hat{x}_1 \\ \hat{x}_2 \\ \hat{x}_3 \\ \hat{x}_4 \end{pmatrix} + \begin{pmatrix} \frac{d}{L_a} \\ \frac{d}{L_b} \\ 0 \\ 0 \end{pmatrix} v_{in} \tag{4.127}$$

4.8.1 Small signal model of ultra-lift Luo converter

Linearized model of NOULLC may be computed by adding perturbations to state space vectors, V_{in}, d. This is done by substituting the following variables into the state space model.

$$i_{la} = I_{La} + \widehat{i_{la}}$$

$$i_{lb} = I_{Lb} + \widehat{i_{lb}}$$

$$v_{ca} = V_{ca} + \widehat{v_{ca}}$$

$$v_{cb} = V_{cb} + \widehat{v_{cb}}$$

$$v_{in} = V_{in} + \widehat{v_{in}}$$

$$d = D + \hat{d}$$

When switch is closed

State space equation is:

$$\frac{d(x_1 + \widehat{x_1})}{dt} = \frac{V_{in} + \widehat{v_{in}}}{L_a} \tag{4.128}$$

$$\frac{d(x_2 + \widehat{x_2})}{dt} = \frac{V_{in} + \widehat{v_{in}}}{L_b} - \frac{x_3 + \widehat{x_3}}{L_b} \tag{4.129}$$

$$\frac{d(x_3 + \widehat{x_3})}{dt} = -\frac{x_2 + \widehat{x_2}}{C_a} \tag{4.130}$$

$$\frac{d(x_4 + \widehat{x_4})}{dt} = \frac{x_2 + \widehat{x_2}}{C_b} - \frac{x_4 + \widehat{x_4}}{RC_b} \tag{4.131}$$

When S has been opened:

State space equation is:

$$\frac{d(x_1 + \widehat{x_1})}{dt} = -\frac{x_3 + \widehat{x_3}}{L_a} \tag{4.132}$$

$$\frac{d(x_2+\widehat{x_2})}{dt}=-\frac{x_3+\widehat{x_3}}{L_b}+\frac{x_4+\widehat{x_4}}{L_b} \tag{4.133}$$

$$\frac{d(x_3+\widehat{x_3})}{dt}=\frac{x_1+\widehat{x_1}}{C_a}-\frac{x_2+\widehat{x_2}}{C_a} \tag{4.134}$$

$$\frac{d(x_4+\widehat{x_4})}{dt}=-\frac{x_4+\widehat{x_4}}{RC_b} \tag{4.135}$$

State space average equations for NOULLC are:

$$\frac{d(x_1+\widehat{x_1})}{dt}=\frac{V_{in}+\widehat{v_{in}}}{L_a}\left(D+\hat{d}\right)-\frac{\left(1-D-\hat{d}\right)}{L_a}(x_3+\widehat{x_3}\ ) \tag{4.136}$$

$$\frac{d(x_2+\widehat{x_2})}{dt}=\frac{V_{in}+\widehat{v_{in}}}{L_b}\left(D+\hat{d}\right)-\frac{(x_3+\widehat{x_3}\ )}{L_b}+\frac{x_4+\widehat{x_4}}{L_b}\left(1-D-\hat{d}\right) \tag{4.137}$$

$$\frac{d(x_3+\widehat{x_3})}{dt}=\frac{\left(1-D-\hat{d}\right)}{C_a}(x_1+\widehat{x_1})-\frac{1}{C_a}(x_2+\widehat{x_2}) \tag{4.138}$$

$$\frac{d(x_4+\widehat{x_4})}{dt}=\frac{\left(D+\hat{d}\right)}{C_b}(x_2+\widehat{x_2})-\frac{x_4+\widehat{x_4}}{RC_b} \tag{4.139}$$

Eliminating all the nonlinear terms like 2nd order and not considering steady state terms, we get the dynamic or linearized state space equation.

State space matrix of linearized model of NOULLC becomes,

This is rewritten as

$$\begin{pmatrix} \dot{\hat{x}}_1 \\ \dot{\hat{x}}_2 \\ \dot{\hat{x}}_3 \\ \dot{\hat{x}}_4 \end{pmatrix} = \begin{pmatrix} 0 & 0 & -\frac{(1-D)}{L_a} & 0 \\ 0 & 0 & -\frac{1}{L_b} & \frac{(1-D)}{L_b} \\ \frac{(1-D)}{C_a} & -\frac{1}{C_a} & 0 & 0 \\ 0 & \frac{D}{C_b} & 0 & -\frac{1}{RC_b} \end{pmatrix} \begin{pmatrix} \hat{x}_1 \\ \hat{x}_2 \\ \hat{x}_3 \\ \hat{x}_4 \end{pmatrix}$$

$$+ \begin{pmatrix} \frac{D}{L_a} & \frac{(V_{in}+x_3)}{L_a} \\ \frac{D}{L_b} & \frac{(V_{in}-x_4)}{L_b} \\ 0 & \frac{-x_1}{C_a} \\ 0 & \frac{x_2}{C_a} \end{pmatrix} \begin{pmatrix} \hat{V}_{in} & \hat{d} \end{pmatrix} \quad (4.140)$$

4.9 CONCLUSION

In this chapter, detailed approach to derive the state space and linearized model of dc converter was discussed. State space method and averaging technique was implemented to get models. Next chapters discuss the controllers that are to be implemented for control of these converters.

CHAPTER 5

LINEAR CONTROLLERS

5.1 INTRODUCTION

Power converters have to be suitably controlled so that desirable output voltages, current, frequency can be obtained by load. There are two methods of control of power converters.

1. Linear Control
2. Non-linear Control

Linear Controllers involves linearized models as it gives better understanding of the steady state performance and variation of outputs with respect to disturbances.

This control method to control a converter depends upon diverse aspects like dynamics of converter, its function, operating range etc. Factors namely rise time, peak overshoot, time of settling, ripples in output changes with the controller used, and gives knowledge about system performance.

Power converters are nonlinear circuitry; therefore the equations are linearized to implement linear controllers. Tuning of these controllers depend on system parameters giving multiple operating points. Hence, robust controlling of converters cannot be achieved. Linearizing the converters, require the use of small signal analysis which makes the derivations complex.

5.2 PRELIMINARIES OF TYPICAL CONTROLLERS NAMELY P, PI & PID

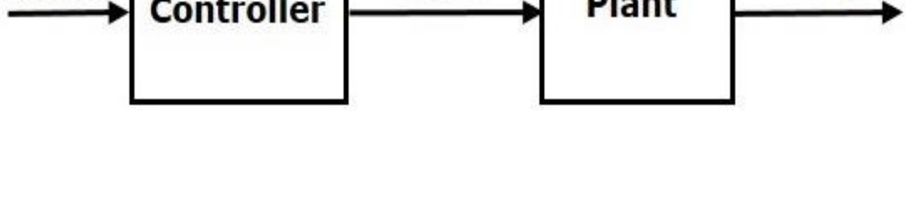

Fig 5.1 OL control of converter

Figure 5.1 represents open loop control system where signal is input to the controller which generates a controlling signal for the plant. Open loop system tends to be unstable and have errors.

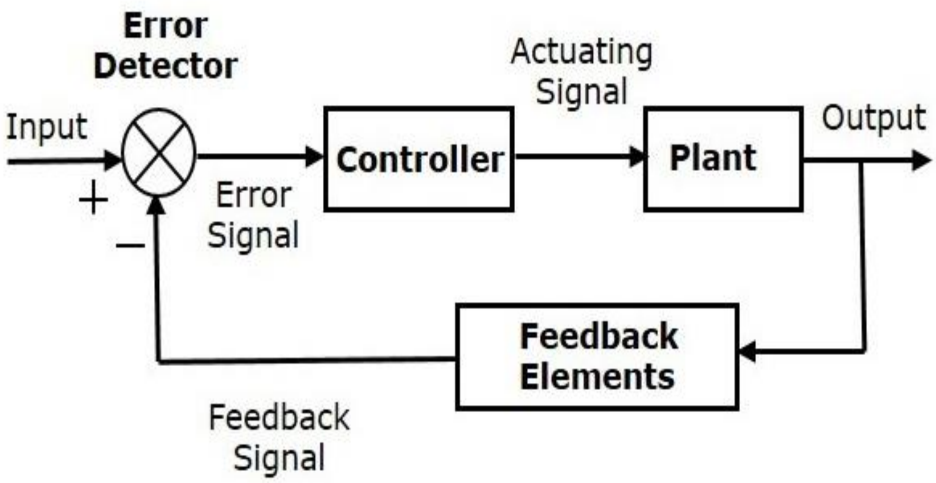

Fig 5.2 CL control of converter

In closed loop control system, feedback element is provided from the output. This signal juxtaposed with a desired input. Error signal is provided to the controller and is then given to the plant. Closed loop system are more stable and have less steady state error.

PID controllers take three primary types of means in usage: P, I D. The integrative and the proportional meanss can also be applied as single controllers while a derivative mean is not frequently applied alone. Following amalgamtions like PI,PID are frequent in the practice.

5.2.1 P Controller

P controller system is one of the linear feedback controllers. It’s more intricate than on/off controller; still it is plainer than PID. So, it can be concluded that the P controller is unable to balance superior processes.
In 1st order functions with one energy storing element, huge gain rise is endured.

A Proportional controller is only capable of stabilizing only the 1st order unstable process. The closed loop dynamics can be changed by changing the controller gain K.

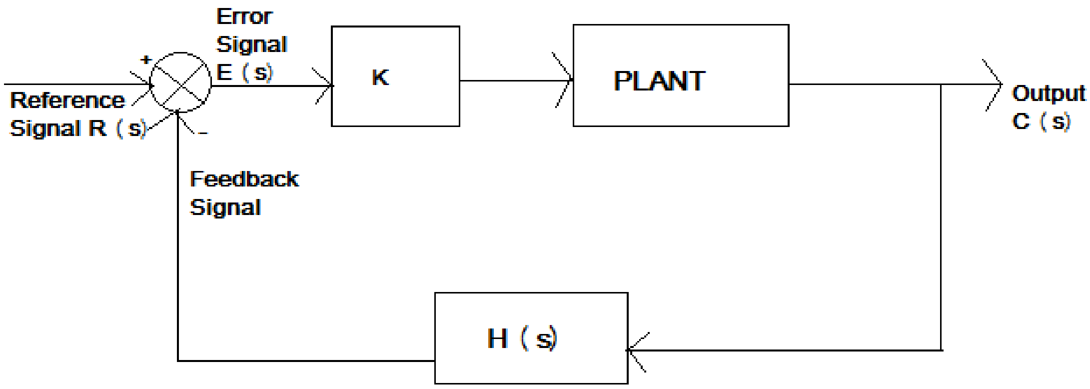

Fig 5.3 Block Diagram for system with P Controller

The errors of the signal are:

$$e(t) = k[r(t) - h(t)] \tag{5.1}$$

5.2.2 PI Controller

Currently, the PI controller is the most practiced in industry because of the plain design and economic. Other than these merits, the PI controller flops when controlled device is extremely nonlinear or complex.

The PI controller will remove imposed vibrations as well as the deviation from reference. Although, presenting the integral means also has an adverse impact upon rate of the response and stability of overall dynamics.

So, PI controller will not make any gain in the speed of the response. We can expect it because the PI controller cannot foretell result of error hereafter. To resolve this issue a derivative mode has been introduced.

It can estimate the result of the error hereafter and hence, for decreasing in the comeback time of controller.

The PI controllers are frequent used , especially when the rate of response is not a problem. We use them without the D mode is used if

1. No need of quick response.
2. Large noises and disturbance is present in the process
3. Single energy storage is present (inductor/capacitor)
4. The system has delays in the large transport.

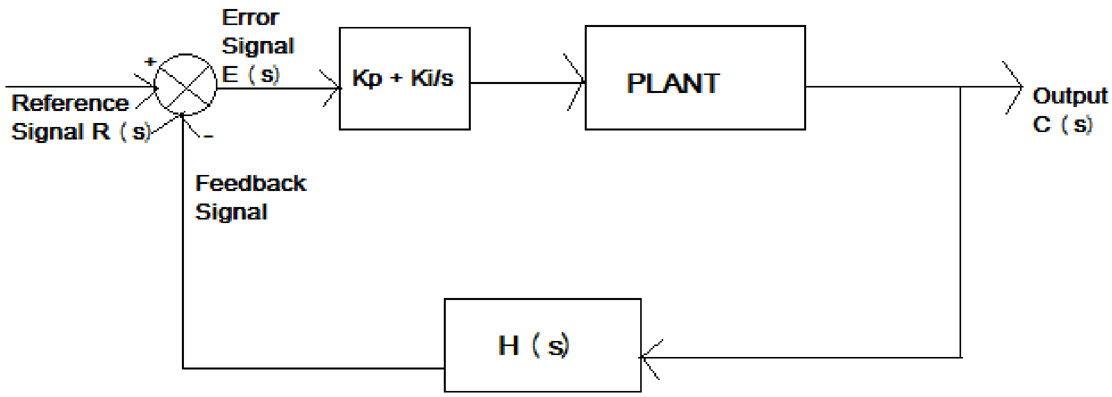

Fig 5.4 Block Diagram for system with PI Controller

The output of controller is

$$u\,(t) = K_P\,.\,e\,(t) + K_i \int e\,(t\,)dt \qquad (5.2)$$

Fig.5.4 shows the block diagram for system with PI controller is a scheme of integral error redress; the output hangs on integration of the signal. This type of redress is introduced by using controller producing output with two parts, firstly proportional to the input and secondly proportional with integration of input. This is the proportional integral controller.

5.2.3 Proportional Integral Derivative (PID) Controller

PID controller has all of the important tendencies: quick response to alteration in controller input , boosting control signal to make error around zero (I mode) as well as the befitting motion in the control error area for the lessening of oscillations (P mode).

The derivative mode recovers the stability of system as well as permits rise of gain as well as the decrease in the integral time constant Ti, which rises the fastens response speed from controller. The PID controllers are frequently applied in the industry.

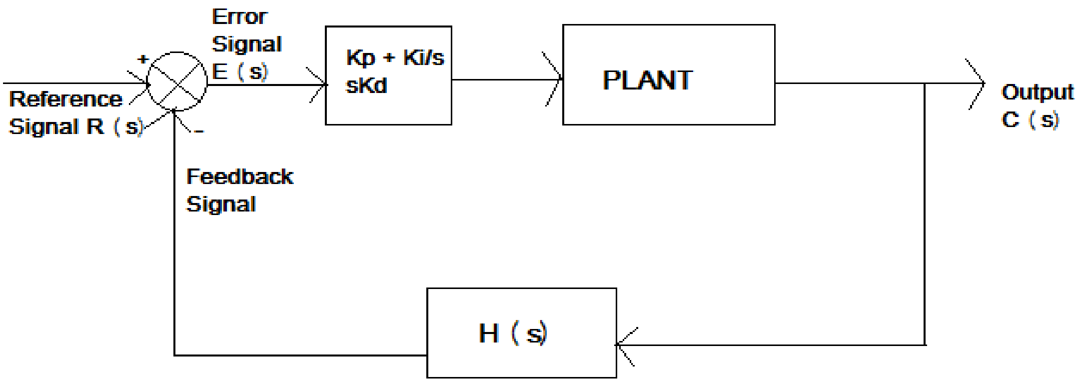

Fig 5.5 Block Diagram for system with PID Controller

y(t) is the output of the controller in the time domain such that,

- K_p= the proportional gain,
- K_d =derivative gain
- K_I *is* integral gain.

$$y(t) = K_p * e(t) + K_d * \frac{d_e(t)}{dt} + K_I \int_0^t e(t) * d\tau \qquad (5.3)$$

- The derivative control will impact the increasing stability of system, it recedes overshoot, raises transient response. The derivative control action when implemented alone is effective only during transient. PID controller generates quicker response from closed loop system with shorter overshoot. When implemented together, system under control has advantage of all three controllers.

5.2.4 Comparison of Gain Response Of P, PI And PID Controllers

Table 5.1 Impact on system under P, PI, PID control

PID Parameters	**Response Speed**	**Stability**	**Accuracy**
Increment in K	Rise	Reduces	Improves
Increment in Ki	Reduces	Reduces	Improves
Increment in Kd	Rise	Rise	No Change

Table 5.2 effects on various system parameter of p, pi and pid controller

Parameter	P Controller	PI Controller	PID Controller
Rise Time	Reduces	Reduces	Minor Reduction
Overshoot	Increase	Increase	Minor Reduction
Settling Time	Minor Change	Increase	Minor Reduction
Steady State Error	Reduces	Large Change	No change

5.3 COMPARISON OF PID, PI and P CONTROLLERS BASED ON PERFORMANCE

When we increase the gain, response speed would increase in the situation of P as well as for PID controller but for PI controller, response gain would decrease.

We can see that in PID controller, there is a very minor reduction or maybe no changes in various parameters of the controller as seen in table 1 and table 2.

As we found that there is no such change in the error of steady state, therefore we can conclude that PI controller is better than P as well as PID controller. But selection of controller will depend on the need of the system to be controlled.
Only the 1st order unstable process can be stabilized by the P controller. We can avoid large disturbances as well as the noise presents during the operation process with the help of the PI controller.

The PID controller are good to use while dealing with capacitive processes of higher order. In the comparative study of P, PI and PID Controller a good response is taken from the PID controller. To evaluate the output response of system different controllers will be used i.e P, PI and PID controller. Based on the various industrial application of the induction motor, a proper controller could be chosen.

In our case, minute overshoot and steady state error won’t affect the systems performance. To reduce the cost and complexity of the system, we have chosen PI Controller for the system as it fits our criteria

5.4 TECHNIQUES FOR OPTIMIZING PARAMETERS OF PI CONTROLLER

Tuning PID values of controller

• System model is needed for the methods like bode plots ,root locus.

• To determine the system model, we can use the system identification method, like measuring an impulse or the step input for output.

• The design techniques of the traditional control are not much accurate if system is unknown;

• Most of the PID controllers are tuned when applied because of the machine and the process variations. Initial setting of PID parameters is done by-passing few tuning parameters.

• In this dissertation, Zeigler-Nichols method is used for tuning PI controller is discussed as this is used to control the converters.

5.4.1 Zeigler- Nichols method of tuning a PI controller

Ziegler and Nichols conducted several experiments as well as provided rules to determine the values of KP, K; and KP based on transient step response of a plant.
They gave more than one technique, but we will restrict ourselves to the first technique of the Ziegler-Nichols in this tutorial. It is applicable to the plants with neither dominant complex-conjugate poles nor integrators, whose unit-step response resemble an S-shaped curve with no overshoot. This S-shaped curve is called the reaction curve.

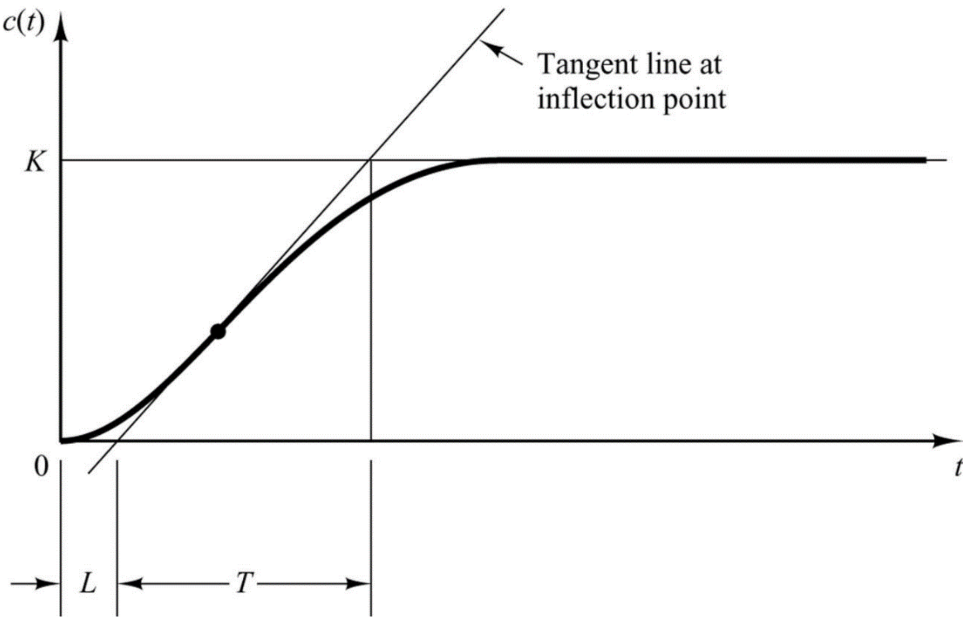

Fig 5.6 Z-N Tuning method

•Begin with closed-loop system having only proportional term.

•Start with small value of gain.

•Increase until a steady state oscillation occurs, this gain is Kcr.

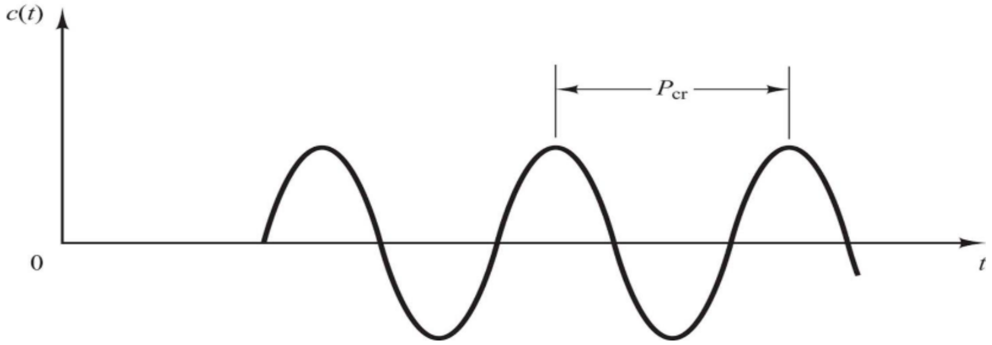

Fig 5.6 Sustained oscillation with period Pcr

Ziegler-Nichols tuning technique for determining an approximate set of the working PID parameters of unknown system

- Some of the controllers even contain extra autotune routines.
- Then we may even start fine-tuning the controller with the help of the basic rules related to each of the parameters to the response characteristics, as already stated.

Table 5.3 Zeigler-Nichols Tuning Table

Controller	Values of proportional, integral, differential gain		
	K_p	**K_i**	**K_d**
P	$K_{cr}/2$	-	-
PI	$K_{cr}/2.2$	$P_{cr}/1.2$	-
PID	$K_{cr}/1.7$	$P_{cr}/2$	$P_{cr}/8$

5.5 CONCLUSION

In this chapter, PI controllers and their tuning is discussed. They are a type of linear controllers. SMC which is a nonlinear controller is discussed in the next chapter. Chapter 7 shows the implementation of PI controller on dc-dc converters and the voltage waveforms under various parameter changes in the converter.

CHAPTER 6

SLIDING MODE CONTROLLER

6.1 INTRODUCTION

The Funtioning of a system or an object in a solicit way is the first and foremost purpose of control engineering. Even if a system engineer has the precise knowledge about the parameters of the system, in real-time the system has to the accomplished the preferable operation in spite of uncertain consequences of the environment on every part of the controlled system, along with the system. The given properties of the system should be preserved and the solicit behaviour of the system must be assured, even though there may be variation of the parameters with external disturbances, time and load. We can say that, to invent such control systems which are tough to the modelling uncertainties and external disturbances, is the main aim of control engineering. Even though, there is uncertainty and complexity in every real-world systems. Thus, the need for strategic control designs has become the need of the hour, as the complexity of control problems rises.

To deal with unmodelled dynamics of a complex system, VSC, SMC due to its easiness and intense toughness on the external disturbances and variations of the system parameter, is one of the competent techniques to manage the complex systems. Based on the philosophy of SMC, for this particular reason, we intend in this dissertation to concentrate on control schemes of novel intelligent designs.

6.2 SLIDING MODE CONTROL

The advantages of using VSC (a non-linear control technique) over the conventional linear controllers is numerous. The so-called sliding motion [34]-[39] displayed by the controlled plant is the main benefit for the system. In the system state space, on the different sides of a predestined surface (generally called as sliding surface), the aim of SMC is to engage distinctive feedback controllers. The system trajectory is driven by each of those controllers and on the occasion, it touches the surface, and stays on it. Graphically the concluding motion of the system can be explained as "sliding" of the system states, as it is bound to the surface. In the example below the concept has been depicted.

Let us consider the following linear time-invariant (LTI) system:

$$x\dot{(t)} = Ax(t) + Bu(t) \quad (6.1)$$

where $x \in R^n$ denotes system state vector, $u \in R^m$ denotes control input vector, $A \in R^{n\times n}$
and $B \in R^{n\times m}$ are constant matrices.

Define a sliding variable vector $s(t) \in R^m$ passing through the state space origin

$$s(t) = Cx(t) \quad (6.2)$$

where $C \in R^{m\times n}$ and $\|CB\| \neq 0$ and C is the parameter vector of sliding mode.

To control the system motion which has been restricted to the sliding mode surface $s(x) = 0$ the technique of equivalent control is a way. On the sliding mode surface, s(x) = 0 and s˙(x) = 0, using expressions we have

$$\dot{s}(t) = C\dot{x}(t) = 0 \quad (6.3)$$

$$C\left(Ax(t) + Bu_{eq}(t)\right) = 0 \quad (6.4)$$

where u_{eq}(t) is viewed as equivalent control.

In (6.4), we can express the equivalent control as

$$u_{eq}(\mathrm{t}) = -(CB)^{-1}CAx(t) \quad (6.5)$$

Substituting (6.5) into (6.1) yields the following differential equation

$$x\dot{(t)} = [I - B(CB)^{-1}C]Ax(t) \quad (6.6)$$

The dynamic motion of the system explained by the system (6.5) is the equivalent system. The equivalent system's properties may be summarized as below:

The system's dynamical behavior is not dependent on the control input. Hence, there is no need for past information of the control input's form for the achievement of determination of the matrix C. Asymptotic stability and prescribed transient response are necessary actions of the response system on the surface of the sliding mode while designing the sliding parameter C. An asymptotically stable solution to the differential equation can be guaranteed, if entire differential equation’s eigenvalues of the sliding mode parameter Vector C have negative real parts, in alignment to the theory of linear control. In sliding mode, the sliding surface could be of any other form with non-linearity, to ensure a system dynamics which is linear; they have a finite time convergence. There are two phases namely: the reaching phase and the sliding phase of the SMC systems. The reaching phase lasts until the controlled plant trajectory has attained the sliding surface. The sliding surface latter governs the plant motion. This shows that the responses of the closed-loop dynamics are not affected by either modeling inaccuracies or external disturbances which is a major enticing characteristic of SMC systems. The system dynamic motion relishes the system order reduction as it is barred to the hypersurface that switches in the sliding mode as further immediate consequence.

6.2.1 Existence condition

This condition makes sure that the system can slide near the sliding surface. The state space system's trajectory must be geared towards the sliding surface., the sliding mode coefficients designed using existence condition, guarantees this.

$$\lim_{s\to 0^-} \dot{s}(x) > 0\,; \qquad when\ s(x) < 0, \dot{s}(x) > 0, u = 1 \qquad (6.7)$$

$$\lim_{s\to 0^+} \dot{s}(x) < 0\,; \qquad when\ s(x) > 0, \dot{s}(x) > 0, u = 0 \qquad (6.8)$$

6.2.2 Reaching Condition

Sliding and reaching phase are included in SMC design. The system dynamics are insured to arrive at the sliding surface so the reaching phase is important in the impression as it would be maintained on it thenceforth

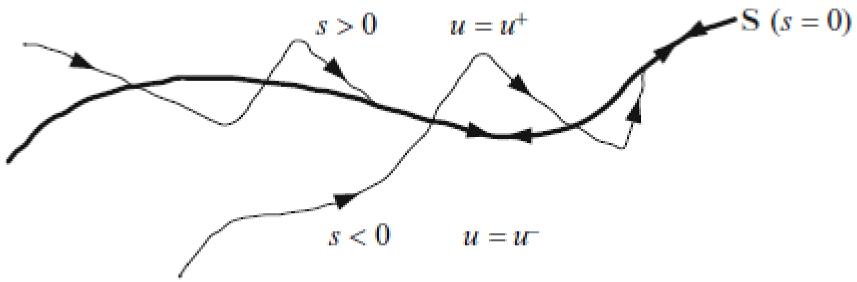

Fig 6.1 Reachability of Surface S in finite time

Figure shows planar representation of the reachability of surface s by a system in finite time.

In order, to achieve reachability of the system, the aim of our controller would be to initiate the sliding variable s to converge to zero.

$$\lim_{t \to \infty} [\dot{s}(x)|_{u=0}] < 0 \tag{6.7}$$

$$\lim_{t \to \infty} [\dot{s}(x)|_{u=1}] > 0 \tag{6.8}$$

Equations (6.7) and (6.8) show the reachability condition of the system under sliding mode controller. These conditions are implemented on the system under sliding mode control and the sliding coefficients can be derived.

6.2.3 Equivalent Control

The equivalent control signal for a system under sliding mode control can be obtained by solving the differential equation of sliding surface equation. The system is said to be under SMC when it satisfies the equations given in (6.9) and (6.10).

$$s(x) = 0 \tag{6.9}$$

$$\dot{s}(x) = 0 \tag{6.10}$$

Figure 6.2 shows the equivalent control for a system under SMC. The equivalent control is derived from the work of Fillipov [48]

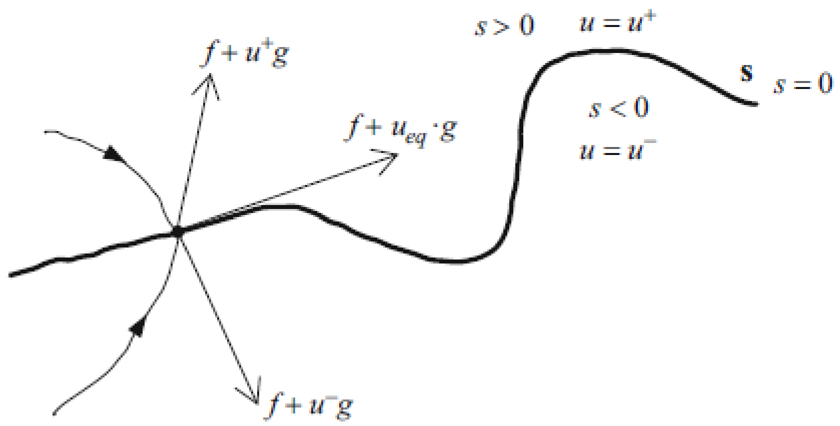

Fig 6.2 Representation of equivalent control for system under SMC

6.2.4 Stability Condition

Stability of the converter under sliding mode control is ensured by deriving the sliding mode coefficients such that the system is stable. The following steps can be followed to check the stability conditions from equivalent control method.

Step 1: The equivalent control law which is derived from equation(6.5) is to be substituted into equation (6.1) in place of control signal u(t).

Step 2: The new equilibrium points for the state space equations derived can be found.
Step 3: Perturbations in state space variables and input and reference voltages are added to the equations.

Step 4: Small signal matrices As, Bs, Cs, Ds can be formed using the above state space equations.

Step 5: If all the poles of the matrix As are on the left half plane of the s-plane, then the closed loop system is said to be stable.

6.3 PROPOSED SLIDING MODE CONTROL

The SMC proposed in this dissertation is designed for the control of buck converter and elementary Luo converter and its voltage lifted configurations. For a buck converter, SMC can be made to control either the current or the voltage. across load. But for converters having higher number of state space variables and which are non-minimum phase in nature, inductor current and load voltage have to be included in the designing of sliding surface. The designing of sliding surface for the converters mentioned in this dissertation are shown in the upcoming sections.

6.3.1 SMC of buck converter

The sliding surface for a buck converter is designed as below

$$s(x) = v_c - v_c^* + \lambda\left(\frac{dv_c}{dt} - \frac{dv_c^*}{dt}\right) \qquad (6.11)$$

Where, v_c is the voltage across load resistor and v_c^* is the desired or reference voltage needed across load. The term λ is the sliding mode coefficient which is a positive value.

In the above equation of sliding surface only one parameter that is output voltage is considered for designing the sliding surface.

Differentiating the above equation (6.11) , we get

$$\dot{s}(x) = \dot{v}_c - \dot{v}_c^* + \lambda(\ddot{v}_c - \ddot{v}_c^*) \tag{6.12}$$

Since the desired or reference voltage is a constant, therefore the terms, $\dot{v}_c^* = \ddot{v}_c^* = 0$. Substituting the value of $\dot{v}_c$ from state space equation of buck converter given in equation (4.22) and (4.23) into equation (6.12), we get

$$\dot{s}(x) = \frac{i_L}{C} - \frac{v_C}{RC} - \lambda\frac{v_C}{LC} + \lambda\frac{u_{eq}V_{in}}{LC} - \lambda\frac{i_L}{RC^2} + \lambda\frac{v_C}{R^2C^2} \tag{6.13}$$

Equating (6.13) to zero, we get the equivalent control law for the designed sliding surface.

$$u_{eq} = \frac{v_C}{V_{in}} + \left(1 - \frac{\lambda}{RC}\right)\frac{LC}{\lambda^2 V_{in}}(v_C - v_C^*) \tag{6.14}$$

Existence Condition

The existence condition mentioned in equation (6.15) has to be satisfied so the space trajectory of buck converter can slide on the designed sliding surface.

$$\lim_{s(x)\to 0^+} \dot{s}(x) < 0 < \lim_{s(x)\to 0^-} \dot{s}(x) \tag{6.15}$$

Case 1: $\lim_{s(x)\to 0^+} \dot{s}(x) > 0 \; when \; s(x) < 0, u_{eq} = 1$

$$\frac{i_L}{C} - \frac{v_C}{RC} - \lambda\frac{v_C}{LC} + \lambda\frac{V_{in}}{LC} - \lambda\frac{i_L}{RC^2} + \lambda\frac{v_C}{R^2C^2} > 0 \tag{6.16}$$

Case 2: $\lim_{s(x)\to 0^-} \dot{s}(x) < 0 \; when \; s(x) > 0, u_{eq} = 0$

$$\frac{i_L}{C} - \frac{v_C}{RC} - \lambda\frac{v_C}{LC} + \lambda\frac{V_{in}}{LC} - \lambda\frac{i_L}{RC^2} + \lambda\frac{v_C}{R^2C^2} < 0 \tag{6.17}$$

Reaching Condition

The reaching condition mentioned in equation (6.18) has to be satisfied so the space trajectory of buck converter can reach the sliding surface.

$$\lim_{t\to\infty}[\dot{s}(x)|_{u_{eq}=0]} < 0 \& \lim_{t\to\infty}[\dot{s}(x)|_{u_{eq}=1]} > 0 \tag{6.18}$$

This equivalent control law (equation (6.14)) is compared with a triangular pulse and is passed as control signal to the MOSFET switch connected in the buck converter.

6.3.2 SMC of POELC

The sliding surface for elementary Luo converter is designed as below:

$$s(x) = \alpha i_{la} + \beta v_{cb} + \gamma \int (\delta v_{cb} - v_{ref}) \tag{6.19}$$

Where, v_{ref} is the desired or reference voltage needed across load. α is the inductor current control coefficient and β is the load voltage control coefficient. γ is the coefficient for error signal $(\delta v_{cb} - v_{ref})$. The proposed sliding surface in equation (6.19 lessens the output oscillations and reduces the system's steady state error. Unlike the sliding surface proposed for buck converter, the sliding surface for Luo converter involves both the inductor current and load voltage as controlling parameters. This is due to the complexity of the converter and considering only output voltage does not meet the existence requirement of the SMC.

Differentiating the above equation (6.19) , we get

$$\dot{s}(x) = \alpha \dot{i_{la}} + \beta \dot{v_{cb}} + \gamma \left(\delta v_{cb} - v_{ref}\right) \tag{6.20}$$

Substituting the value of i_{la} and $\dot{v_{cb}}$ from state space equation of elementary Luo converter given in equation (4.45) to (4.48) into equation (6.20), we get

$$\dot{s}(x) = \alpha \frac{v_{in}\, u_{eq}}{L_a} - \alpha \frac{\left(1 - u_{eq}\right)}{L_a} x_3 + \beta \frac{x_2}{C_b} - \beta \frac{x_4}{RC_b} + \gamma \left(\delta V_{cb} - v_{ref}\right) \tag{6.21}$$

Equating (6.21) to zero, we get the equivalent control law for the designed sliding surface.

$$u_{eq} = \frac{\alpha \frac{x_3}{L_a} - \beta \frac{ic_b}{C_b} - \gamma \left(\delta V_{cb} - v_{ref}\right)}{\alpha \frac{V_{in}}{L_a} + \alpha \frac{x_3}{L_a}} \tag{6.22}$$

Existence Condition

The existence condition mentioned in equation (6.15) has to be satisfied so the space trajectory of elementary Luo converter can slide on the designed sliding surface.

Case 1: $\lim_{s(x)\to 0^+} \dot{s}(x) > 0 \; when \; s(x) < 0, u_{eq} = 1$

$$\alpha \frac{v_{in}}{L_a} + \beta \frac{x_2}{C_b} - \beta \frac{x_4}{RC_b} + \gamma \left(\delta V_{cb} - v_{ref}\right) > 0 \qquad (6.23)$$

Case 2: $\lim_{s(x)\to 0^-} \dot{s}(x) < 0 \; when \; s(x) > 0, u_{eq} = 0$

$$-\alpha \frac{1}{L_a} x_3 + \beta \frac{x_2}{C_b} - \beta \frac{x_4}{RC_b} + \gamma \left(\delta V_{cb} - v_{ref}\right) < 0 \qquad (6.24)$$

The above equations (6.23) and (6.24) must be satisfied to derive the existing condition.

Reaching Condition

The reaching condition mentioned in equation (6.25) has to be satisfied so the space trajectory of elementary Luo converter can reach the sliding surface.

$$\lim_{t\to\infty} [\, \dot{s}(x)|_{u_{eq}=0}] < 0 \& \lim_{t\to\infty} [\, \dot{s}(x)|_{u_{eq}=1}] > 0 \qquad (6.25)$$

The reaching condition mentioned in equation (6.25) can be solved with the steady state values of state space variables taken as X=[∞ 0 -v_{in} 0] when $u_{eq} = 1$ and X=[0 0 0 0] when $u_{eq} = 0$.

Stability Condition

The stability of the sliding surface designed can be ensured by substituting the value of u_{eq} from equation (6.22) into the state space equations given in equations (4.45) to (4.48). Small perturbation is added to the state space variables, inputs and reference signals and the resultant matrix As must have all the poles on the left half of s-plane.

The sliding mode coefficients are derived from the above three conditions and the resultant equivalent control law (equation (6.22)) is compared with a triangular pulse and is passed as control signal to the MOSFET switch connected in the elementary Luo converter.

6.3.3 SMC of POSLLC

The sliding surface for self-lift Luo converter is designed as below:

$$s(x) = \alpha i_{la} + \beta v_{cb} + \gamma \int (\delta v_{cb} - v_{ref}) \qquad (6.26)$$

Where, v_{ref} is the desired or reference voltage needed across load. α is the inductor current control coefficient and β is the load voltage control coefficient. γ is the coefficient for error signal $(\delta v_{cb} - v_{ref})$. The proposed sliding surface in equation (6.26) lessens the output oscillations and reduces the system's steady state error. Unlike the sliding surface proposed for buck converter, the sliding surface for Luo converter involves both the inductor current and load voltage as controlling parameters. This is due to the complexity of the converter and considering only output voltage does not meet the existence requirement of the SMC.

Differentiating the above equation (6.26) , we get

$$\dot{s}(x) = \alpha \dot{i_{la}} + \beta \dot{v_{cb}} + \gamma \left(\delta v_{cb} - v_{ref}\right) \qquad (6.27)$$

Substituting the value of i_{la} and $\dot{v_{cb}}$ from state space equation of self-lift Luo converter given in equation (4.73) to (4.76) into equation (6.27), we get

$$\dot{s}(x) = \alpha \frac{V_{in}}{L_a} - \alpha(1-d)\frac{x_3}{L_a} + \beta \frac{x_2}{C_b} - \beta \frac{x_4}{RC_b} + \gamma \left(\delta v_{cb} - v_{ref}\right) \qquad (6.28)$$

Equating (6.28) to zero, we get the equivalent control law for the designed sliding surface.

$$u_{eq} = \frac{-\alpha \frac{V_{in}}{L_a} + \alpha \frac{x_3}{L_a} - \beta \frac{x_2}{C_b} + \beta \frac{x_4}{RC_b} - \gamma \left(\delta V_{cb} - v_{ref}\right)}{\alpha \frac{x_3}{L_a}} \qquad (6.29)$$

Existence Condition

The existence condition mentioned in equation (6.15) has to be satisfied so the space trajectory of self-lift Luo converter can slide on the designed sliding surface.

Case 1: $\lim_{s(x)\to 0^+} \dot{s}(x) > 0 \; when \; s(x) < 0, u_{eq} = 1$

$$\alpha \frac{V_{in}}{L_a} + \beta \frac{x_2}{C_b} - \beta \frac{x_4}{RC_b} + \gamma \left(\delta V_{cb} - v_{ref}\right) > 0 \qquad (6.30)$$

Case 2: $\lim_{s(x)\to 0^-} \dot{s}(x) < 0 \; when \; s(x) > 0, u_{eq} = 0$

$$\alpha\frac{V_{in}}{L_a} - \alpha\frac{x_3}{L_a} + \beta\frac{x_2}{C_{cb}} - \beta\frac{x_4}{RC_{cb}} + \gamma\left(\delta V_{cb} - v_{ref}\right) < 0 \quad (6.31)$$

The above equations (6.30) and (6.31) must be satisfied to derive the existing condition.

Reaching Condition

The reaching condition mentioned in equation (6.32) has to be satisfied so the space trajectory of self-lift Luo converter can reach the sliding surface.

$$\lim_{t\to\infty}[\dot{s}(x)|_{u_{eq}=0]} < 0 \& \lim_{t\to\infty}[\dot{s}(x)|_{u_{eq}=1]} > 0 \quad (6.32)$$

The reaching condition mentioned in equation (6.32) can be solved with the steady state values of state space variables taken as X=[∞ $\frac{v_{in}}{R}$ 0 0] when $u_{eq} = 1$ and X=[0 0 0 0] when $u_{eq} = 0$.

Stability Condition

The stability of the sliding surface designed can be ensured by substituting the value of u_{eq} from equation (6.29) into the state space equations given in equations (4.73) to (4.76). Small perturbation is added to the state space variables, inputs and reference signals and the resultant matrix As must have all the poles on the left half of s-plane.

The sliding mode coefficients are derived from the above three conditions and the resultant equivalent control law (equation (6.29)) is compared with a triangular pulse and is passed as control signal to the MOSFET switch connected in the self-lift Luo converter.

6.3.4 SMC of POSLC

The sliding surface for super-lift Luo converter is designed as below:

$$s(x) = \alpha i_l + \beta v_{cb} + \gamma\int(\delta v_{cb} - v_{ref}) \quad (6.33)$$

Where, v_{ref} is the desired or reference voltage needed across load. α is the inductor current control coefficient and β is the load voltage control coefficient. γ is the coefficient for error signal $(\delta v_{cb} - v_{ref})$. The proposed sliding surface in equation (6.33) lessens the output oscillations and reduces the system's steady state error. Unlike the sliding surface proposed for buck converter, the sliding surface for Luo converter involves both the inductor current and load voltage as controlling parameters. This is due to the complexity of the converter and considering only output voltage does not meet the existence requirement of the SMC.

Differentiating the above equation (6.33) , we get

$$\dot{s}(x) = \alpha \dot{i_l} + \beta \dot{v_{cb}} + \gamma \left(\delta v_{cb} - v_{ref}\right) \tag{6.34}$$

Substituting the value of i_l and $\dot{v_{cb}}$ from state space equation of super-lift Luo converter given in equation (4.99) to (4.101) into equation (6.34), we get

$$\dot{s}(x) = \alpha \frac{V_{in}}{L} - \alpha\left(1 - u_{eq}\right)\frac{x_2}{L} - \alpha\left(1 - u_{eq}\right)\frac{x_3}{L} + \beta \frac{x_1}{C_b}\left(1 - u_{eq}\right) - \beta \frac{x_3}{RC_b} + \gamma \left(\delta V_{cb} - v_{ref}\right) \tag{6.35}$$

Equating (6.35) to zero, we get the equivalent control law for the designed sliding surface.

$$u_{eq} = \frac{\alpha \frac{V_{cb}}{L} + 2\alpha \frac{V_{in}}{L} - \beta \frac{i_{l1}}{C_b} + \beta \frac{V_{cb}}{RC_b} - \gamma \left(\delta V_{cb} - v_{ref}\right)}{\frac{V_{cb} - V_{in}}{L} + \beta \frac{i_l}{C_b}} \tag{6.36}$$

Existence Condition

The existence condition mentioned in equation (6.15) has to be satisfied so the space trajectory of super-lift Luo converter can slide on the designed sliding surface.

Case 1: $\lim_{s(x)\to 0^+} \dot{s}(x) > 0 \; when \; s(x) < 0, u_{eq} = 1$

$$\alpha \frac{V_{in}}{L} - \beta \frac{V_b}{RC_b} + \gamma \left(\delta V_{cb} - v_{ref}\right) > 0 \tag{6.37}$$

Case 2: $\lim_{s(x)\to 0^-} \dot{s}(x) < 0 \; when \; s(x) > 0, u_{eq} = 0$

$$-\alpha \frac{V_{cb}}{L} + \beta \frac{i_{L1}}{C_b} - -\beta \frac{V_{cb}}{RC_b} + \gamma \left(\delta V_{cb} - v_{ref}\right) < 0 \tag{6.38}$$

The above equations (6.37) and (6.38) must be satisfied to derive the existing condition.

Reaching Condition

The reaching condition mentioned in equation (6.39) has to be satisfied so the space trajectory of super-lift Luo converter can reach the sliding surface.

$$\lim_{t\to\infty}[\,\dot{s}(x)|_{u_{eq}=0}] < 0\& \lim_{t\to\infty}[\,\dot{s}(x)|_{u_{eq}=1}] > 0 \qquad (6.39)$$

The reaching condition mentioned in equation (6.39) can be solved with state space variables' steady state values taken as X=[∞ V_{in} 0] when $u_{eq} = 1$ and X=[0 -V_{in} 0] when $u_{eq} = 0$.

Stability Condition

The stability of the sliding surface designed can be ensured by substituting the value of u_{eq} from equation (6.36) into the state space equations given in equations (4.99) to (4.101). Small perturbation is added to the state space variables, inputs and reference signals and the resultant matrix As must have all the poles on the left half of s-plane.

The sliding mode coefficients are derived from the above three conditions and the resultant equivalent control law (equation (6.36)) is compared with a triangular pulse and is passed as control signal to the MOSFET switch connected in the super-lift Luo converter.

6.3.5 SMC of NOULLC

The sliding surface for ultra-lift Luo converter is designed as below:

$$s(x) = \alpha i_{la} + \beta v_{cb} + \gamma \int (\delta v_{cb} - v_{ref}) \qquad (6.40)$$

Where, v_{ref} is the desired or reference voltage needed across load. α is the inductor current control coefficient and β is the load voltage control coefficient. γ is the coefficient for error signal $(\delta v_{cb} - v_{ref})$. The proposed sliding surface in equation (6.40) lessens the output oscillations and reduces the system's steady state error. Unlike the sliding surface proposed for buck converter, the sliding surface for Luo converter involves both the inductor current and load voltage as controlling parameters. This is due to the complexity of the converter and considering only output voltage does not meet the existence requirement of the SMC.

Differentiating the above equation (6.40) , we get

$$\dot{s}(x) = \alpha \dot{i_{la}} + \beta \dot{v_{cb}} + \gamma\left(\delta v_{cb} - v_{ref}\right) \tag{6.41}$$

Substituting the value of i_{la} and $\dot{v_{cb}}$ from state space equation of ultra-lift Luo converter given in equation (4.123) to (4.126) into equation (6.41), we get

$$\dot{s}(x) = \alpha \frac{V_{in}}{L_a} u_{eq} - \alpha\left(1 - u_{eq}\right)\frac{x_3}{L_a} + \beta \frac{x_2\, u_{eq}}{C_b} - \beta \frac{x_4}{RC_b} + \gamma\left(\delta V_{cb} - v_{ref}\right) \tag{6.42}$$

Equating (6.42) to zero, we get the equivalent control law for the designed sliding surface.

$$u_{eq} = \frac{\alpha \frac{x_3}{L_a} + \beta \frac{x_4}{RC_b} - \gamma\left(\delta V_{cb} - v_{ref}\right)}{\alpha \frac{V_{in}}{L_a} + \alpha \frac{x_3}{L_a} + \beta \frac{x_2}{C_b}} \tag{6.43}$$

Existence Condition

The existence condition mentioned in equation (6.15) has to be satisfied so the space trajectory of ultra-lift Luo converter can slide on the designed sliding surface.

Case 1: $\lim_{s(x)\to 0^+} \dot{s}(x) > 0 \; when \; s(x) < 0, u_{eq} = 1$

$$\alpha \frac{V_{in}}{L_a} + \beta \frac{x_2}{C_b} - \beta \frac{x_4}{RC_b} + \gamma\left(\delta V_{cb} - v_{ref}\right) > 0 \tag{6.44}$$

Case 2: $\lim_{s(x)\to 0^-} \dot{s}(x) < 0 \; when \; s(x) > 0, u_{eq} = 0$

$$-\alpha \frac{x_3}{L_a} - \beta \frac{x_4}{RC_b} + \gamma\left(\delta V_{cb} - v_{ref}\right) < 0 \tag{6.45}$$

The above equations (6.44) and (6.45) must be satisfied to derive the existing condition.

Reaching Condition

The reaching condition mentioned in equation (6.46) has to be satisfied so the space trajectory of ultra-lift Luo converter can reach the sliding surface.

$$\lim_{t\to\infty}[\,\dot{s}(x)|_{u_{eq}=0}] < 0 \& \lim_{t\to\infty}[\,\dot{s}(x)|_{u_{eq}=1}] > 0 \qquad (6.39)$$

The reaching condition mentioned in equation (6.39) can be solved with the steady state values of state space variables taken as X=[∞ 0 V_{in} 0] when $u_{eq} = 1$ and X=[0 0 0 0] when $u_{eq} = 0$.

Stability Condition

The stability of the sliding surface designed can be ensured by substituting the value of u_{eq} from equation (6.43) into the state space equations given in equations (4.123) to (4.126). Small perturbation is added to the state space variables, inputs and reference signals and the resultant matrix As must have all the poles on the left half of s-plane.

The sliding mode coefficients are derived from the above three conditions and the resultant equivalent control law (equation (6.43)) is compared with a triangular pulse and is passed as control signal to the MOSFET switch connected in the ultra-lift Luo converter.

6.4 CONCLUSION

In this chapter, SMC is discussed and a sliding surface is proposed for implementation on dc-dc converters mentioned in this dissertation. The value of circuit elements considered is given in appendix A.. The next chapter shows the simulation waveforms of the converters under uncontrolled, PI controller and sliding mode controllers. Results under all three conditions are tabulated and compared.

CHAPTER 7
RESULT AND DISCUSSION

The converters and the discussed PI and Sliding mode controllers are implemented on MATLAB-Simulink software. The output waveforms under different conditions for each converter are observed in parts that follow.

7.1 BUCK CONVERTER

Output waveforms of buck converter under certain parameter disturbances are presented below.

7.1.1 Uncontrolled buck converter

Waveforms of output showing results for uncontrolled buck converter are given:

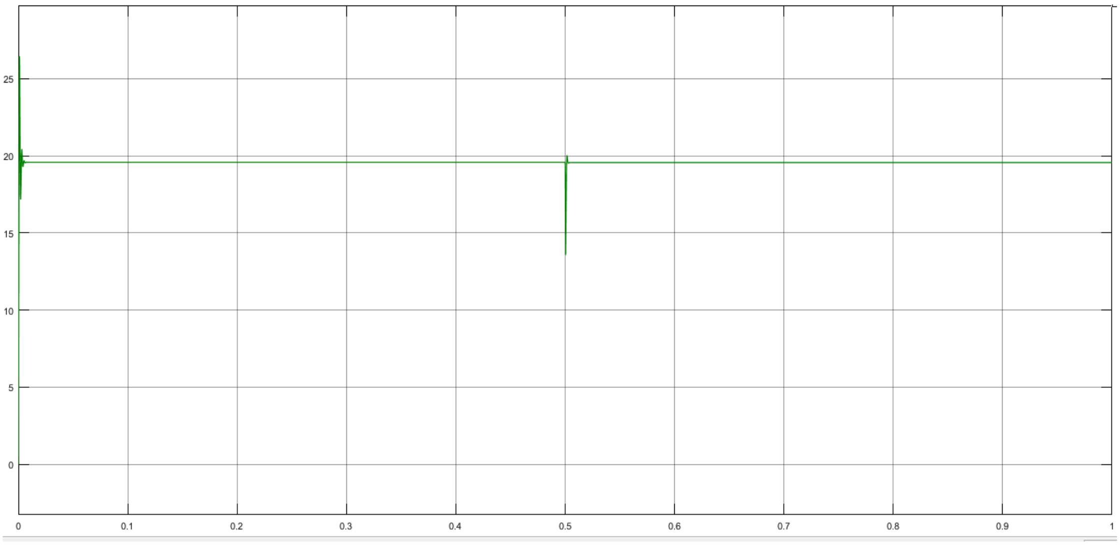

Fig 7.1: Voltage at output of uncontrolled buck having change in load resistance

In figure 7.1, load resistance of buck decreases by 50% at 0.5 sec. At this disturbance, voltage at output undergoes a transient change and drops from 19.58V to a new value of 19.56V.

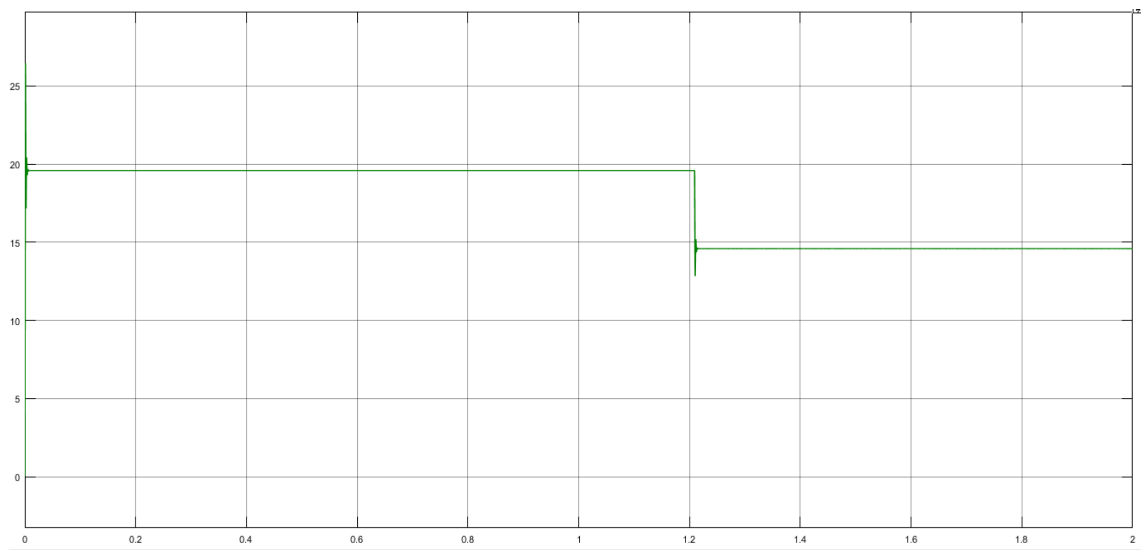

Fig 7.2: Voltage at output of uncontrolled buck with change in voltage at supply

In fig 7.2, voltage at supply decreases from 20V to 15V at time 1.2 seconds. At disturbance, the output voltage drops from 19.58V to 14.58V.

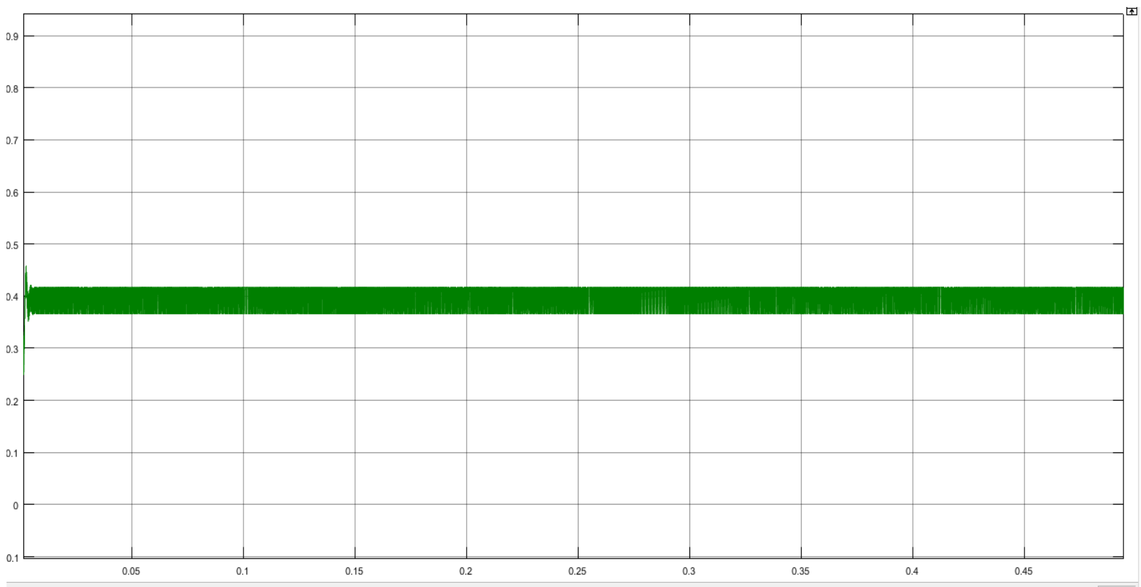

Fig 7.3: Inductor current of uncontrolled buck

In fig 7.3, the i_L of the uncontrolled buck is shown with r.m.s value is 0.39A and ripples in the inductor current are 0.51A.

7.1.2 Buck converter controlled using PI Controller

Waveforms of output showing results for this are shown:

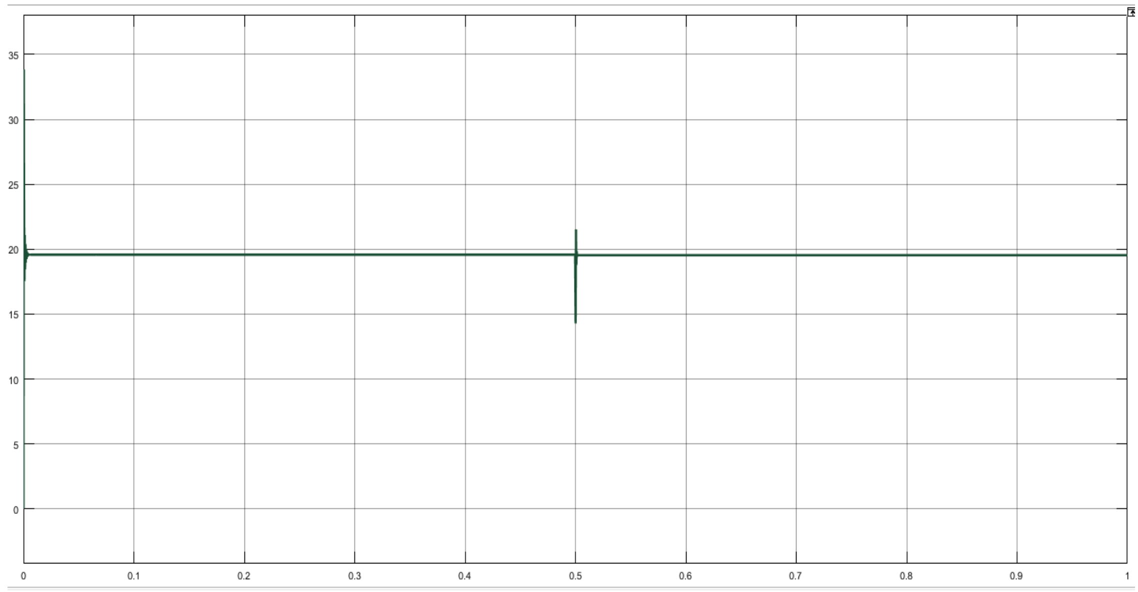

Fig 7.4: Voltage at output under buck under PI with change in load R

In figure 7.4, the load resistance of buck under PI control is decreased by 50% at 0.5 sec. At disturbance, output voltage undergoes a transient change but remains on the same voltage level of 19.98V.

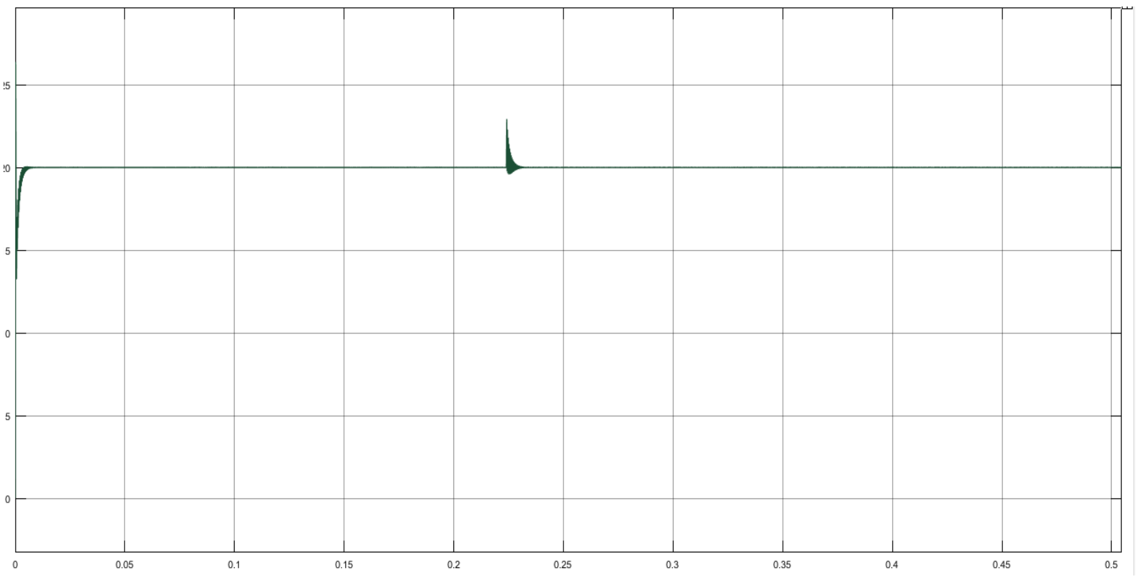

Fig 7.5: Voltage at output under buck under PI with change in input voltage

In figure 7.5, supply to buck converter increases from 20V to 30V at time 0.225 seconds. The output voltage shows some fluctuations but stabilizes around reference voltage 19.98 V.

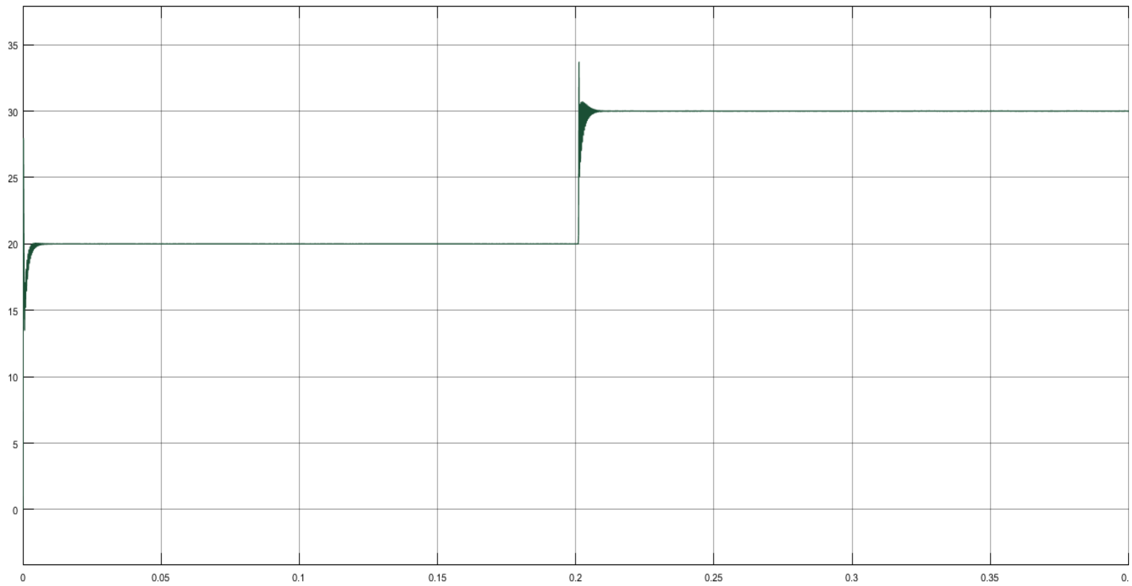

Fig 7.6: Voltage at output under PI control buck converter with reference voltage change

In fig 7.6, reference voltage increases from 20V to 30V at time 0.2 seconds. The output voltage fluctuates for 16.812 seconds then stabilizes to the new value of reference voltage 29.98 V.

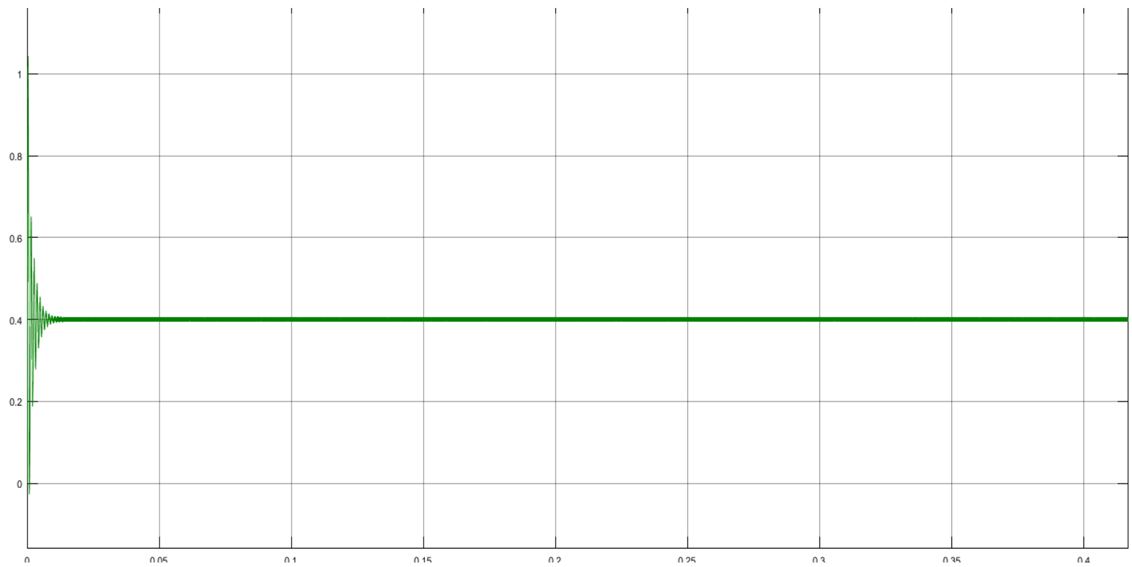

Fig 7.7: Current through inductor under PI control for buck converter

In fig 7.7, the current through inductor is shown whose r.m.s value is 0.43A and ripples in the inductor current are 0.11A.

7.1.3 Buck converter under SMC

Waveforms of output showing results for SMC of buck converter are given:

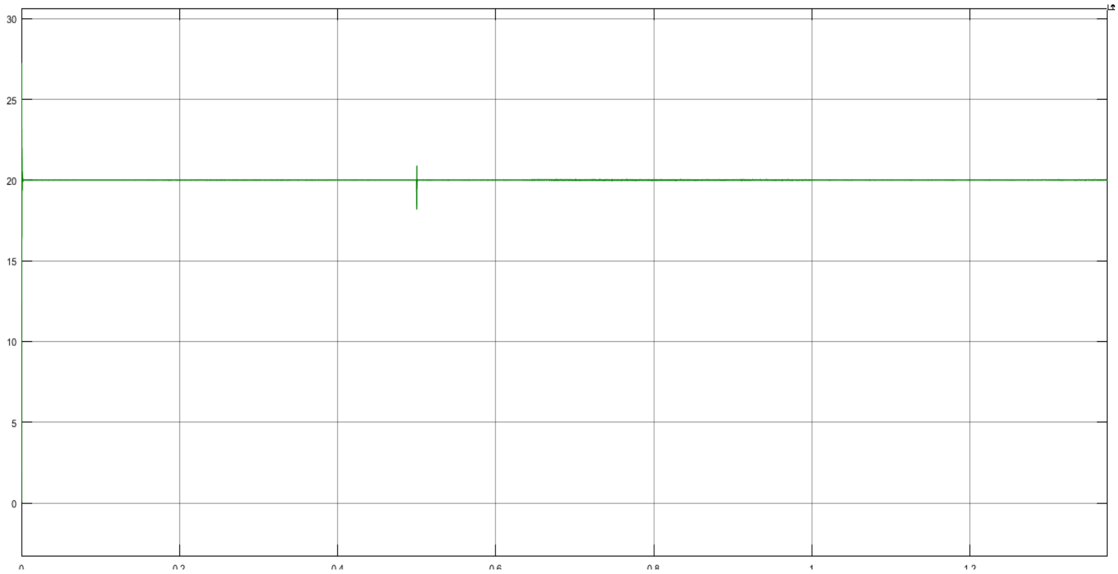

Fig 7.8: Voltage at output for buck converter under SMC when load resistance changes

In figure 7.8, the load resistance of PI controlled buck converter is decreased by 50% at 0.5 sec. At disturbance, output voltage undergoes a transient change but remains on the same voltage level of 20V.

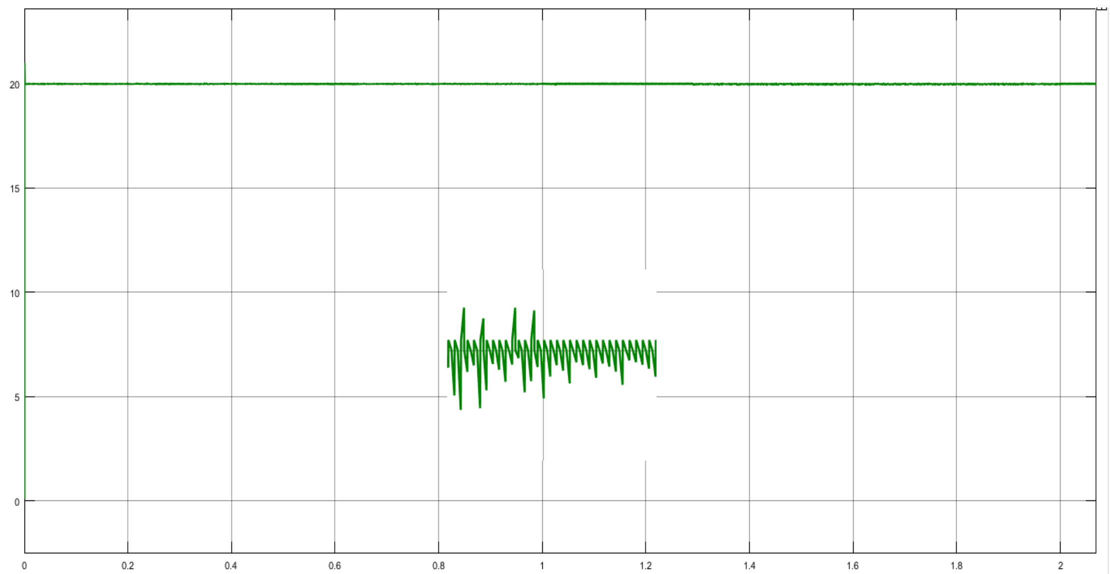

Fig 7.9: Voltage at output for buck under SMC when supply voltage changes

In fig 7.9, input voltage decreases from 40V to 30V at time 1 second. The output voltage shows negligible change. The inset shows the ripple in output voltage before and after disturbance which is at 0.01V.

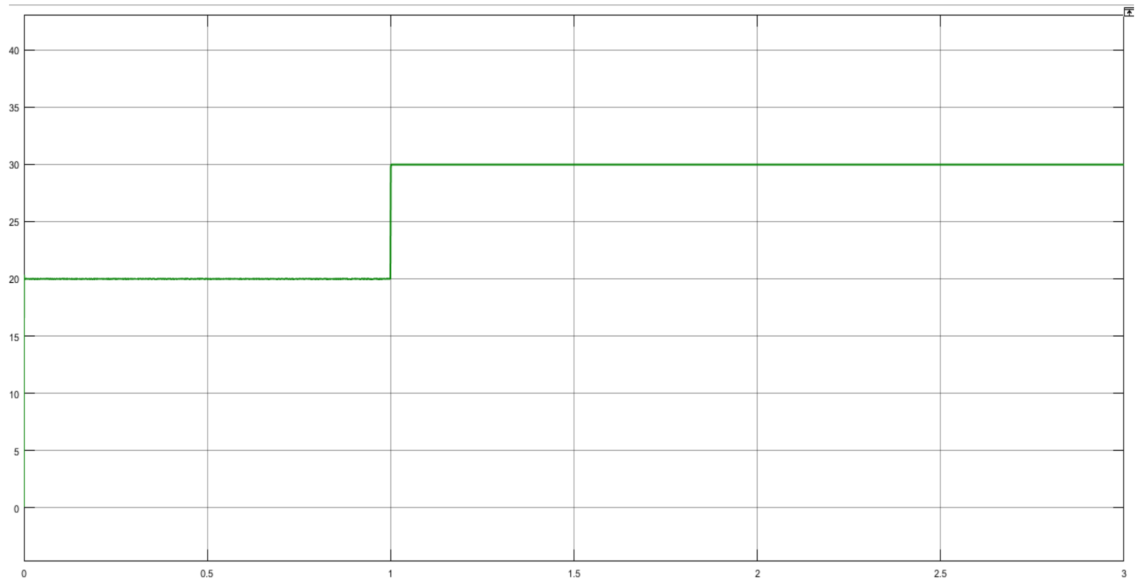

Fig 7.10: Voltage at output for buck converter under SMC when ref changes.

In fig 7.10, reference voltage increases from 20V to 30V at time 1 second. The output voltage changes to the new value of reference voltage 30 V after time 0.73 seconds.

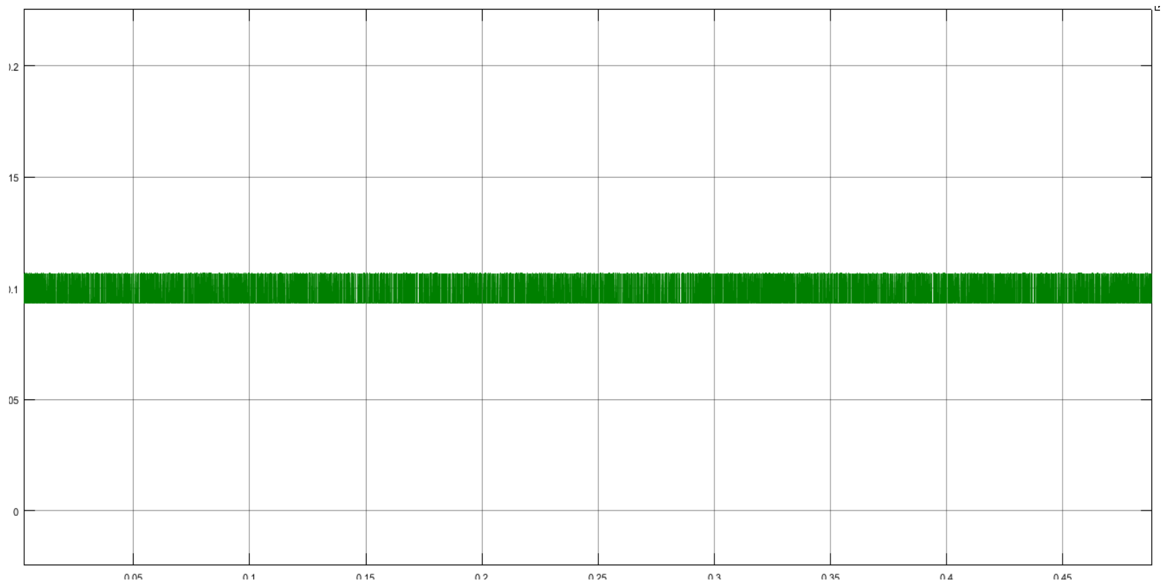

Fig 7.11: Inductor current buck with SMC

In fig 7.11, the current through inductor of buck with SMC buck having r.m.s value 0.10A and the ripples in the inductor current are 0.01A.

Table 7.1 Comparison of data of buck converter with PI and SMC

Performance Parameters	**Uncontrolled buck converter**	**Buck with PI**	**Buck with SMC**

Rise time (μsec)	107.983	753.97	117.969
Settling time(msec)	2.951	5.115	0.084
Overshoot(%)	74.561	61.933	1.531
Voltage ripple(mV)	16	20	10
Inductor current ripple(A)	0.51	0.11	0.012
Steady state error(mv)	560	60	0
Time taken to recover from disturbance(msec)	20	13.77	0.730

7.1.4 Conclusion

Table 7.1 presents the data from the uncontrolled, PI controlled and sliding mode controlled configurations of buck converter. Rise time shows that sliding mode controlled converter is faster than PI controlled. It settles faster than uncontrolled and PI controlled converter models. Percentage overshoot is also significantly less in sliding mode configuration than the other two configurations. Ripple in voltage at output and current through inductor is reduced in sliding mode. Steady state error is zero for buck converter in SMC. After disturbances are introduced in the system, SMC takes minimum time to achieve the new steady state. Sliding mode provide better rejection of disturbances. Hence, SMC provides better system performance than a PI.

7.2 POSITIVE OUTPUT ELEMENTARY LUO CONVERTER

Output waveforms of POELC under certain parameter disturbances are presented below.

7.2.1 Uncontrolled POELC

Waveforms of output showing results for uncontrolled elementary Luo converter are given:

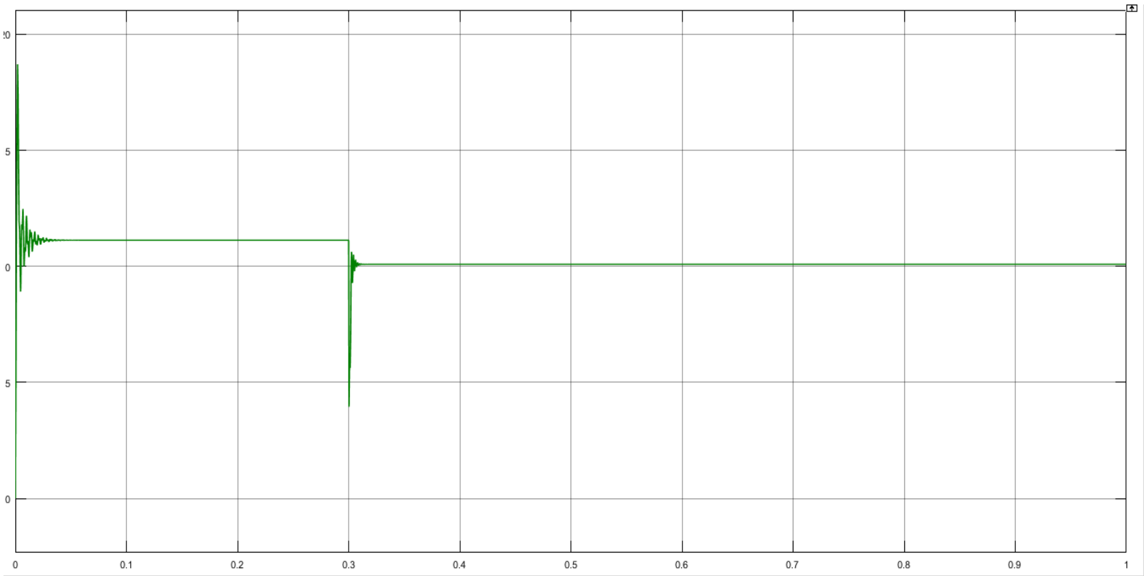

Fig 7.12: Voltage at output of uncontrolled POELC with change in load resistance

In figure 7.12, resistance at load for POELC decreases by 50% at 0.3 sec. At disturbance, output voltage undergoes a transient change and drops from 11.13V to a new value of 10.09V with a time of 16.16 msec.

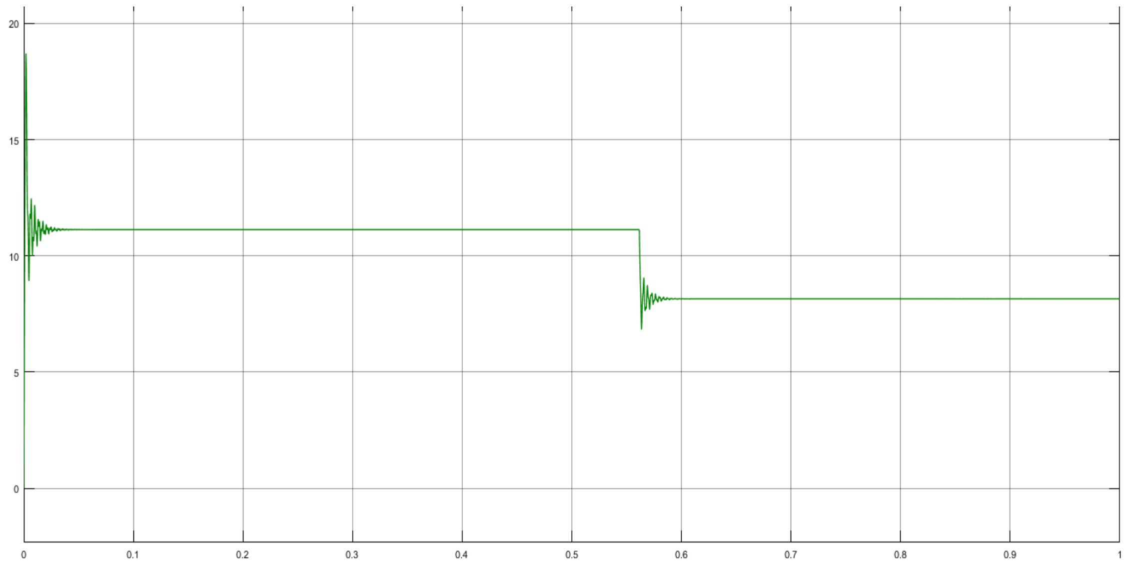

Fig 7.13: Voltage at output of uncontrolled POELC with change in voltage at supply

In fig 7.13, input voltage of POELC decreases from 12V to 9V at 0.55 sec. At disturbance, output voltage alters from 11.13V to 8.14V.

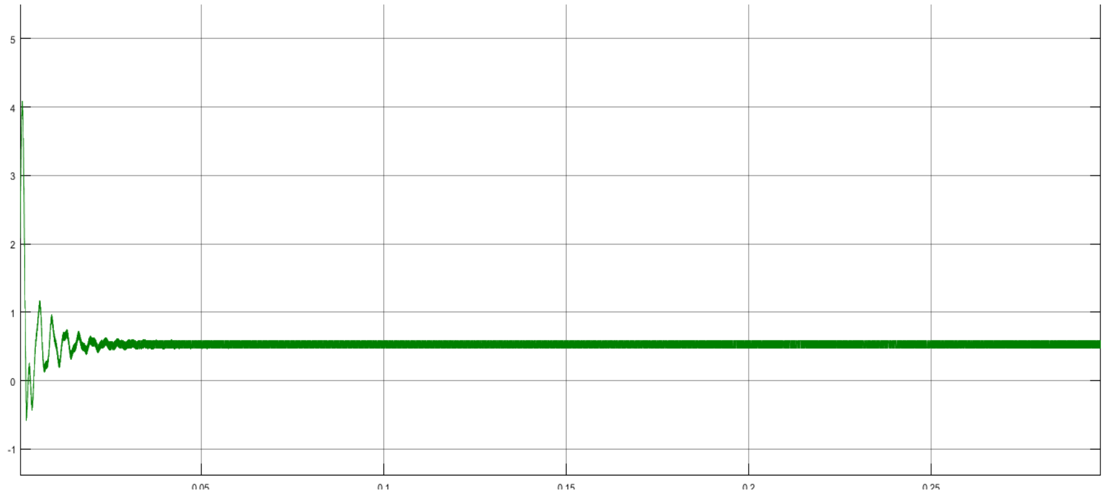

Fig 7.14: Inductor current of uncontrolled POELC

In fig 7.14, current through inductor of uncontrolled POELC is shown whose r.m.s value is 0.53A with ripples in the inductor current are 0.11A.

7.2.2 PI controlled positive output elementary Luo converter

Waveforms of output showingresults for PI controlled elementary Luo converter are given:

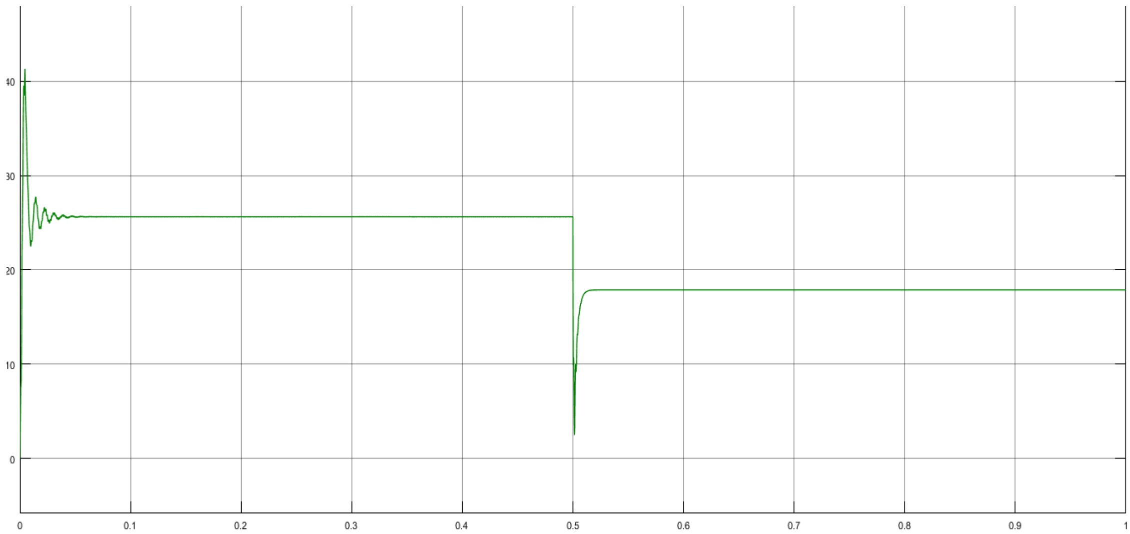

Fig 7.15: Voltage at output under PI control POELC with change in load resistance

In figure 7.15, the load resistance of PI controlled elementary Luo converter is decreased by 50% at 0.5 sec. At disturbance, output voltage alters from 25.6V to 17.8V

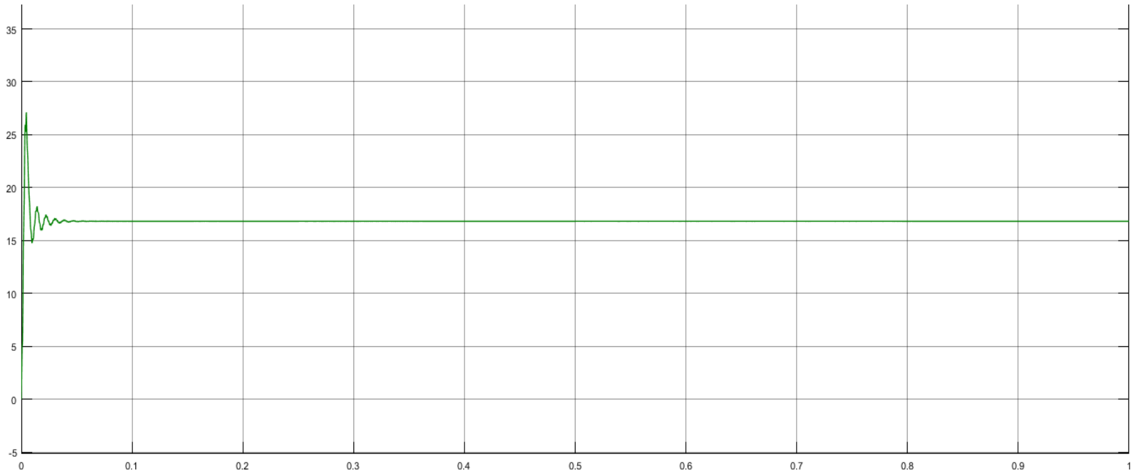

Fig 7.16: Voltage at output under PI control POELC with change in input voltage

In fig 7.16, input voltage of POELC decreases from 12V to 9V at 0.52 sec. Output voltage remains on the same value 16.8V.

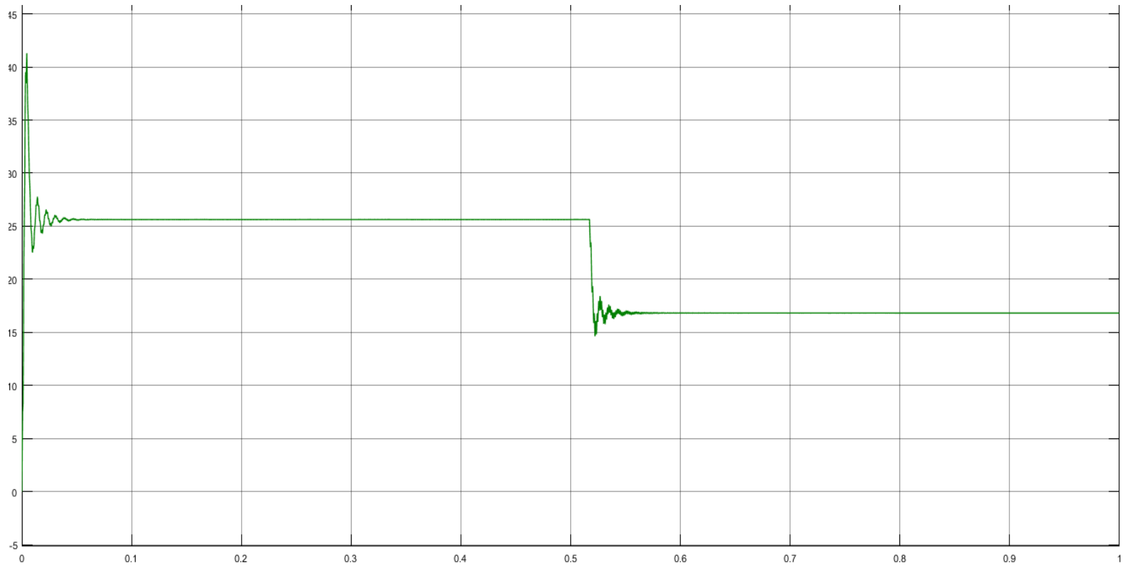

Fig 7.17: Voltage at output under PI control POELC with change in reference voltage

In fig 7.17, reference voltage decreases from 25V to 15V at 0.52 sec. Output voltage changes from 25.6V to 16.82V.

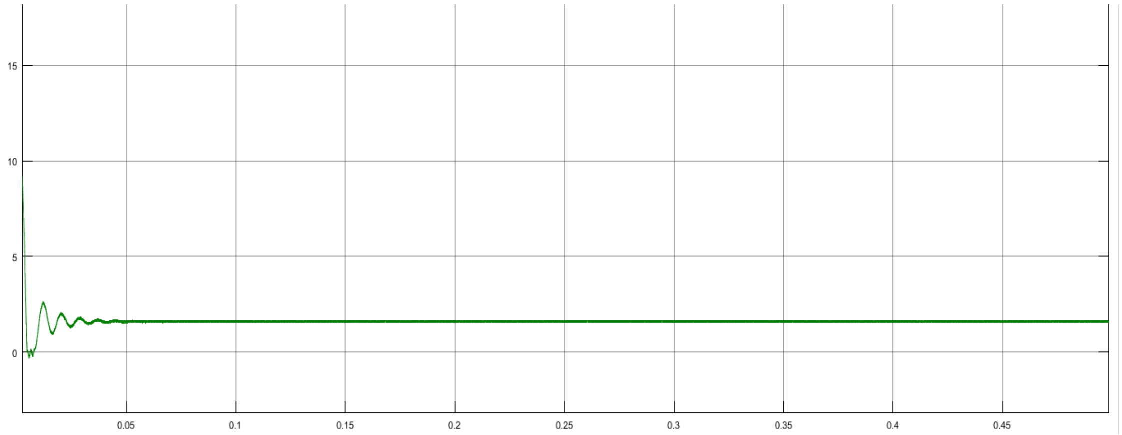

Fig 7.18: Inductor current of PI controlled POELC

In figure 7.18, current through inductor for PI controlled POELC whose r.m.s value is 1.69A with ripples 0.13A.

7.2.3 Sliding mode controlled positive output elementary Luo converter

Waveforms of output showing results for sliding mode controlled elementary Luo converter are given:

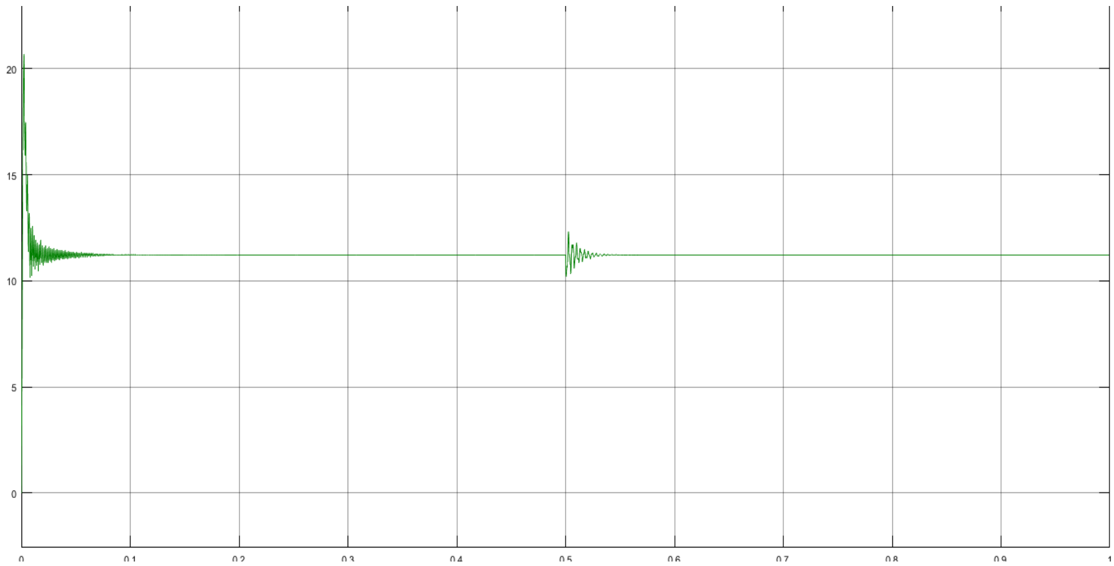

Fig 7.19: Voltage at output of POELC with SMC when load resistance is changed.

In figure 7.19, the load resistance of sliding mode controlled elementary Luo converter is suddenly decreased by 50% at 0.5 sec. At disturbance, output voltage undergoes a transient change but remains on the same voltage level of 11.22V.

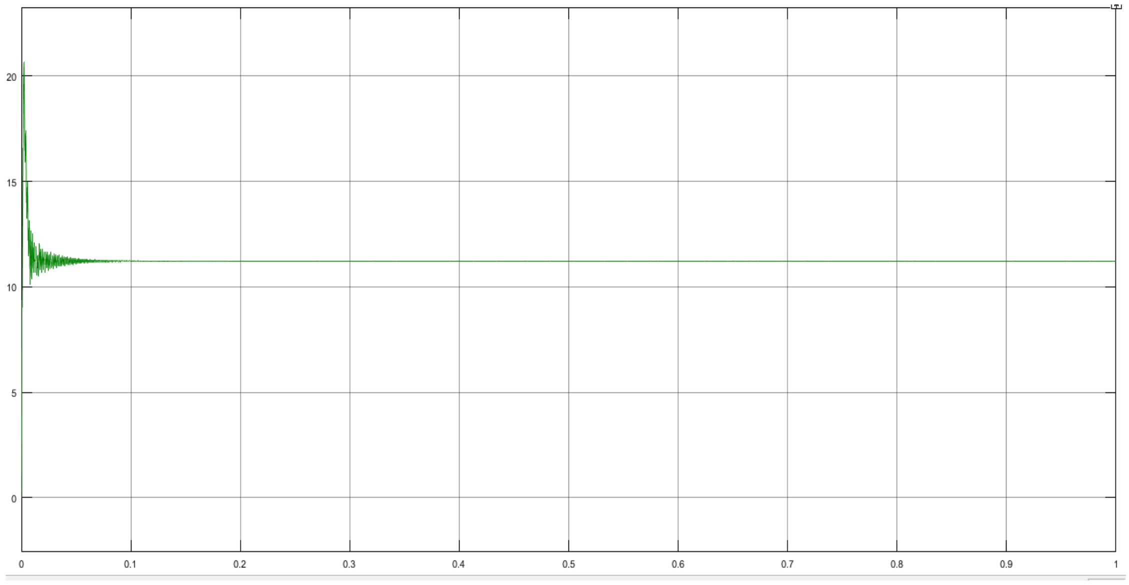

Fig 7.20: Voltage at output of POELC with SMC when supply voltage is changed..

In fig 7.20, voltage from supply decreases from 12V to 9V at 0.52 sec and output voltage remains at 11.22V.

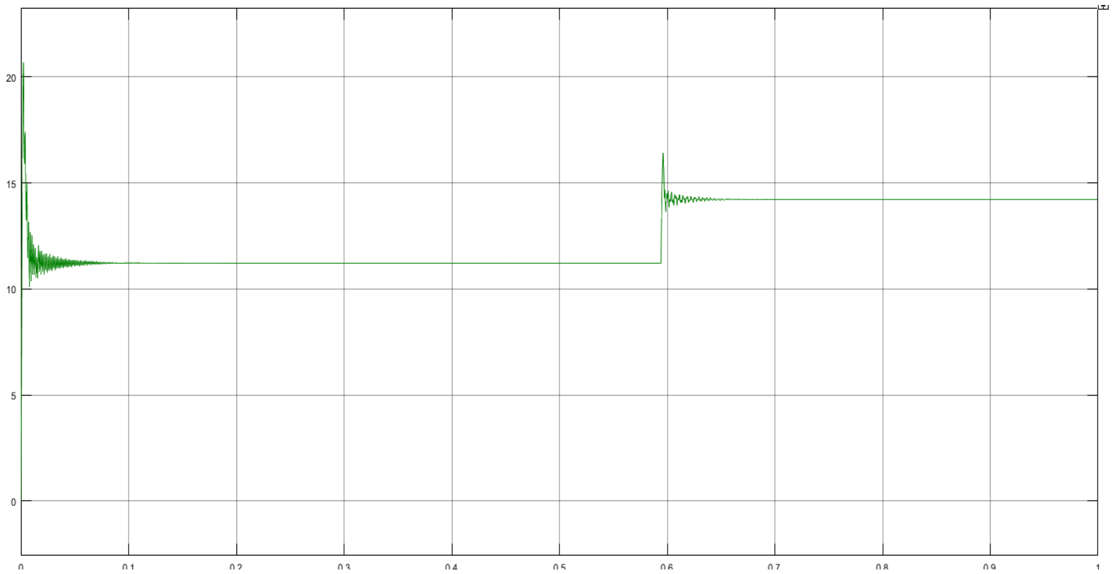

Fig 7.21: Voltage at output of POELC under SMC when reference voltage changed

In figure 7.21, the reference voltage of POELC increases from 12V to 15V at 0.5 sec. Output voltage alters from 11.22V to 14.23V.

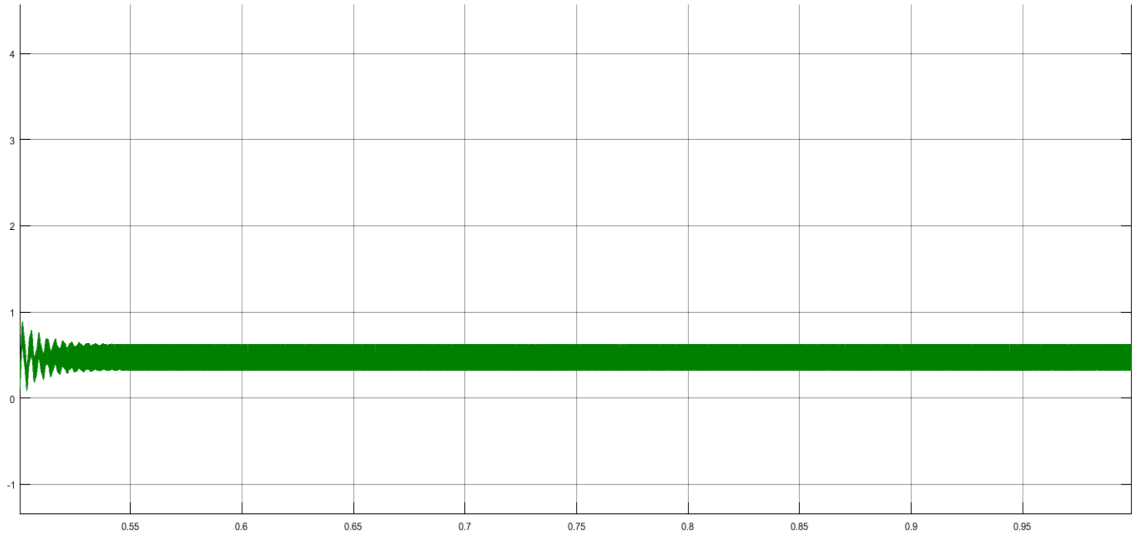

Fig 7.22: Inductor current of POELC under SMC

In figure 7.22, inductor current has r.m.s value 0.33A with ripples of 0.29A.

Table 7.2 Comparison of data of POELC with PI and SMC

Performance Parameters	Uncontrolled elementary Luo converter	PI controlled elementary Luo converter	Sliding mode controlled elementary Luo converter
Rise time (µsec)	407.98	406.44	131.85
Settling time(msec)	10.11	74.06	100.18
Overshoot(%)	77.53	174.71	165.42
Voltage ripple(mV)	0	2.17	0
Inductor current ripple(A)	0.11	0.13	0.29
Steady state error(mv)	0.87	0.62	0.78
Time taken to recover from disturbance(msec)	16.16	20.33	40.15

7.2.4 Conclusion

Table 7.2 presents the data from the uncontrolled, PI controlled and sliding mode controlled configurations of elementary Luo converter. Rise time shows that sliding mode controlled converter is faster than PI controlled. It takes large time to settle as compared with uncontrolled and PI controlled converter models. Percentage overshoot is also significantly less in sliding mode configuration than the PI controller. Ripples in output voltage are zero in sliding mode. From the waveforms, it's concluded that SMC tends to follows reference voltage under variations in circuit. It provides better rejection of disturbances.

7.3POSITIVE OUTPUT SELF-LIFT LUO CONVERTER

The output waveforms of POSLLC under certain parameter disturbances are presented below.

7.3.1 Uncontrolled positive output self-lift Luo converter

Waveforms of output showing results of uncontrolled POSLLC are presented:

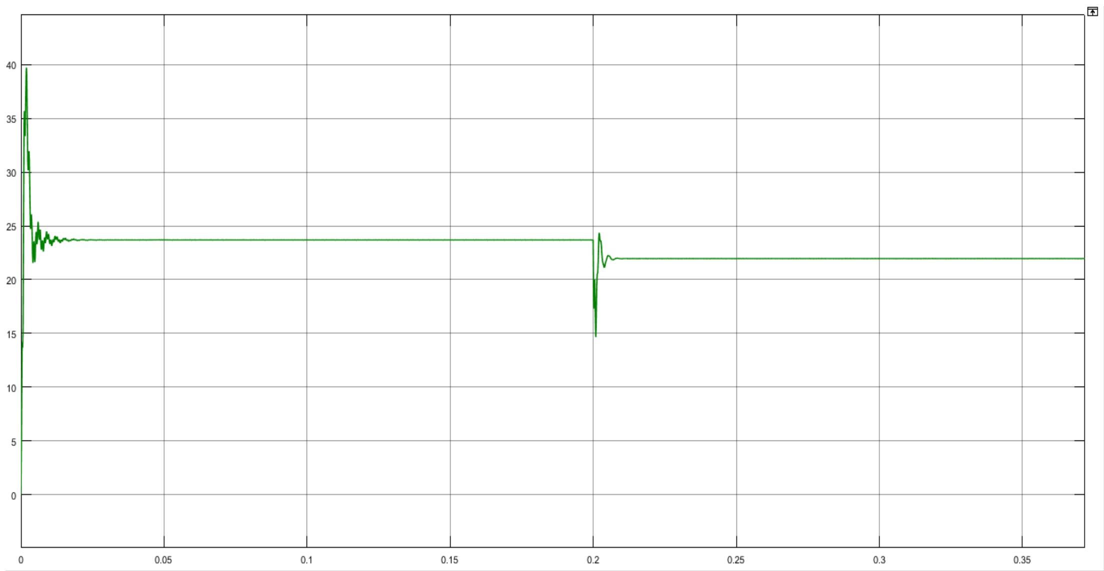

Fig 7.23: Voltage at output of uncontrolled POSLLC with change in load resistance.

In figure 7.23, the load resistance of the self-lift converter is suddenly decreased by 50% at 0.3 seconds. At disturbance, output voltage undergoes a transient change and drops from 23.69V to 21.96V with a time of 8.925 msec.

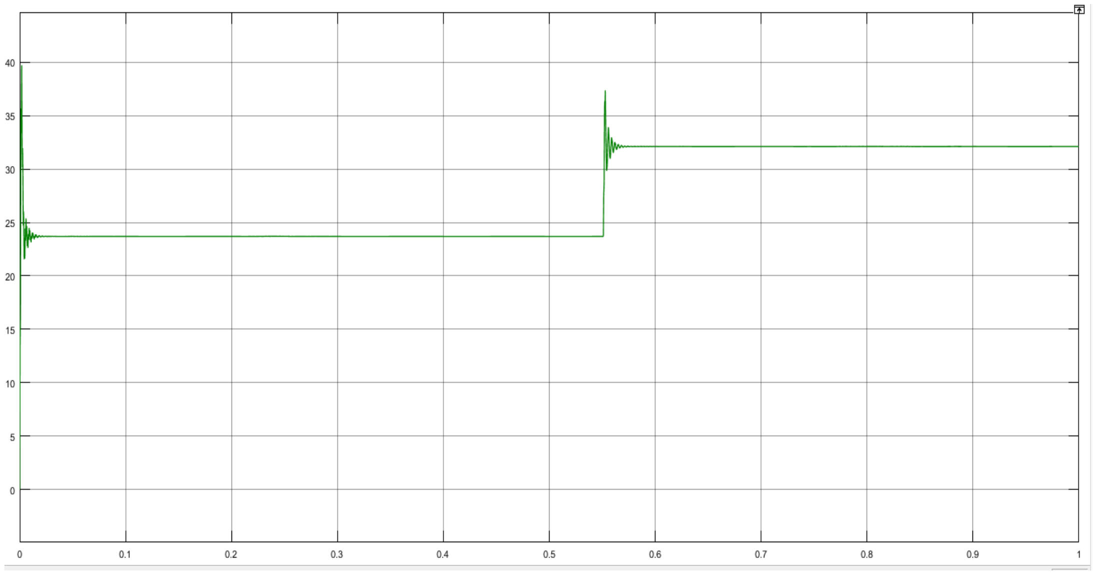

Fig 7.24: Voltage at output of uncontrolled POSLLC with change in voltage at supply

In fig 7.24, voltage at supply of POSLLC decreases from 12V to 9V at 0.55 sec. At disturbance, output voltage drops suddenly from 32.12V to 23.69V.

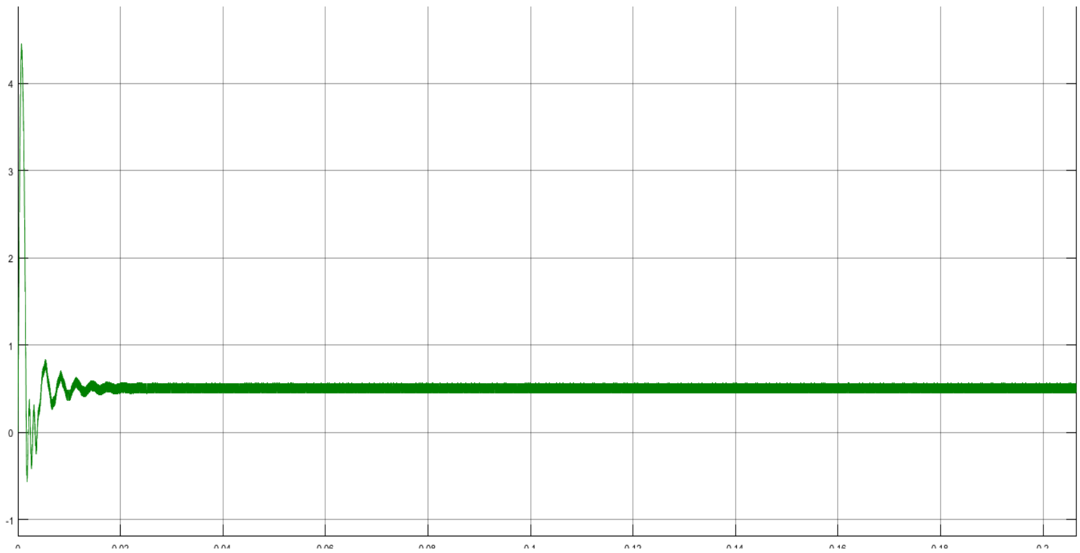

Fig 7.25: Inductor current of uncontrolled POSLLC

In figure 7.25, current through inductor of uncontrolled POSLLC with r.m.s value of 0.57A and the ripples in the inductor current are 0.11A.

7.3.2 PI controlled positive output self-lift Luo converter

Waveforms of output showing results for PI controlled POSLLC are given:

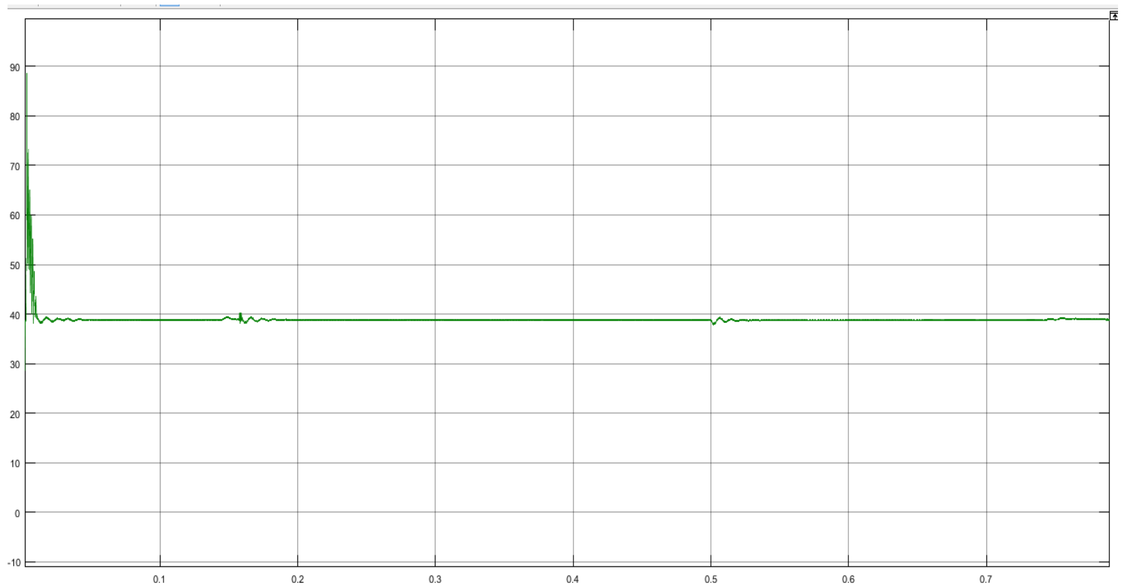

Fig 7.26: Voltage at output under PI control POSLLC with change in load resistance.

In figure 7.26, the load resistance of PI controlled self-lift Luo converter is suddenly decreased by 50% at time 0.5 seconds. Waveform shows no observable changes in load voltage.

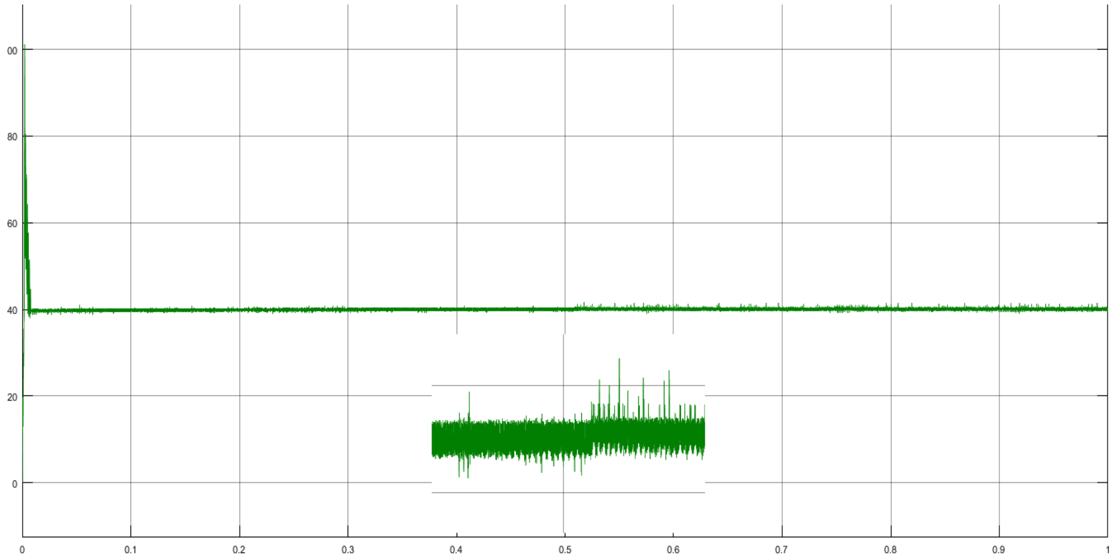

Fig 7.27: Voltage at output under PI control POSLLC with changes in supply voltage.

In fig 7.27, input voltage of self-lift Luo converter increases from 12V to 15V at time 0.5 seconds. Voltage at output increases by 0.19V. The ripples in output voltage also increases from 1.3V to 1.47V with increase in input voltage.

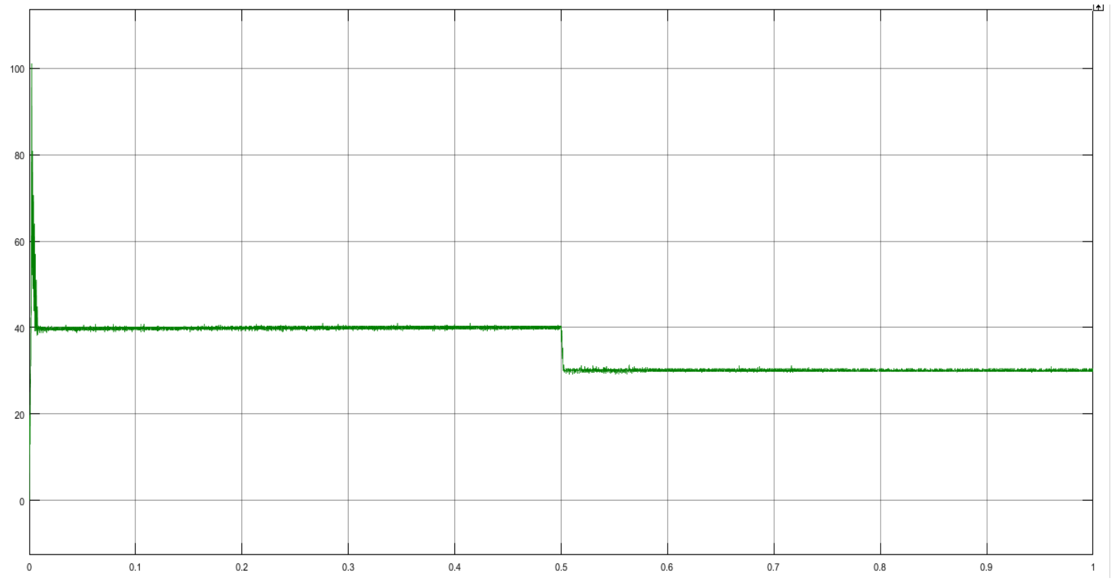

Fig 7.28: Voltage at output under PI control POSLLC with change in reference voltage.

In fig7.28, reference voltage of POSLLC decreases from 40V to 30V at 0.5 sec and output voltage changes from 39.9V to 30.02V.

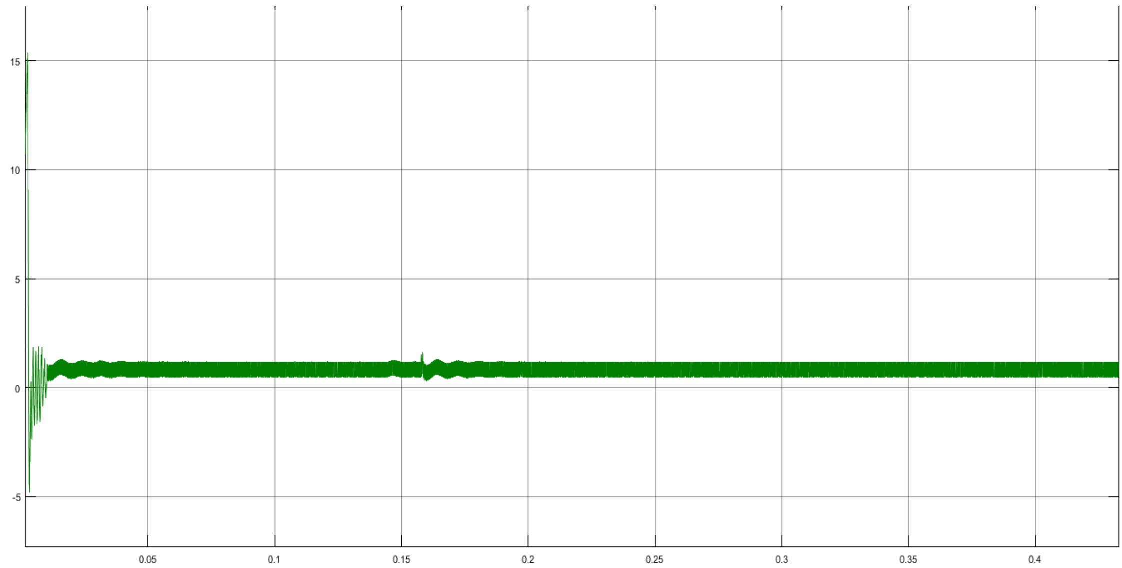

Fig 7.29: Current through inductor of POSLLC with PI controller

In fig 7.29, inductor current of PI controlled POSLLC whose r.m.s value is 1.13A with ripples of 0.64A.

7.3.3 Sliding mode controlled positive output self-lift Luo converter

Waveforms of output showing results for sliding mode controlled POSLLC are given:

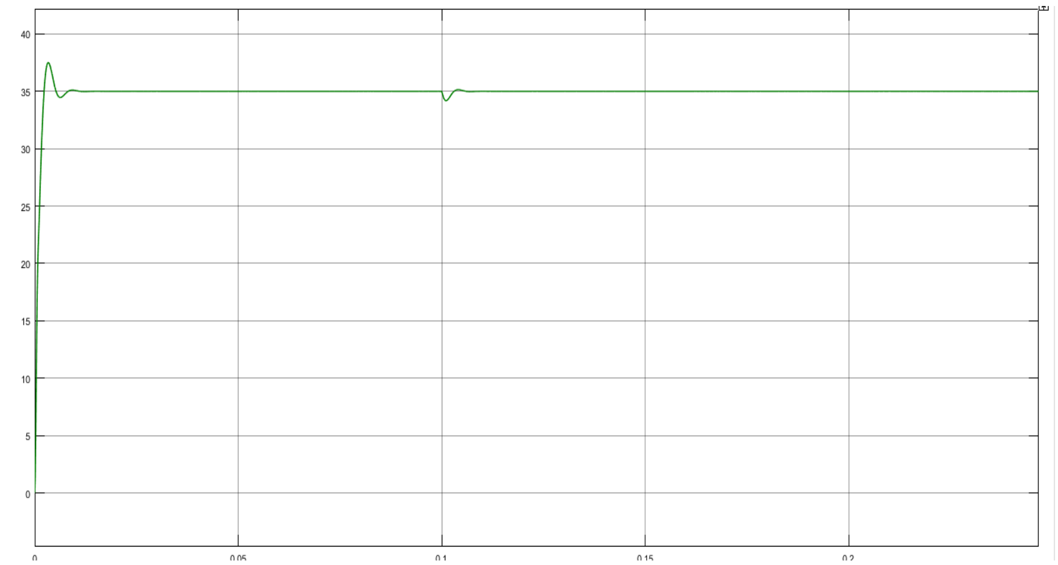

Fig 7.30: Voltage at output of POSLLC under SMC with change in load resistance.

In figure 7.30, the load resistance of sliding mode controlled self-lift Luo converter is suddenly decreased by 50% at time 0.1 second. At disturbance, the output voltage slightly drops and immediately rises again to the reference voltage value of 35V.

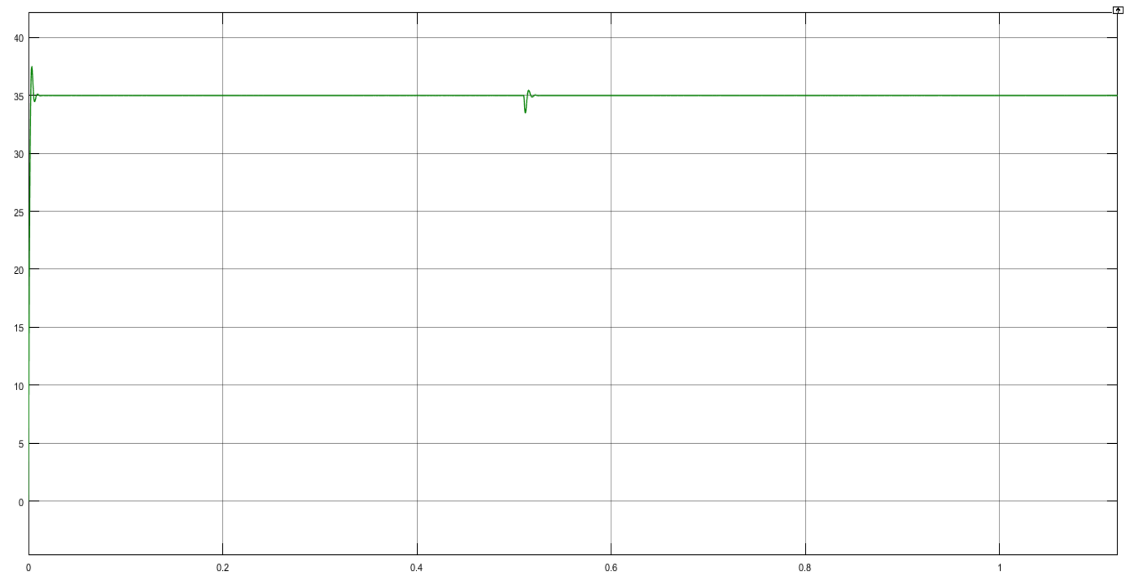

Fig 7.31: Voltage at output of POSLLC under SMC with change in supply

In fig 7.31, supply of POSLLC decreases from 12V to 9V at 0.5 sec. Voltage at output drops At disturbance but immediately regains a value of 35V same as the reference voltage.

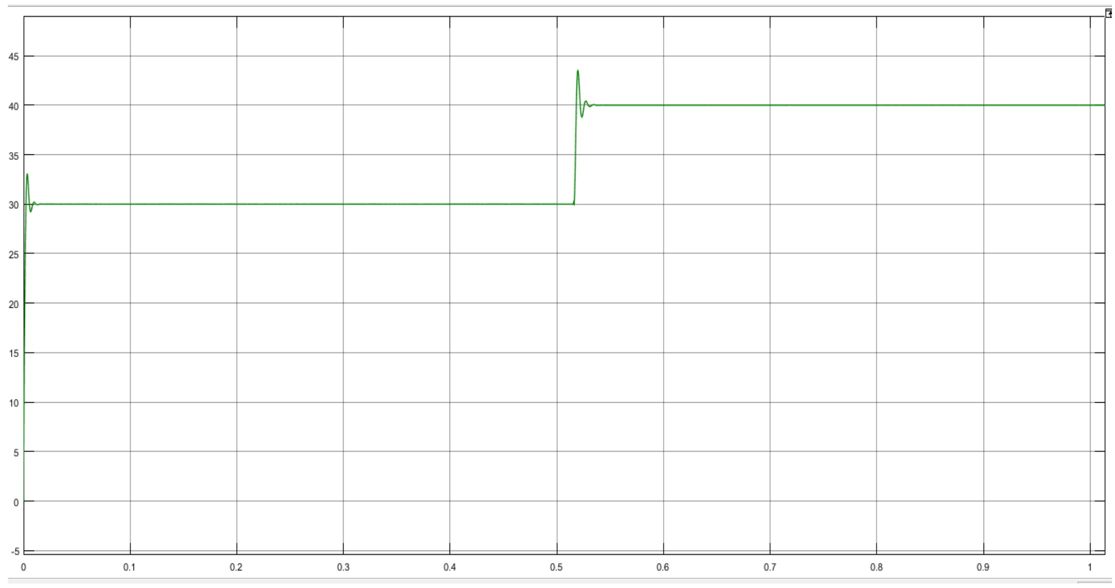

Fig 7.32: Voltage at output of POSLLC under SMC with change in reference voltage.

In figure 7.32, the reference voltage of the self-lift Luo converter increases from 30V to 40V at 0.52 sec. Voltage at output immediately follows the reference voltage and changes from 30V to 40V.

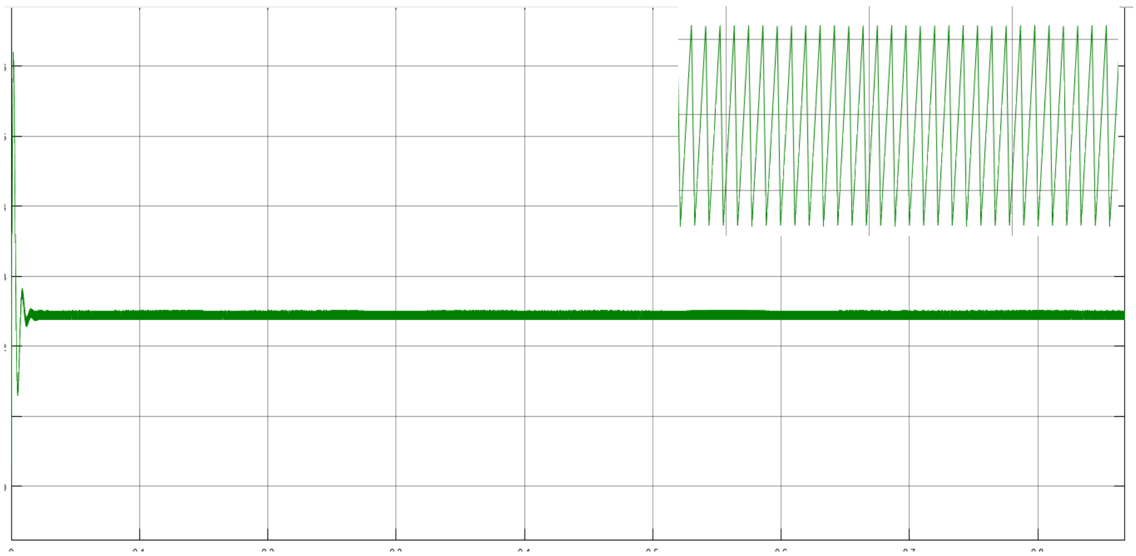

Fig 7.33: Inductor current of POSLLC under SMC

In figure 7.33, inductor current of SMC POSLLC whose r.m.s value is 1.14A with ripples 0.16A.

Table 7.3 Comparison of data of POSLLC under PI and SMC

Performance	Uncontrolled	PI controlled	Sliding mode

Parameters	POSLLC	POSLLC	controlled POSLLC
Rise time (msec)	0.17	0.26	1.61
Settling time(msec)	14.816	53.871	4.076
Overshoot (%)	121.226	180.019	6.989
Voltage ripple(mV)	20	226	6.862
Inductor current ripple(A)	0.116	0.643	0.16
Steady state error(V)	1.31	1.1	0
Time taken to recover from disturbance(msec)	8.925	23.197	3.406

7.3.4 Conclusion

Table 7.3 presents the data from the uncontrolled, PI controlled and sliding mode controlled configurations of self-lift Luo converter. Sliding mode controlled converter is slower as compared to the other two configurations but it settles faster than uncontrolled and PI controlled converter models. Percentage overshoot is significantly less in sliding mode configuration than the other two. Ripple in voltage at output and current through inductor is reduced in sliding mode control. Steady state error is zero for sliding mode controlled self-lift Luo converter. After disturbances are introduced in the system, sliding mode control takes minimum time to achieve the new steady state. Hence, sliding mode control provides better system performance than a PI controller for the control of self-lift Luo converter.

7.4 SUPER-LIFT LUO CONVERTER

The output waveforms of super-lift Luo converter under certain parameter disturbances are presented below.

7.4.1 Uncontrolled super-lift Luo converter

Waveforms of output showing results for uncontrolled super-lift Luo converter are given:

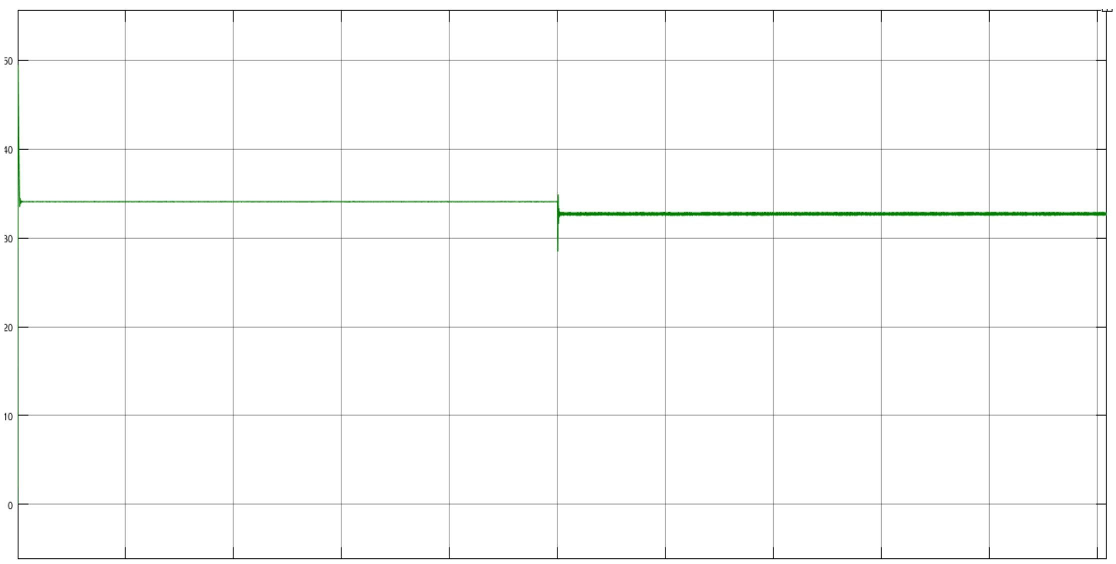

Fig 7.34: Voltage at output of uncontrolled POSLC with change in load resistance.

In figure 7.34, the load resistance of the super-lift converter is suddenly decreased by 50% at 0.3 sec. At disturbance, output voltage undergoes a transient change and drops from 34.05V to 32.55V with a time of 2.526 msec.

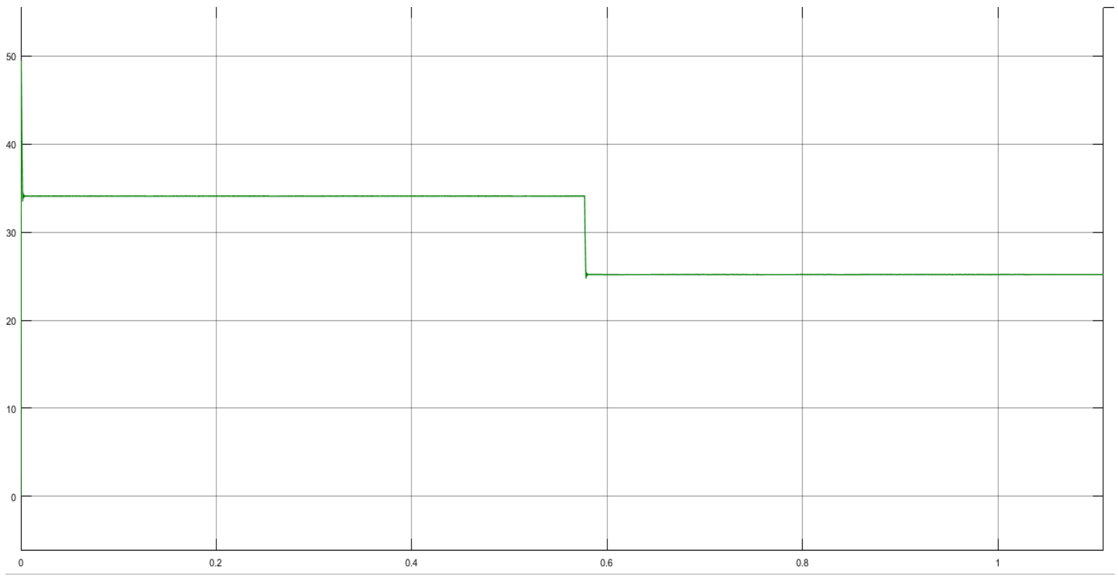

Fig 7.35: Voltage at output of uncontrolled POSLC with change in supply

In fig 7.35, the supply of super-lift Luo converter is suddenly decreased from 12V to 9V at 0.55 sec. At disturbance, output voltage drops from 34.06V to 25.18V.

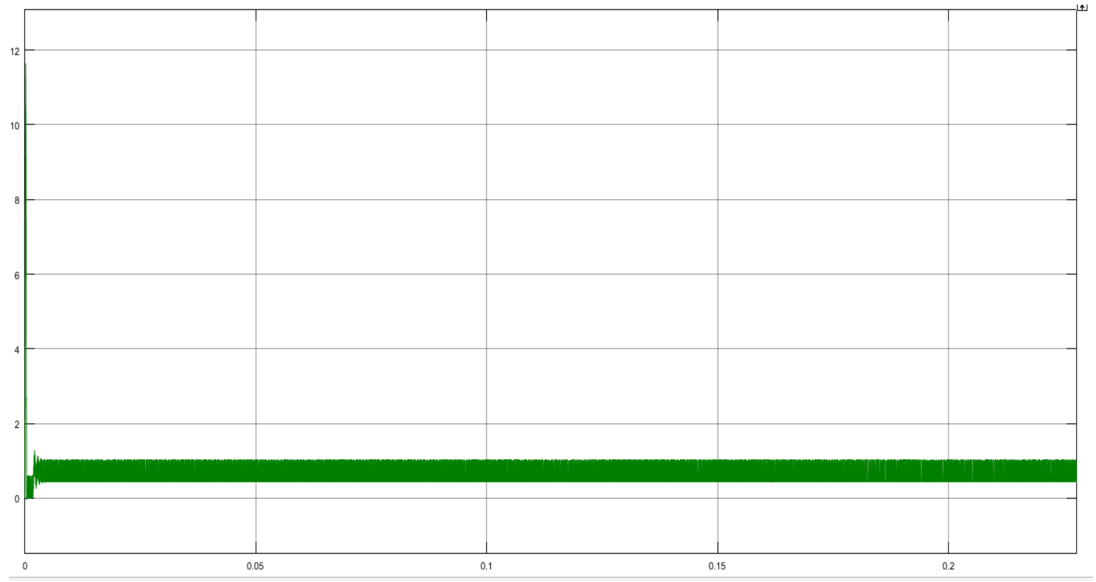

Fig 7.36: Inductor current of uncontrolled POSLC.

In figure 7.36, the current through inductor of uncontrolled super-lift Luo converter with r.m.s value 0.87A and ripples 0.59A.

7.4.2 PI controlled super-lift Luo converter

Waveforms of output showing results for PI controlled super-lift Luo converter are given:

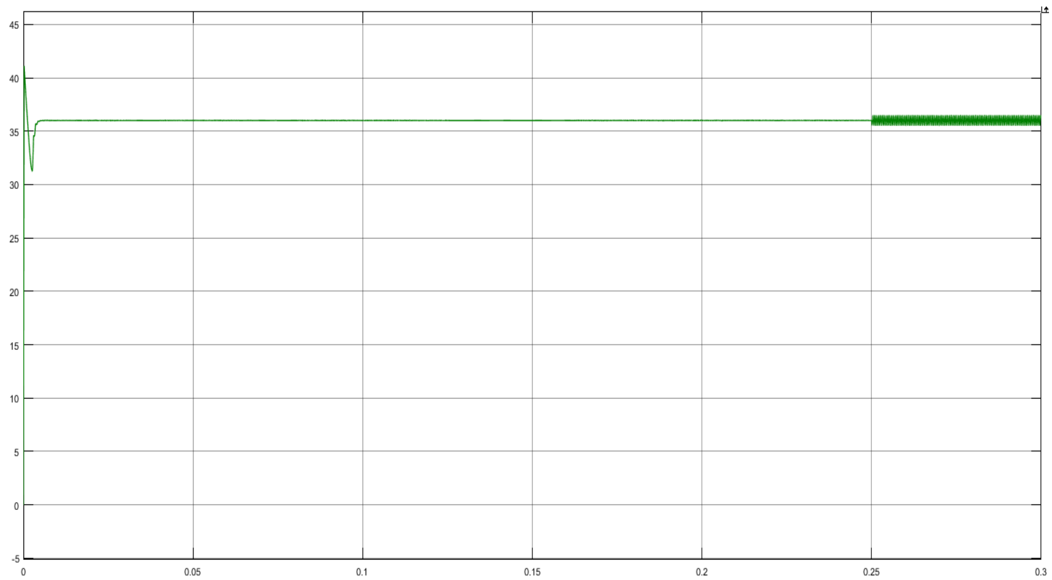

Fig 7.37: Voltage at output under PI control POSLC with change in load resistance.

In figure 7.37, the load resistance of PI controlled super-lift Luo converter is decreased by 50% at time 0.25 seconds. The ripples in output voltage increases from 0.03V to 0.97V.

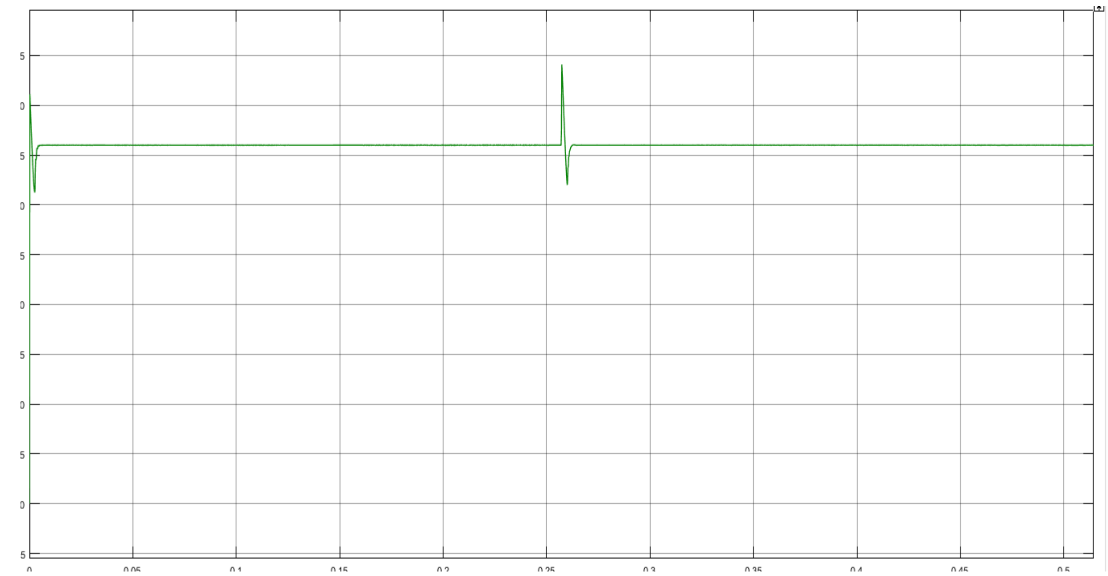

Fig 7.38: Voltage at output under PI control POSLC with change in input voltage.

In figure 7.38, supply of POSLC is increased from 12V to 15V at 0.5 sec. Output voltage alters from 39.9V to 40V. The ripples in output voltage decreases from 0.22V to 0.13V

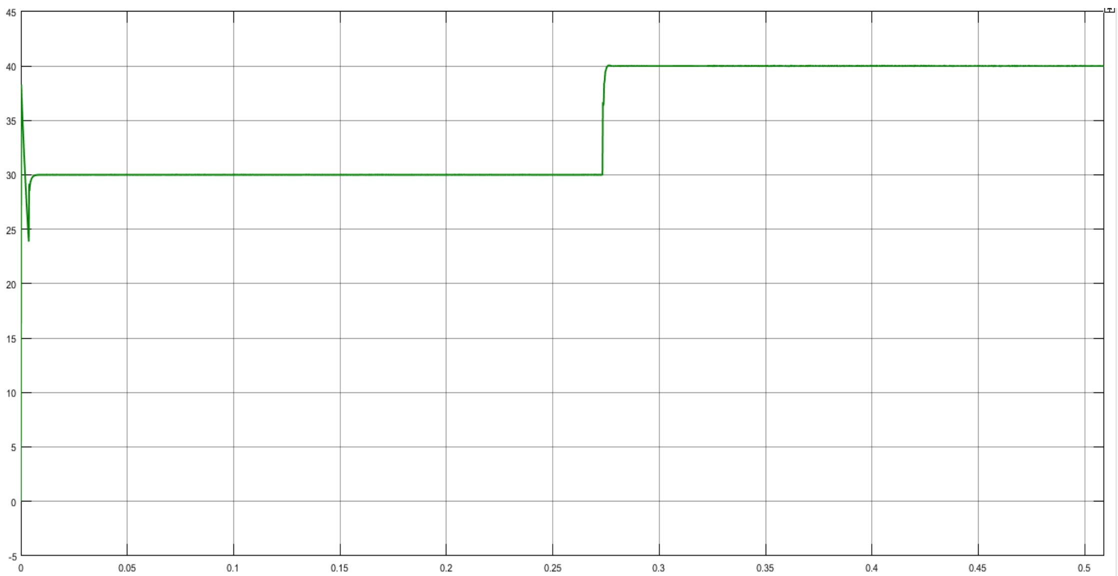

Fig 7.39: Voltage at output under PI control POSLC with change in reference voltage.

In figure 7.39, reference voltage of super-lift Luo converter is increased from 30V to 40V at 0.5 seconds. Output voltage follows reference and changes from 30V to 39.9V.

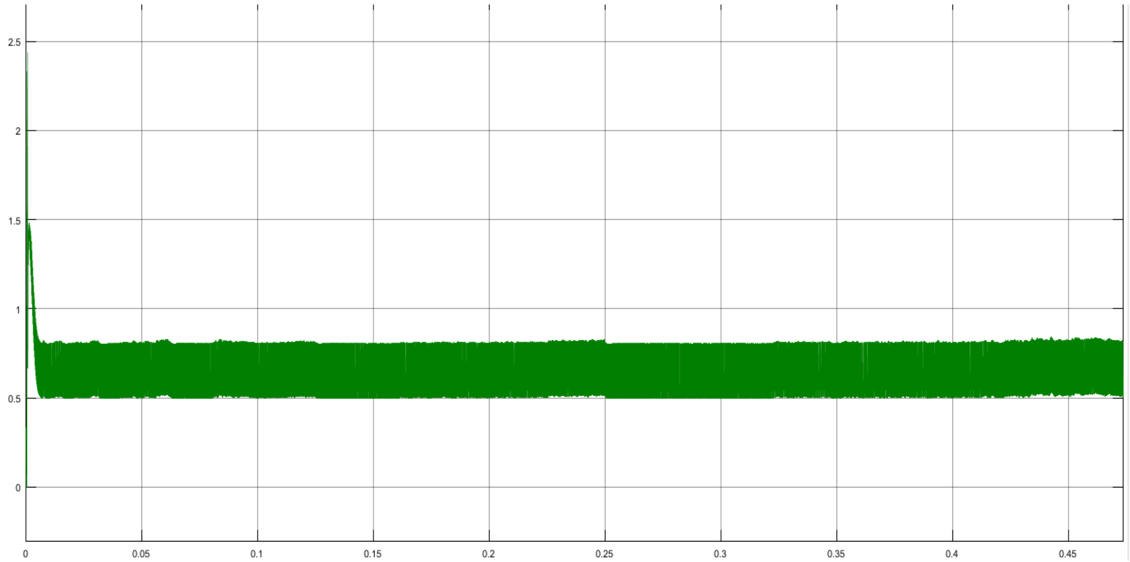

Fig 7.40: Current through inductor POSLC with PI

In fig 7.40, current through inductor of POSLC with PI whose r.m.s value is 0.67A with ripples 0.3A.

7.4.3 Sliding mode controlled super-lift Luo converter

Waveforms of output showing results for sliding mode controlled super-lift Luo converter are given:

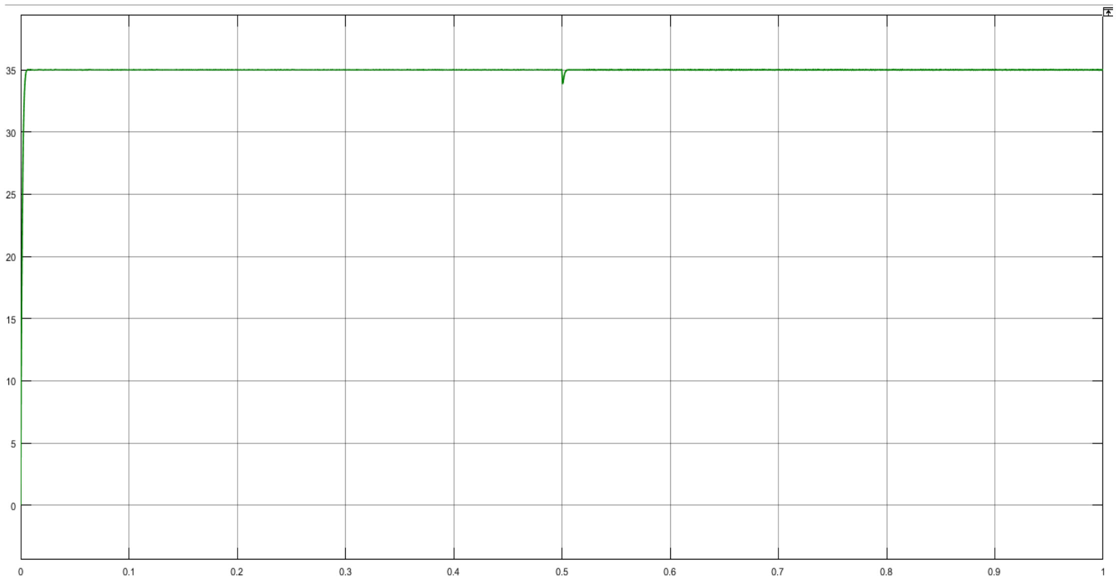

Fig 7.41: Voltage at output of POSLC under SMC with change in load resistance

In figure 7.41, the load resistance of sliding mode controlled super-lift Luo converter is suddenly decreased by 50% at time 0.5 second. At disturbance, the output voltage slightly drops and immediately rises again to the reference voltage value of 35V.

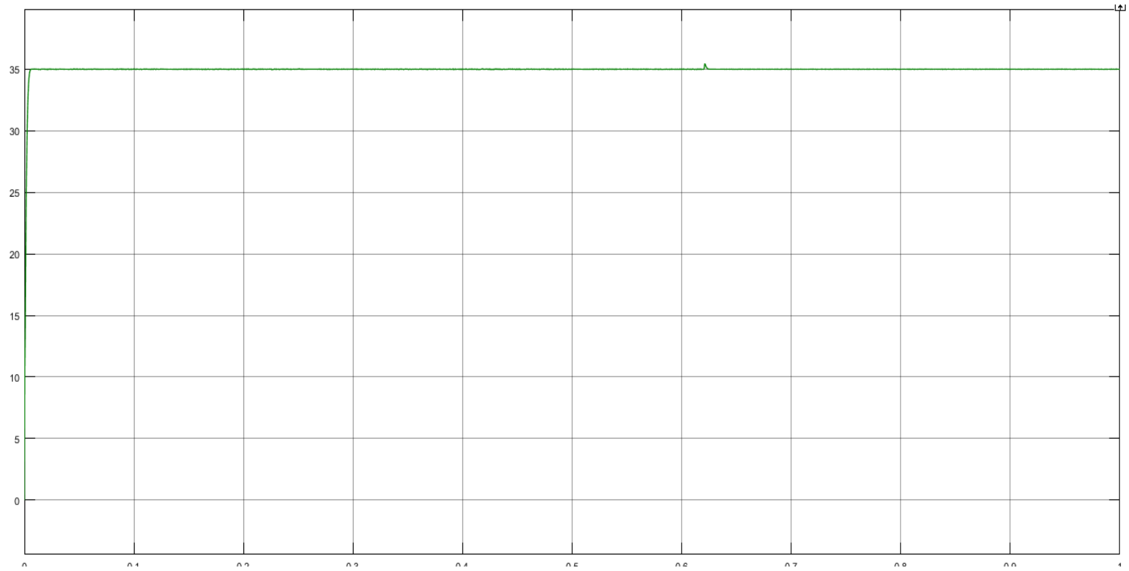

Fig 7.42: Voltage at output of POSLC under SMC with change in input voltage.

In figure 7.42, supply voltage of POSLC decreases from 12V to 9V at 0.5 sec. Voltage across output drops at disturbance but immediately regains a value of 35V same as the reference voltage.

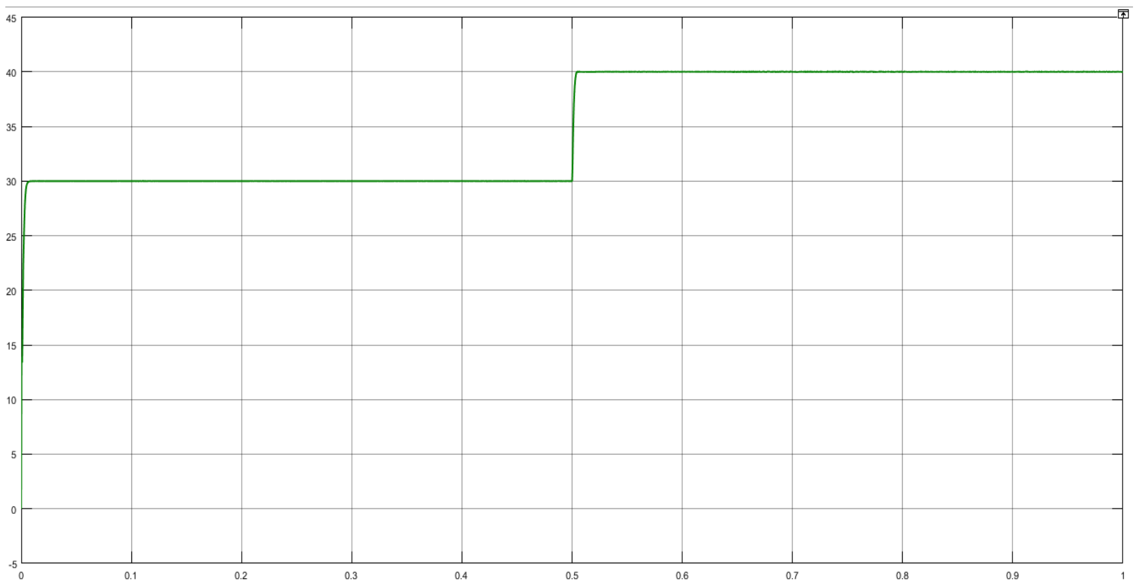

Fig 7.43: Voltage at output of POSLC with SMC when reference voltage is changed.

In figure 7.43, the reference voltage of the super-lift Luo converter increases from 30V to 40V at 0.5 sec. Voltage at output immediately follows the reference voltage and changes from 30V to 40V.

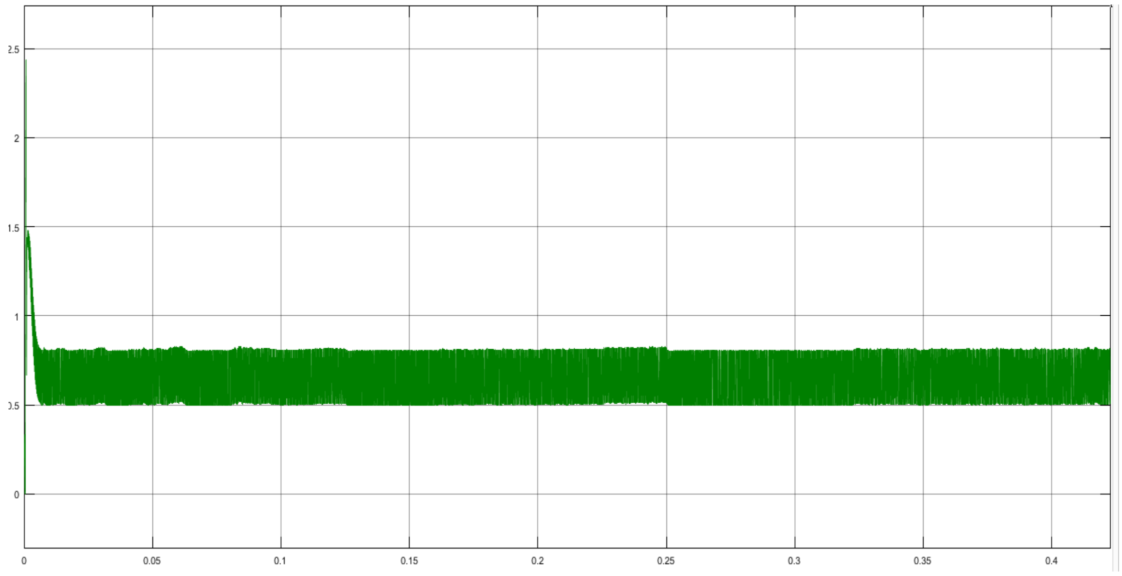

Fig 7.44: Inductor current of POSLC under SMC

In figure 7.44, the inductor current of POSLC with SMC whose r.m.s value is 0.67A and ripples is 0.3A.

Table 7.4 Comparison of data of POSLC under PI and SMC

Performance Parameters	Uncontrolled super-lift Luo converter	PI controlled super-lift Luo converter	Sliding mode controlled super-lift Luo converter
Rise time (msec)	0.122	0.118	2.427
Settling time(msec)	2.215	3.410	2.77
Overshoot (%)	65.625	20.161	0.714
Voltage ripple(mV)	60	30	40
Inductor current ripple (A)	0.59	0.3	0.3
Steady state error(V)	0.82	0.03	0
Time taken to recover from disturbance(msec)	2.526	4.435	4.06

7.4.4 Conclusion

Table 7.4 presents the data from the uncontrolled, PI controlled and sliding mode controlled configurations of super-lift Luo converter. Sliding mode controlled converter is slower as compared to the other two configurations but it settles faster than PI controlled converter. Percentage overshoot is significantly less in sliding mode configuration than the other two. Ripples in current across inductor and output voltage reduce under sliding mode control. Steady state error becomes zero for sliding mode controlled super-lift Luo converter. After disturbances are introduced in the system, sliding mode control takes minimum time to achieve the new steady state. Hence, sliding mode control provides better system performance than a PI controller.

7.5 ULTRA-LIFT LUO CONVERTER

Waveforms of output voltage for NOULLC under certain parameter disturbances are presented below.

7.5.1 Uncontrolled ultra-lift Luo converter

Waveforms of output showing results for uncontrolled ultra-lift Luo converter are given:

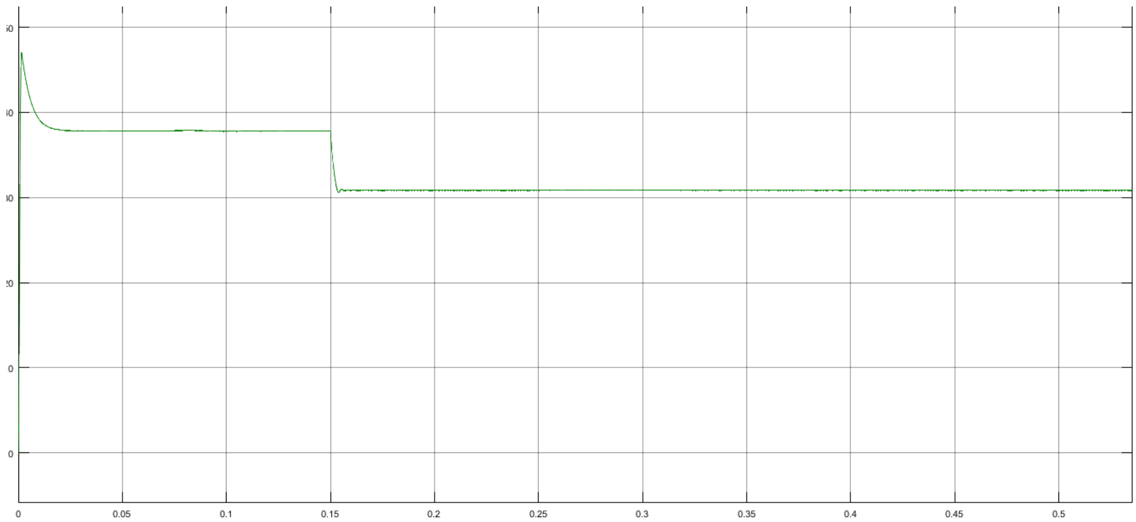

Fig 7.45: Voltage at output of uncontrolled NOULLC with change in load resistance.

In figure 7.45, resistance at load of the NOULLC decreases by 50% at 0.15 sec. At disturbance, output voltage undergoes a transient change and drops from 37.8V to 30.8V with a time of 16.07 msec

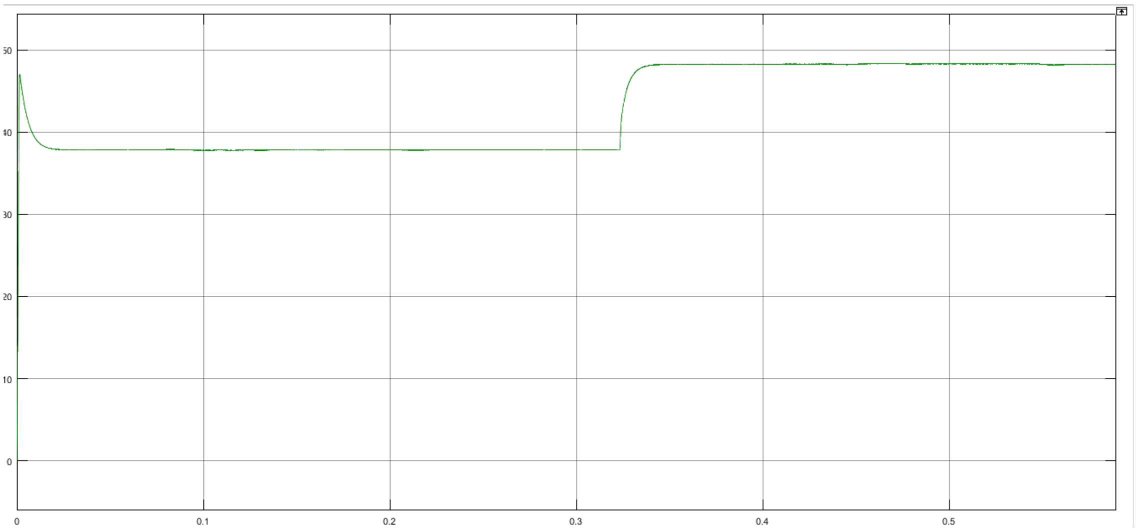

Fig 7.46: Voltage at output of uncontrolled NOULLC with change in input voltage.

In figure 7.46,supply voltage of NOULLC increases from 12V to 15V at 0.32 sec. Output voltage alters from 37.8V to 40.23V.

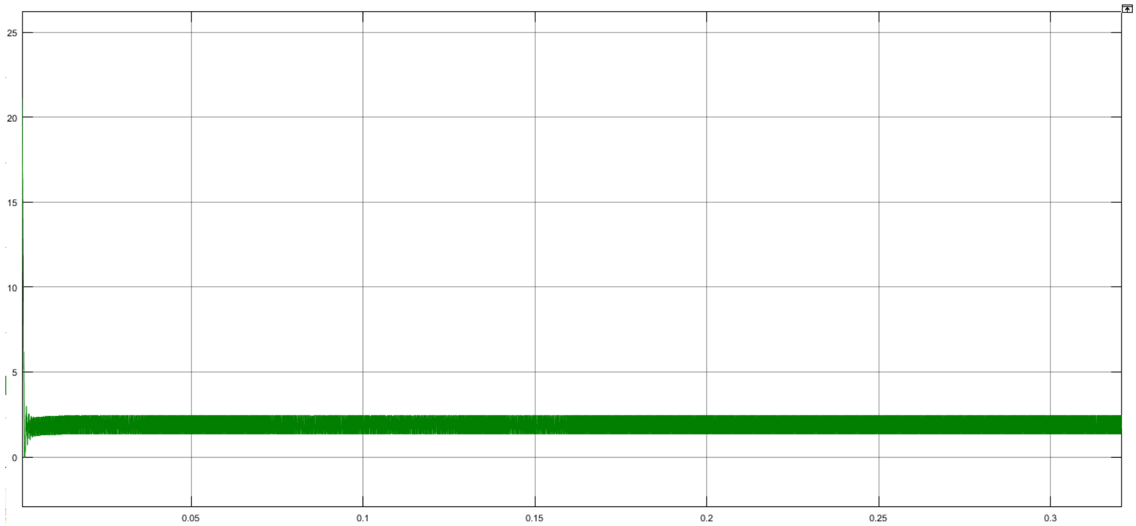

Fig 7.47: Inductor current of uncontrolled NOULLC

In figure 7.47, current across inductor of uncontrolled NOULLC whose r.m.s value is 1.61A and ripple present is 1.09A.

7.5.2 PI controlled ultra-lift Luo converter

Waveforms of output showingresults for PI controlled ultra-lift Luo converter are given:

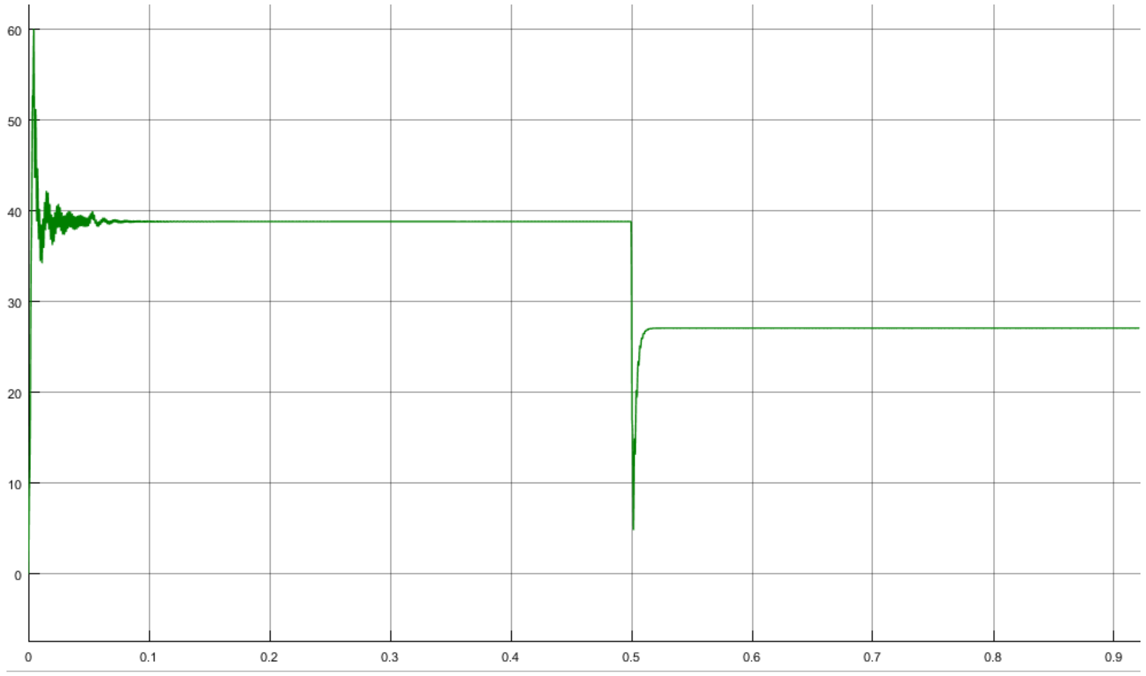

Fig 7.48: Voltage at output under PI control NOULLC with change in load resistance.

In figure 7.48, the load resistance of PI controlled ultra-lift Luo converter is decreased by 50% at time 0.5 seconds. Voltage at output increases from 38.8V to 27V.

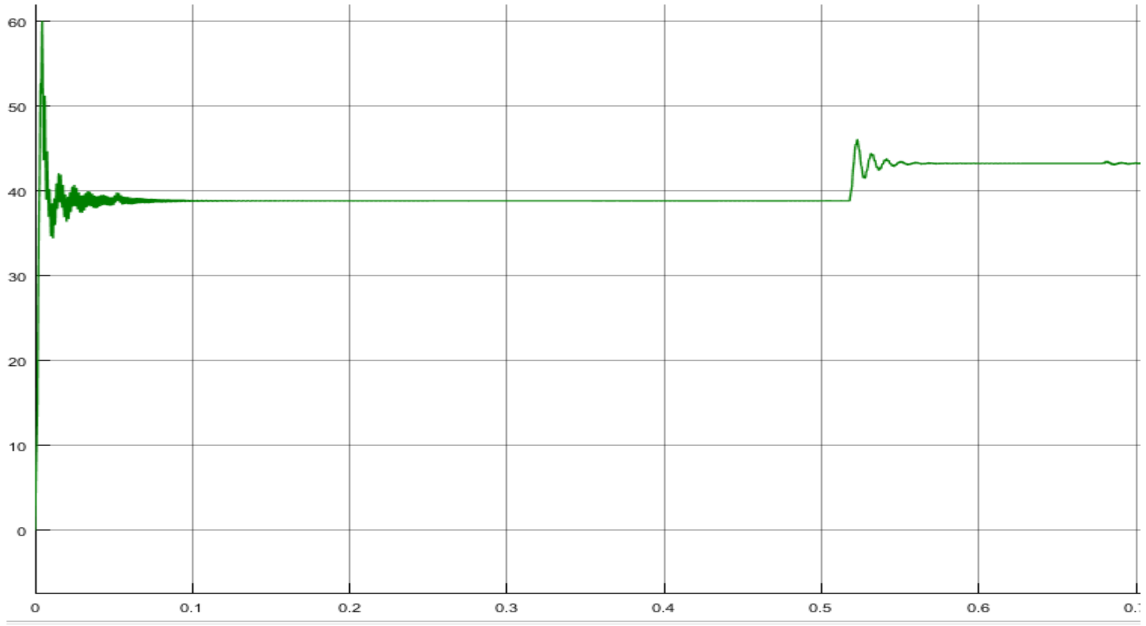

Fig 7.49: Voltage at output under PI control NOULLC with change in supply

In fig 7.49, supply of NOULLC is increased from 12V to 15V at time 0.51 seconds. The output voltage increases from 38.8V to 43.2V.

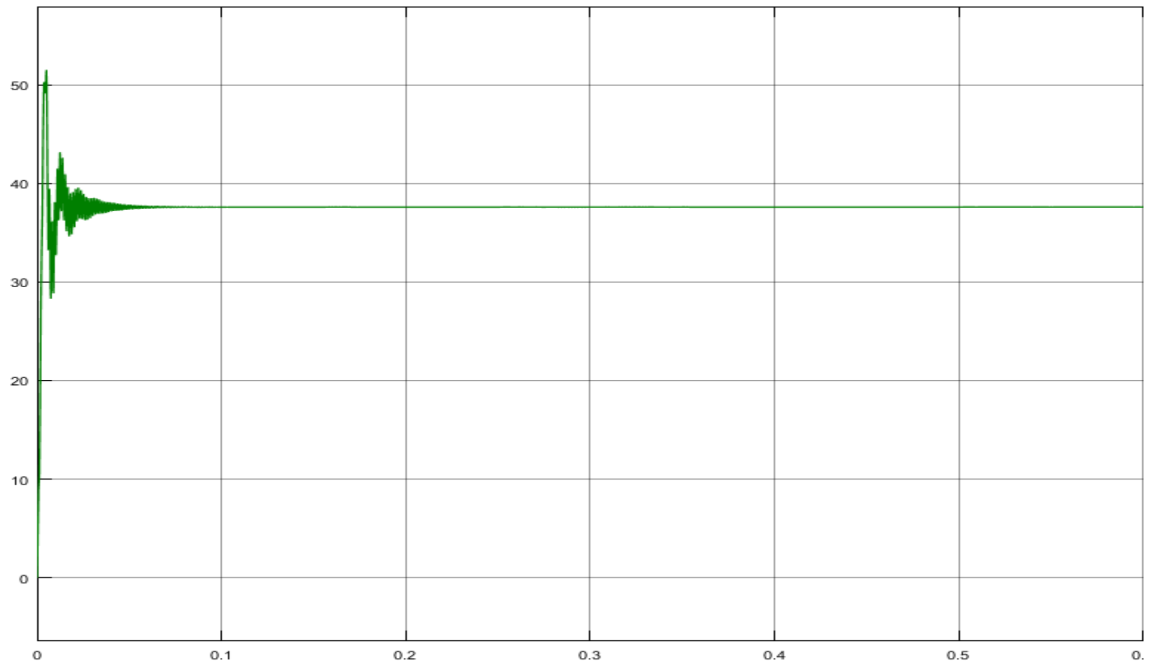

Fig 7.50: Voltage at output under PI control NOULLC with change in reference voltage.

In figure 7.50, the reference voltage of ultra-lift Luo converter is increased from 40V to 50V at time 0.25 seconds. No observable change is there in voltage across load.

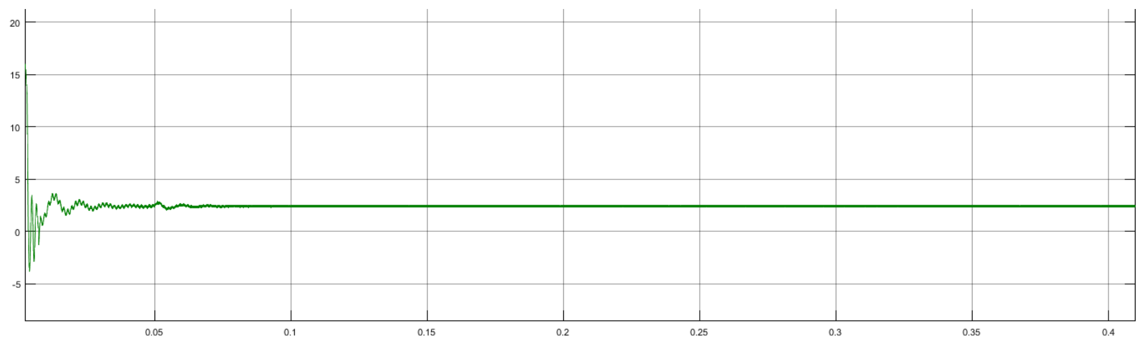

Fig 7.51: Inductor current of PI controlled NOULLC

In fig 7.51, current through inductor of PI controlled NOULLC whose r.m.s value is 2.691A and ripples are 0.19A.

7.5.3 Sliding mode controlled ultra-lift Luo converter

Waveforms of output showing results for SMC NOULLC are given:

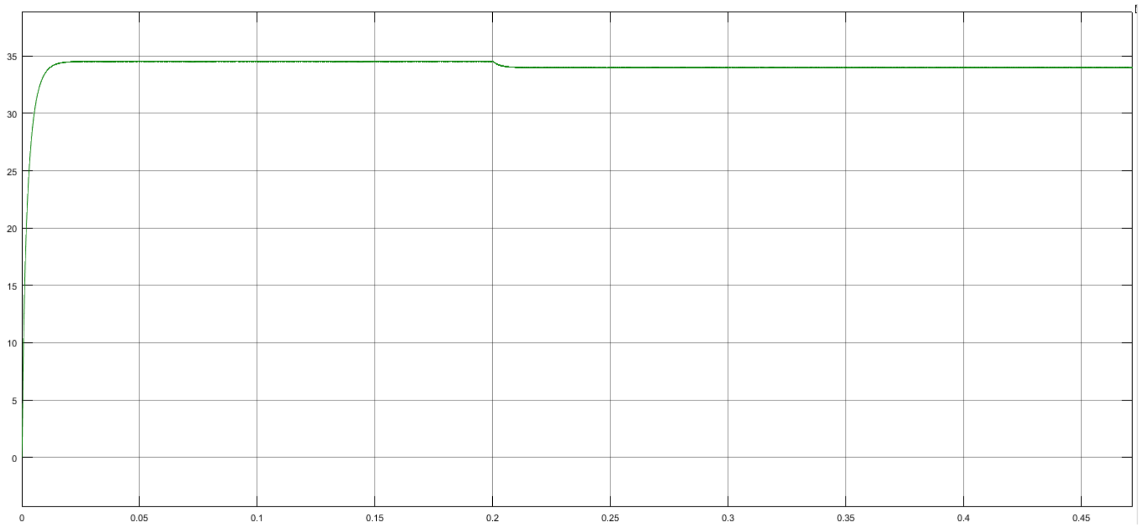

Fig 7.52: Voltage at output of NOULLC under SMC when change in load resistance.

In figure 7.52, the load resistance of sliding mode controlled ultra-lift Luo converter is suddenly decreased by 50% at 0.2 sec. Output voltage alters from 34.56V to 33.99V.

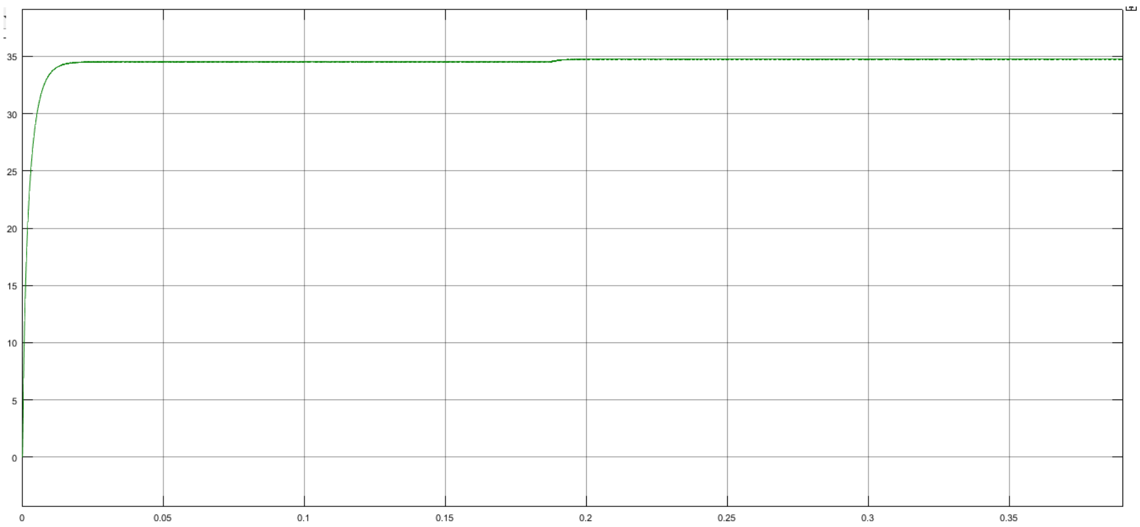

Fig 7.53: Voltage across output of NOULLC under SMC when change in supply

In fig 7.53, supply voltage of NOULLC increases from 9V to 12V at 0.2 sec.Output voltage alters from 34.56V to 34.74V.

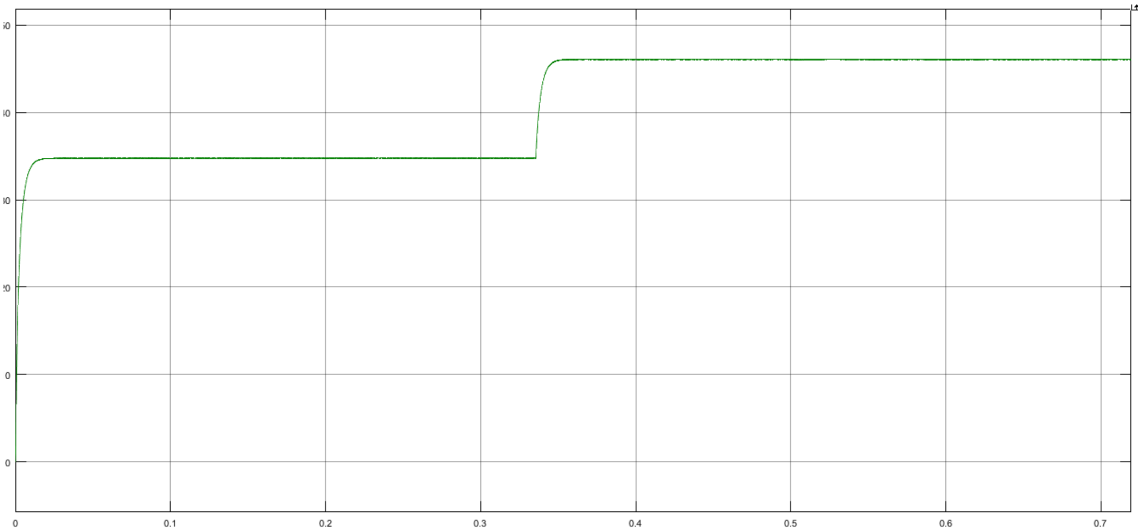

Fig 7.54: Voltage across output of NOULLC under SMC when change in reference voltage.

In figure 7.54, the reference voltage of the ultra-lift converter is increased from 35V to 45V at 0.32 sec. The output voltage alters from 34.79V to 46.07V.

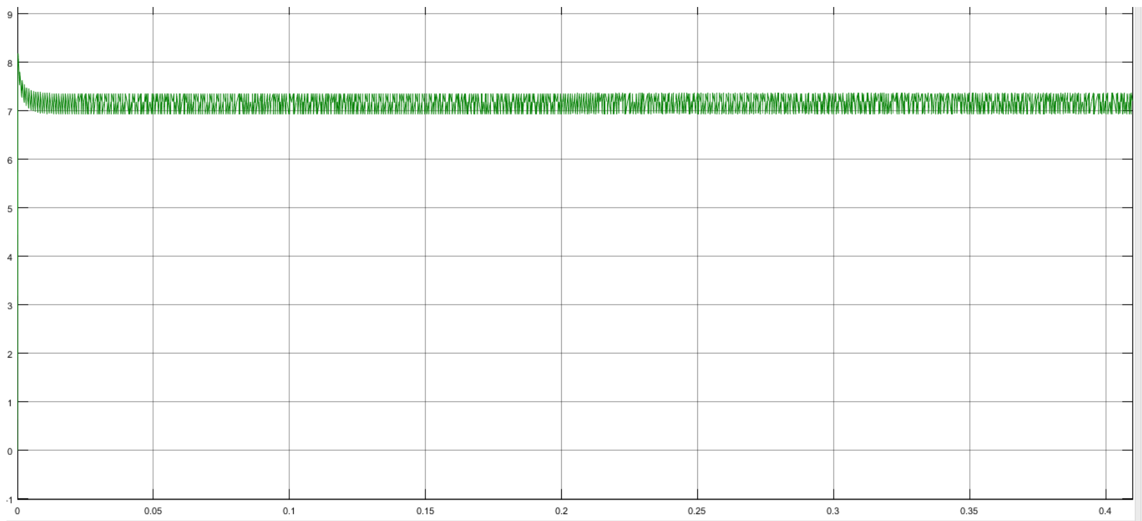

Fig 7.55: Inductor current of NOULLC under SMC

In figure 7.55, current through inductor of NOULLC is presented having r.m.s value 7.15A and ripple 0.44A.

Table 7.5 Comparison of data of NOULLC under PI and SMC

Performance Parameters	Uncontrolled NOULLC	PI controlled NOULLC	Sliding mode controlled NOULLC
Rise time (msec)	0.51	0.58	5.40
Settling time(msec)	11.70	40.20	8.13
Overshoot (%)	24.37	185.46	1.50
Voltage ripple(mV)	50	2.19	8
Inductor current ripple(A)	1.05	0.17	0.47
Steady state error(V)	2.87	1.18	0.47
Time taken to recover from disturbance(msec)	16.09	45.69	6.13

7.5.4 Conclusion

Table 7.5 presents the data from the uncontrolled, PI controlled and sliding mode controlled configurations of ultra-lift Luo converter. Sliding mode controlled converter is slower as compared to the other two configurations but it settles faster than both. Percentage overshoot significantly lessens in SMC configuration than the other two. Ripple in current through inductor and output voltage reduces under sliding mode control. Steady state error significantly lessens for NOULLC with SMC. After disturbances are introduced in the system, sliding mode control takes minimum time to achieve the new steady state. Hence, sliding mode control provides better system performance than a PI controller for the control of NOULLC.

CHAPTER 8

CONCLUSION AND FUTURE WORK

The primary goal of this dissertation was to investigate and analyze modeling of dc-dc converters , implementing controlling methods which can offer stable environment to the closed loop system under load, line disturbances. For this PI control and SMC have been instated on the dc-dc power converters.

From the analysis provided in this dissertation, it is inferred that dc-dc converters show better performance under sliding mode control. The sliding surface proposed in this dissertation for Luo converters includes an integration of output voltage error signal. Therefore, steady state error and the time taken to recover from a disturbance both are very less in SMC in comparison to PI controller and open loop system. The settling time of the system under SMC is significantly less than open loop and PI controlled system. PI controller is difficult to implement when higher order nonlinear converters are involved. Small signal state space analysis becomes complex when the order of converter is increased.

SMC is robust in nature and suitable for nonlinear power converters. But it also has certain disadvantages. Chattering phenomenon described as high frequency oscillation present in voltage at output is one of the major drawbacks of SMC. Certain methodologies can be implemented to reduce the chattering but it cannot be completely eliminated.

This dissertation includes the study and analysis of buck converter, elementary Luo converter, self-lift Luo converter, super-lift Luo converter and ultra-lift Luo converter. All the necessary details studied during the coursework have been presented in this dissertation along with parameters, calculation and results.

8.1 FUTURE WORK TO BE DONE

Based on research discussed in this dissertation, following researches can be carried out in future.

Circuital analysis of converters mentioned in this dissertation were performed both in CCM and DCM. However, modeling and control of these converters is performed only under continuous conduction mode. In practical applications DCM operation is also available. Therefore, modeling and control of these converters in discontinuous conduction is recommended.

The designed dc-dc converters along with controllers can be practically built and tested for various applications like electric drives, fast charging applications in electric vehicles. Effects of electromagnetic interference can also be studied.

APPENDIX

APPENDIX A

Parameters for buck converter

Supply Voltage V_{in} = 12V

Inductor L= 1 mH

Capacitor C = 10 μF

Load resistance R = 2 Ω

Switching frequency f = 100 kHZ

Parameters for Luo converter

Supply Voltage V_{in} = 12V

Inductor L_a= 1 mH

Inductor L_b=1 mH

Capacitor C_a = 47 μF

Capacitor C_b= 100 μF

Load resistance R = 12 Ω

Switching frequency f = 100 kHZ

APPENDIX B

Transfer function of converters and tuning PI controller.

For buck converter

Transfer function derived of converter and parameters mentioned in appendix A are:

$$\frac{\widehat{v_o}}{\hat{v}_{in}} = \frac{5x10^7}{s^2 + 10000\, s + 1x10^8}$$

$$\frac{\widehat{v_o}}{\hat{d}} = \frac{1.2x10^9}{s^2 + 10000\, s + 1x10^8}$$

Using Z-N tuning method, values of k_p ,k_i values obtained for buck converter are k_p = 0.055 and k_i = 72

For elementary Luo converter

Transfer function derived of converter and parameters mentioned in appendix A are:

$$\frac{\widehat{v_o}}{\hat{v}_{in}} = \frac{5x10^6\, s^2 \,+\, 1.421x10^{-7}\, s \,-\, 0.006715}{s^4 \,+\, 833.3\; s^3 \,-\, 6.383x10^5\, s^2 \,-\, 8.865x10^9\, s \,-\, 5.319x10^{13}}$$

$$\frac{\widehat{v_o}}{\hat{d}} = \frac{2.4x10^8\, s^2 -\, 2.128x10^{11}\, s \,+\, 0.1451}{s^4 \,+\, 833.3\; s^3 \,-\, 6.383x10^5\, s^2 \,-\, 8.865x10^9\, s \,-\, 5.319x10^{13}}$$

Using Z-N tuning method, the value of k_p and k_i values obtained for elementary Luo converter are k_p = 0.13, k_i = 8.87

For self-lift Luo converter

Transfer function derived of converter and parameters mentioned in appendix A are:

$$\frac{\widehat{v_o}}{\hat{v}_{in}} = \frac{2x10^7\, s^2 +\, 1.137x10^{-6}\, s +\, 6.84x10^{14}}{s^4 \,+\, 200\; s^3 +\, 1.18x10^8\, s^2 +\, 1.96x10^{10}\, s +\, 2.35x10^{14}}$$

$$\frac{\widehat{v_o}}{\hat{d}} = \frac{6.99x10^8\, s^2 -\, 1.095x10^{12}\, s +\, 2.4x10^{16}}{s^4 \,+\, 200\; s^3 +\, 1.18x10^8\, s^2 +\, 1.96x10^{10}\, s +\, 2.35x10^{14}}$$

Using Z-N tuning method, the value of k_p and k_i values obtained for self-lift Luo converter are $k_p = 0.3$, $k_i = 40$

For super-lift Luo converter

Transfer function derived of converter and parameters mentioned in appendix A are:

$$\frac{\widehat{v_o}}{\hat{v}_{in}} = \frac{1.064x10^7\ s\ +\ 3.024x10^{-7}}{s^3\ +\ 833.3\ s^2\ +\ 7.979x10^6\ s\ +\ 2.216x10^9}$$

$$\frac{\widehat{v_o}}{\hat{d}} = \frac{-3.83x10^5 s^2\ +\ 5.106x10^8\ s\ -\ 3.056x10^{11}}{s^3\ +\ 833.3\ s^2\ +\ 7.979x10^6\ s\ +\ 2.216x10^9}$$

Using Z-N tuning method, the value of k_p and k_i values obtained for super-lift Luo converter are $k_p = 0.015$ and $k_i = 74$

For ultra-lift Luo converter

Transfer function derived of converter and parameters mentioned in appendix A are:

$$\frac{\widehat{v_o}}{\hat{v}_{in}} = \frac{1.064x10^7\ s\ +\ 3.024x10^{-7}}{s^3\ +\ 833.3\ s^2\ +\ 7.979x10^6\ s\ +\ 2.216x10^9}$$

$$\frac{\widehat{v_o}}{\hat{d}} = \frac{-3.83x10^5 s^2\ +\ 5.106x10^8\ s\ -\ 3.056x10^{11}}{s^3\ +\ 833.3\ s^2\ +\ 7.979x10^6\ s\ +\ 2.216x10^9}$$

Using Z-N tuning method, the value of k_p and k_i values obtained for ultra-lift Luo converter are $k_p = 0.061$ and $k_i = 10.02$

REFERENCES

1. Chakraborty, S.; Vu, H.-N.; Hasan, M.M.; Tran, D.-D.; Baghdadi, M.E.; Hegazy, O. DC-DC Converter Topologies for Electric Vehicles, Plug-in Hybrid Electric Vehicles and Fast Charging Stations: State of the Art and Future Trends. Energies **2019**, 12, 1569. https://doi.org/10.3390/en12081569
2. Y. S. Lin, K. W. Hu, T. H. Yeh, and C. M. Liaw An electric vehicle IPMSM drive with interleaved front-end DC/DC converter IEEE Trans. Veh. Technol., vol. 65, no. 6, pp. 4493–4504, Jun. 2016.
3. C. H. Rivetta, A. Emadi, G. A. Williamson, R. Jayabalan, and B. Fahimi Analysis and control of buck DC-DC converter operating with constant power load in sea and undersea vehicles IEEE Trans. Ind. Appl., vol. 42, no. 2, pp. 559–572, Mar./Apr. 2006.
4. J. Sun Small-signal modeling of variable-frequency pulse width modulators IEEE Trans. Aerosp. Electron. Syst., vol. 38, no. 3, pp. 1104–1108, Jul. 2002.
5. Z. Rehman, I. Al-Bahadly, and S. Mukhopadhyay Multi input DC-DC converters in renewable energy applications- An overview Renew. Sustain. Energy Rev., vol. 41, pp. 521–539, 2015.
6. R. T. Naayagi, A. J. Forsyth, and R. Shuttleworth High power bidirectional DC-DC converter for aerospace applications IEEE Trans. Power Electron., vol. 27, no. 11, pp. 4366–4379, Nov. 2012.
7. Power Electronics Converters, Applications and Design(Ned Mohan, ToreM.Undeland, William P. Robbins),John Wiley and Sons,Inc,2003.
8. R. W. Erickson and D. Maksimovic, “Fundamentals of power electronics (Second Edition)”, Kluwer Academic Publishers, c2001.
9. M. H. Rashid, “Power electronics: circuits, devices and applications”, Prentice Hall, Upper Saddle River, NJ, USA, c1993, second edition.
10. P. N. Kanna and B. Meenakshi, "Analysis and design of DC-DC/AC non isolated cuk converter using sliding mode controller," 2015 International Conference on Circuits, Power and Computing Technologies [ICCPCT-2015], 2015, pp. 1-8, doi: 10.1109/ICCPCT.2015.7159294.
11. S. Cúk and R. D. Middlebrook, “A new optimum topology switching DC-TO-DC converter”, in the proceedings of the IEEE Power Electronics Specialists conference, PESC’ 1977, June 14 -16, 1977, pp. 160 – 179.

12. F. L. Luo, “Advance dc-dc converters”, CRC Press, Boca Raton, FL, USA, c2004.
13. Fang Lin Luo, Luo-Converters, a series of new DC-DC step-up (boost) conversion circuits at Proceedings of Second International Conference on Power Electronics and Drive Systems, 1997, pp. 882-888 vol.2, doi: 10.1109/PEDS.1997.627511.
14. F. L. Luo, “Positive output Luo converters: voltage lift technique”, IEEE proceedings Electric Power Applications, VOL. 146, NO. 4, July. 1999, pp. 415 –432.
15. F. L. Luo, “Negative output Luo converters: voltage lift technique”, IEEE proceedings Electric Power Applications, VOL. 146, NO. 2, March 1999, pp. 208– 224.
16. F. L. Luo and H. Ye, “Positive output super-lift converters”, IEEE Transactions on POWER ELECTRONICS, VOL. 18, NO. 1, January. 2003, pp. 105 – 113.
17. F. L. Luo and H. Ye, “Negative output super-lift converters”, IEEE Transactions on Power Electronics, VOL. 18, NO. 5, September 2003, pp. 1113 – 1121.
18. F. L. Luo, “Re-Lift converter: design, test, simulation and stability analysis”, IEEE proceedings on Electrical Power Applications, VOL. 145, NO. 4, July 1998, pp. 315 – 325.
19. Fang Lin Luo and Hong Ye, "Ultra-lift Luo-converter," 2004 International Conference on Power System Technology, 2004. PowerCon 2004, pp. 81-86 Vol.1, doi: 10.1109/ICPST.2004.1459970.
20. Fang Lin Luo, Luo-converters, voltage lift technique, PESC 98 Record. 29th Annual IEEE Power Electronics Specialists Conference (Cat. No.98CH36196), 1998, pp. 1783-1789 vol.2, doi: 10.1109/PESC.1998.703423
21. R. D. Middlebrook and S. Cúk, “A general unified approach to modeling switching-converter power stages”, International Journal of Electronics, VOL. 42,NO. 6, 1977, pp. 521 – 550.
22. A. J. Forsyth and S. C. Mollov, “Modeling and control of DC-DC converters”,Power Engineering Journal, Vol. 12, No. 5, October 1998, pp. 229 – 236
23. R. D. Middlebrook and S. Cúk, “Advances in switched-mode power conversion:Volumes I and II”, TESLAco, Pasadena, Calif., c1983.
24. S. Banerjee and G. C. Verghese, “Nonlinear phenomena in power electronics attractors, bifurcations, chaos and nonlinear control”, the Institute of Electrical and Electronics Engineers, IEEE press, New York, USA, c2001.
25. D. Czarkowski and M. K. Kazimierczuk, “Circuit models of PWM dc-dc converters”, in proceedings of the IEEE 1992 National Aerospace and Electronics Conference, 1992. NAECON’ 1992, VOL. 1, 18-22 May 1992, pp. 407 – 413.
26. A. R. Nikhar, S. M. Apte and R. Somalwar, "Review of various control techniques for DC-DC interleaved boost converters," 2016 International Conference on Global Trends in Signal

Processing, Information Computing and Communication (ICGTSPICC), 2016, pp. 432-437, doi: 10.1109/ICGTSPICC.2016.7955340.

27. Mumtaz, F.; Zaihar Yahaya, N.; Tanzim Meraj, S.; Singh, B.; Kannan, R.; Ibrahim, O. Review on non-isolated DC-DC converters and their control techniques for renewable energy applications. Ain Shams Eng. J. 2021.
28. Z. Chen, "PI and Sliding Mode Control of a Cuk Converter," in IEEE Transactions on Power Electronics, vol. 27, no. 8, pp. 3695-3703, Aug. 2012, doi: 10.1109/TPEL.2012.2183891.
29. K.Ogata, Modern Control Engineering, (5 th ed) , Prentice Hall, 2010, pp 681-724
30. P. Cominos and N. Munro, PID Controllers: Recent Tuning Methods and Design to Specification, IEE Proceedings Control Theory & Applications, Vol. 149, No. I, January 2002.
31. M.Beschi, S. Dormido, J. Sanchez, and A. Visioli. “An automatic tuning procedure for an event-based PI controller” in Proc. IEEE 52nd Annu. Conf. Decision Control (CDC), Dec. 2013, pp. 7437–7442.
32. H. Sira-Ramirez, and M. Ilic, “Exact linearization in switched mode dc to dc power converters”, International Journal of Control, VOL. 50, NO. 2, August 1989, pp. 511 – 524.
33. D. Liebal, P. Vijayraghavan, and N. Sreenath, “Control of dc-dc buck-boost converter using exact linearization techniques”, Power Electronics Specialists Conference, 1993. PESC '93 Record, 24th Annual IEEE, 20-24 June 1993, pp.203 – 207.
34. Utkin, V., Guldner, J., and Shi, J.X.: ‘Sliding mode control in electromechanical systems’ (Taylor and Francis, London, UK, 1999)
35. V. Utkin, Sliding Modes in Control Optimization. Berlin, Germany: Springer-Verlag, 1992.
36. C. Edwards and S. K. Spurgeron, Sliding Mode Control: Theory and Applications. London, U.K.: Taylor & Francis, 1998.
37. M. Salimi, J. Soltani, G. R. Arab-Markadeh, and N. R. Abjadi Adaptive nonlinear control of the DC-DC buck converters operating in CCM and DCM Int. Trans. Electr. Energy., vol. 23, no. 8, pp. 1536–1547, 2013.
38. F. Bilalovi´c, O. Mu˘si´c, and A. ˘Sabanovi´c, “Buck converter regulator operating in the sliding mode,” in Proc. 7th Int. Conf. PCI, Apr. 1983,pp. 331–340.
39. R. Venkataramanan, A. Šabanovic´, and S. C´ uk, “Sliding mode control of DC-to-DC converters,” in Proc. IEEE Conf. IECON, 1985, pp. 251–258.
40. S. P. Huang, H. Q. Xu, and Y. F. Liu, “Sliding-mode controlled C´ uk switching regulator with fast response and first-order dynamic characteristic,” in Proc. IEEE PESC Rec., Jun. 1989, pp. 124–129.

41. P. Mattavelli, L. Rossetto, G. Spiazzi, and P. Tenti, “General-purpose sliding-mode controller for DC/DC converter applications,” in Proc. IEEE PESC Rec., Jun. 1993, pp. 609–615.
42. H. Sira-Ramirez, “On the generalized PI sliding mode control of DC- DC power converters: A tutorial,” Int. J. Control, vol. 76, no. 9/10, pp. 1018–1033, 2003.
43. J. Mahdavi, A. Emadi, and H. A. Toliyat, “Application of state space averaging method to sliding mode control of PWM DC/DC converters, ”in Proc. Conf. Rec. IEEE IAS Annu. Meeting, Oct. 1997, vol. 2,pp. 820–827.
44. S. Tan, Y. M. Lai and C. K. Tse, "General Design Issues of Sliding-Mode Controllers in DC–DC Converters," in IEEE Transactions on Industrial Electronics, vol. 55, no. 3, pp. 1160-1174, March 2008, doi: 10.1109/TIE.2007.909058.
45. Tan, S., Lai, Y., Tse, C., & Martínez-Salamero, L. (2007). Special family of PWM-based sliding-mode voltage controllers for basic DC-DC converters in discontinuous conduction mode. Iet Electric Power Applications, 1, 64-74.
46. Y. He and F. L. Luo, "Study of sliding mode control for DC-DC converters," 2004 International Conference on Power System Technology, 2004. PowerCon 2004, Singapore, 2004, pp. 1969-1974 Vol.2, doi: 10.1109/ICPST.2004.1460324.
47. Y. He and F.L. Luo, Sliding-mode control for dc–dc converters with constant switching frequency, IEE Proc.-Control Theory Appl., Vol. 153, No. 1, pp. 37-45, January 2006
48. Filippov AF (1960) Differential equations with discontinuous right hand side. Am Math Soc Transl 62:199–231